HIGH RESOLUTION SEDIMENTOLOGY AND RESERVOIR PROPERTIES OF ULAYYAH RESERVOIR EQUIVALENT, UPPER JURASSIC HANIFA FORMATION, OUTCROP APPROACH, CENTRAL SAUDI ARABIA

BY

Hussam Eldin Elzain Osman Elzain

A Thesis Presented to the
DEANSHIP OF GRADUATE STUDIES

KING FAHD UNIVERSITY OF PETROLEUM & MINERALS

DHAHRAN, SAUDI ARABIA

In Partial Fulfillment of the
Requirements for the Degree of

MASTER OF SCIENCE

In

GEOLOGY

MAY 2015

KING FAHD UNIVERSITY OF PETROLEUM & MINERALS

DHAHRAN- 31261, SAUDI ARABIA

DEANSHIP OF GRADUATE STUDIES

This thesis, written by **Hussam Eldin Elzain Osman Elzain** under the direction his thesis advisor and approved by his thesis committee, has been presented and accepted by the Dean of Graduate Studies, in partial fulfillment of the requirements for the degree of **MASTER OF SCIENCE IN GEOLOGY.**

Dr. Osman M. Abdullatif
(Advisor)

Dr. Abdulaziz Al-Shaibani
Department Chairman

Prof. Gabor Korvin
(Member)

Dr. Salam A. Zummo
Dean of Graduate Studies

Dr. Michael Kaminski
(Member)

25/6/15
Date

To my mother

ACKNOWLEDGMENTS

I would like to express my sincere gratitude to King Fahd University of Petroleum & Minerals for giving me the opportunity to pursue MSc study and supporting me. I would like to express my thanks to Dr. Osman Abdulatif for his administration as a Chairman of my Thesis Committee. I also would like to thank the Committee members; Dr. Gabor Korvin and Dr. Michael Kaminski for their supervision, and helpful comments .The faculty member, all my course instructors and all staff at the Earth Sciences, Department are also thankfully acknowledged for wonderful and educational learning skills.

I would like to thank the chairman of the Earth Sciences Department, Dr. Abdulaziz Al-Shaibani and faculty in the department and in the research institute for the support and continuing help during different stages of the study. Thanks also to my colleagues in Earth Sciences Department and to Sudanese community at KFUPM.

TABLE OF CONTENTS

LIST OF TABLES

LIST OF FIGURES

ABSTRACT

Full Name : [HUSSAM ELDIN ELZAIN OSMAN ELZAIN]

Thesis Title : [HIGH RESOLUTION SEDIMENTOLOGY AND RESERVIOR PROPERTIES OF ULAYYAH RESERVIOR EQUIVELNT, UPPER JURRASIC HANIFA FORMATION, OUTCROP APPROACH, CENTRAL SAUDI ARABIA]

Major Field : [Geology]

Date of Degree : [May, 2015]

The Jurassic carbonates in Saudi Arabia host vast hydrocarbon resources. Because of their economic importance, numerous petroleum-related studies have been carried out on the Jurassic carbonates in Saudi Arabia. However, most sedimentological and micropalentological framework studies have focused only on the reservoir units themselves. A more encompassing approach is needed to enhance and improve understanding of the intra-reservoir stratigraphy, sedimentology and heterogeneity within the inter-well spacing in individual oil fields. This study uses high resolution outcrop analog to characterize a strata equivalent to the Middle Jurassic Upper Ullayah reservoir units of Hanifa Formation exposed in central Saudi Arabia. The study utilized a multidisciplinary approach involving the integration of sedimentological, chemostratigraphical, biostratigraphical and gamma ray data. The Upper Jurassic (Oxfordian-Kimmeridgian) Upper Ullayah Reservoir strata of Hanifa formation are composed of medium- to thick-bedded, mostly grainy limestones with various skeletal (brachiopods, bivalves, foraminifera, Cladocoropsis, encrusting stromatoporoid, corals and echinoderms) and non-skeletal (peloids, ooids, intraclasts, and oncoids) components. Facies analysis documents low- to high-energy environments, including, deep lagoonal,

lagoonal shoal flank, and barrier sand shoal. The field analysis revealed six high frequency sequences of fourth-order depositional sequences in each of the four stratigraphic measured sections. High stand systems tracts (HST) show shallowing-upward trends in which deep-water facies are overlain by shallow-water facies. Correlation of depositional sequences in the studied sections shows that relatively shallow marine (shallow lagoonal, lagoonal shoal flank and barrier shoal sand) conditions dominated in the study area. These alternated condition with deep-water open-marine wackestone and mudstones representing zones of maximum flooding. The controlling factors on the sedimentation pattern and geometries are: (a) relative sea-level variations, at different scales: third order of eustatic/tectonic origin, fourth order and fifth order of eustatic/climatic origin (Milankovitch type) (b) input of siliciclastic sands from local high shield area. Size, morphology and reproductive characters of grainstone seem to be directly related to changes in water depth (accommodation). Spectral Gamma Ray (SGR) and chemical analysis signatures show moderate correlation with lithofacies for each high frequencies sequence, their sequence hierarchy and stacking pattern. The chemical profiles defined the regressive and transgressive phases and reflect cyclic depositional patterns within Upper Ullayah reservoir member. The geochemical data shows marked differences in character and distribution of different lithofacies, which might help in reservoir layering and zonation. This study provides outcrop analog for Upper Ullayah carbonate reservoir. It is predictive and provides quantitative information at the sub-seismic scale with regard to the distribution, size and heterogeneities of the reservoir rock lithofacies. The best reservoir potential is attributed to the cross-stratified well sorted and laminated sandy grainstone of sand shoal with a maximum porosity value of 32-25 %. Best reservoirs are located in the platform

margin. The outcrop analog 3D model revealed heterogeneity of the reservoir lithofacies at a higher resolution than that in the subsurface model. Capturing the small-scale lithofacies heterogeneity is important since it influences the distribution of porosity and permeability in the subsurface reservoirs.

ملخص الرسالة

الاسم الكامل: حسام الدين الزين عثمان الزين

عنوان الرسالة: دراسة تفصيلية للرسوبيات وخصائص المكمن لخزان الغُلّيا البترولي لتكوين حنيفة الجوراسي باستخدام شبيه سطحي ، وسط المملكة العربية السعودية

التخصص: جيولوجيا

تاريخ الدرجة العلمية: مايو ، 2015

صخور الكربونات ذات العمر الجوراسي تعتبر من أهم الصخور المستضيفة للموارد الهيدروكربونية في المملكة العربية السعودية, وبسبب أهميتها الاقتصادية, فإن العديد من الدراسات البترولية قد أجريت على هذه الصخور في المنطقة. لكن, وعلى الرغم مما ذُكر, فإن معظم الدراسات الرسوبية والإحاثية التي تمت للتعرف على هذه الصخور بشكل أوسع أجريت على الوحدات التي تُشكِّل مكامن تخزين الهيدروكربونات.

في الحقيقة نحن بحاجة الى وضع منهج أكثر شمولاً ودقةً من أجل تعزيز وتحسين فهمنا فيما يختص بطبقية وترسب الوحدات الداخلية للمكمن, بالإضافة الى عدم التجانس الكبير الذي يظهر في المسامات الداخلية لحقول البترول.

هذه الدراسة تقوم باستقراء تناظرية الطبقات البارزة على سطح الأرض بدقة عالية من أجل توصيف ما يعادل أو يماثل صخور الكربونات ذات العمر الجوراسي الوسيط المنتمية الى تكوين حنيفة في مكمن غُلية في وسط المملكة العربية السعودية.

استخدمت هذه الدراسة نهجاً متعدد التخصصات يتعلق بتكامل البيانات الرسوبية والكيميائية والأحيائية للطبقات, بالإضافة الى قراءات اشعاعات جاما. الصخور ذات العمر الجوراسي العلوي (الأكسفوردي) المنتمية لتكوين حنيفة في مكمن غُلية تتكون من حبيبات حجر جيري متوسطة الى سميكة الطبقية, وتحتوي على بقايا كائنات حية عظمية (ذوات القوائم الذراعية وذوات الصدفتين والمنخريات والشعاب المرجانية وشوكيات الجلد وبقايا أخرى), وبقايا كائنات حية غير عظمية (البيليوبدز والأنكويدز والأويدز والانتراكلاستس).

أظهر تحليل السحنات بيئات رسوبية ذات طاقة حركية منخفضة الى عالية, منها بيئات البحيرات العميقة والبحيرات الضحلة (لاغونيه) والمياه الضحلة ذات الحاجز الرملي. أظهر التحليل الميداني ستة تسلسلات عالية التردد من الترتيب الرابع للتسلسلات الترسيبية في كل واحدة من المقاطع الطبقية الأربعة التي تمت دراستها. أظهر تحليل المساحات ذات الأنظمة العالية توجهاً يزداد ضحالة بصورة تصاعدية الى أعلى حيث تكون سحنات المياه العميقة موجود بالأعلى من سحنات المياه الضحلة. مقارنة ارتباط الطبقات

الترسيبية في المقاطع التي تمت دراستها أظهرت أن الظروف البحرية الضحلة (البحيرات الضحلة والمياه الضحلة ذات الحاجز الرملي) هي السائدة في منطقة الدراسة, ولكنها تناوبت مع سحنات الواكستون والصخور الطينية المنتمية للمياه المفتوحة العميقة في تقديم مناطق الحد الأقصى من الفيضانات.

العوامل المتحكمة في نمط وشكل الترسيب هي (أ) التغيرات في مستوى سطح البحر بمقاييس مختلفة. الترتيب الثالث من الأصل التكتوني والترتيب الرابع والخامس من الأصل المناخي (نوع ميلانكوفيتش). (ب) المدخلات الرملية ذات الأصل السليكي القادمة من مناطق الدروع المحلية العالية. بالإضافة الى حجم وشكل صخور الجرينستون المرتبطة مباشرةً بتغيرات عمق المياه.

طريقة أشعة جاما الطيفية والتحليل الكيميائي أظهرا علاقةً قوية بين السحنات الطبقية لأي تسلسل متوسط التردد. التحاليل الكيميائية ساهمت في تعريف حالات التراجع والتأخر للدورات الترسيبية بأنماطها المختلفة في الجزء العلوي من مكمن عُلية. أظهرت البيانات الجيو-كيميائية اختلافات واضحة في توزيع السحنات الطبقية, وهذا قد يساعد في عمليتي تقسيم المناطق وطبقية المكمن.

تُقدِّم هذه الدراسة استقراءاتٍ لتناظرية الطبقات البارزة على سطح الأرض لصخور الكربونات الموجودة في الجزء العلوي من مكمن عُلية. كما أنها تقوم بتقديم معلومات كمية على المقياس الزلزالي فيما يختص بتوزيع وحجم وتباين السحنات الطبقية لصخور المكمن. ويُعزى أفضل انتاج للمكمن الى صخور الجرينستون التي تحتوي على بقايا الفورامنفرا والتي ترسبت في بيئات البحيرات ذات الأجنحة الرملية والتي توصف بأنها جيدة التوزيع الحبيبي الرملي بمسامية بين حبيبية تتراوح بين 15% و 25%.

كشف النموذج التناظري للطبقات البارزة على سطح الأرض عن تباين كبير في السحنات الطبقية للمكمن, بدقة أكبر من النموذج التناظري للطبقات تحت سطح الأرض. التقاط التباين في السحنات الطبقية على المقياس الصغير ذو أهمية كبيرة في تحديد توزيع المسامية والنفاذية لصخور المكمن تحت سطح الأرض.

CHAPTER 1

INTRODUCTION

1.1 Overview

Carbonate rocks make up less than 10% of the rock record, yet they contain half of the world's oil and gas reserves, about 60% of which remain in place after primary recovery methods have been completed on established fields. Many of these fields are classified as "giant fields" and still contain large reserves of petroleum. Jurassic carbonates have economic importance in the Middle East region, their petrographic properties have received considerable attention. The Late Oxfordian Uppermost part of Ulayyah Member reservoir basin-margin grainstone-dominated facies presents good hydrocarbon reservoir facies and its juxtaposition to intra-shelf, potential source-rock basinal sediments provides important new exploration target (Hughes et al., 2008).

The study of outcrop model provides the opportunity to investigate and quantify the geometry and the distribution of sedimentary bodies along a depositional profile. Field-based, 2-D and 3-D geological data play an essential role for the characterization of sub-surface reservoir properties). Which cannot be accessed using geophysical imaging tools and wells (Kerans et al., 1994; Grammer et al., 2004; Jones et al., 2008). The establishment of a high resolution sedimentology and stratigraphy strategy designed to capture the geological heterogeneity observed in the sedimentary record remains challenging for the

building of a realistic 3-D geological model for carbonate deposits .The predictable nature of facies heterogeneity was questioned by field observations and statistical analyses on shallow-water carbonate rocks (Ginsburg, 1971; Hardie and Shinn, 1986; Pratt and James, 1986; Read, 1995; Drummond and Wilkinson, 1993; Wilkinson et al., 1997, 1999). The latter studies showed the common occurrence of a random distribution of facies in the sedimentary record, caused by the predominance of internal factors (auto-cyclic model) on sedimentation such as tidal-flat progradation, variability of carbonate production and transport, unfilled accommodation, clastic input, and storms. In the effort of integration, recent studies (Wright and Burgess, 2005; Burgess, 2008; Strasser and Védrine, 2009) have highlighted that the predictable or random nature of carbonate heterogeneity is dependent of the scale of observation. Whereas at the basin scale, the association of facies exhibits gradational and ordered trends along a proximal-distal depositional profile, facies distribution, at the bedding scale, lacks clear trends in facies-to-facies transitions, leading to an unpredictable spatial arrangement. These recent advances of carbonate sedimentology modified previous conceptions on carbonate heterogeneity and brought new viewpoints, which need to be considered for the improvement carbonate outcrop modeling.

1.2 Problem Statement

Carbonates have more varied facies and diagenetic patterns than their siliciclastic counterparts, thus offering a greater challenge to reservoir evaluation. Studies of modern analogs are valuable because they constrain interpretations and lend predictability to unraveling facies patterns in reservoirs. These patterns help to understand the lateral continuity of stratification, variation within layers, heterogeneity, and performance of

reservoirs examples. Carbonate depositional systems, are complex from the scale of a producing field right down to that of a pore throat.

The problem is how to model the sedimentary facies , their sequence hierarchy and stacking pattern of the Ulayyah Member Reservoir at the outcrop analog level with a high order of resolution based on their sedimentological, stratigraphic, and petrophysical properties.

Outcrop analogs provide important information on the stacking pattern and lateral correlation of reservoirs rocks. This information is a useful proxy that could facilitate the understanding of the reservoir architecture elements, and might help to overcome the limitations of subsurface data. Many researchers have pointed out that the outcropping strata equivalents to the reservoirs in the Jurassic Shaqra Group have similar age and similar geometry as their subsurface equivalent (Le Nindre et al., 1987; Mitchell et al., 1988; Hughes, 2004a, 2004b, 2009, 2010) which allows for direct comparison between surface and subsurface strata. Study of outcropping strata of the Hanifa Reservoir will help understanding the architectural elements and reservoir components and increase the predictability of the geological parameters that control the Hanifa reservoir equivalents in the subsurface. The integrated methodology proposed for this study is expected to provide a better understanding and prediction for the reservoir quality and architecture for carbonate reservoir unit within the Ulayyah Member Reservoir.

1.3 Objective

The present study will use integrative approach for characterizing Ulayyah Member Reservoir with the focus placed on the outcrop analogs. The study objectives include

- Propose the paleo-depositional environment based on lithofacies zones description and their biofacies assemblages of the outcrop succession
- Develop high resolution 3-D sedimentological and stratigraphical models.

- Characterize the outcrop using Spectral Gamma Ray (SGR) logs and geochemical signature

- Distribute outcrop porosity and permeability data into the high resolution 3-D facies model.

1.4 Area of Study

The Upper Ulayyah member reservoir of jurassic Hanifa formation investigated in this research, crop out as hill in Jabal Abakkayn along the northern Hisyan Pass in the north-west Riyadh district (Figure 1-1), the outcrop located about 18.9 km to the west from the Uyayna Town and to the south east from the Sadoos village.

Jabal Abakkayn outcrop was chosen for the study on basis of accessibility, style of exposure and quality. The deposits at the selected outcrop area comprise carobonate Hanfa formation excellently exposed in both vertical cliff faces, ranging from 90 m to 110 m with vast lateral extend in these specific area Therefore, the Hanifa outcrop allows detailed high-resolution sedimentological analysis of the Upper Ulayyah reservoir equivalent member architecture (e.g. lithofacies spatial distribution and proportions, geometry of bounding surfaces and sedimentary bodies). This outcrop encompasses the Upper Ulayyah member and its lower boundary with Lower Hawatah member of Hanifa formation (Figure 2-1) and extends from west to east providing a very good cross section of the Upper Ulayyah member.

Figure 1.1 Map showing the location of Hanifa refrence section (Jabal Abakkayn) in central Saudi Arabia (Google maps revised February, 2013).

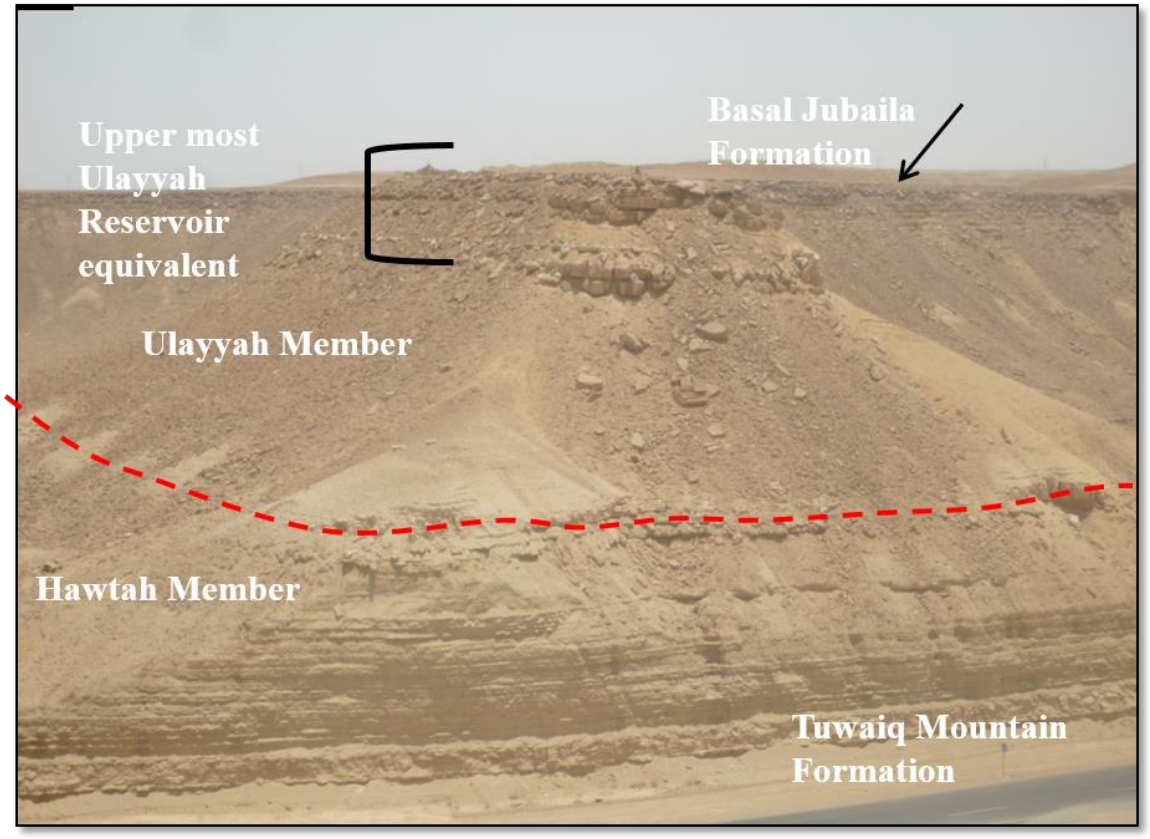

Figure 1.2 Jabal Abakkayn outcrop encompasses the Upper Ulayyah member and its lower boundary with Lower Hawatah member of Hanifa formation.

1.5 Literature Review

1.5.1 Tectonic Setting of Arabian Plate

The consolidation of the Arabian Shield in the eastern part during the Late Precambrian took place by the accretions between the micro-plates. The most important Amar collision was before 640 – 620 Ma, when the Al-Rayn micro-plate moved westward and collided with the Arabian Shield through the N – S Amar suture (Figure 1-3). This collision formed a number of anticlines that extend N – S and were surrounded by NE Bin Batin and NW Abu Jifan faults (Al-Husseini, 2000). Then, a stage of extension occurred, due to A-type granitic pluton, causing some collapse in the shield. The last stage of that extension resulted

in the Najd fault system that moved the whole area in a left-lateral side about 300 km; this caused rifts to form in NE direction (Al-Husseini, 2000).

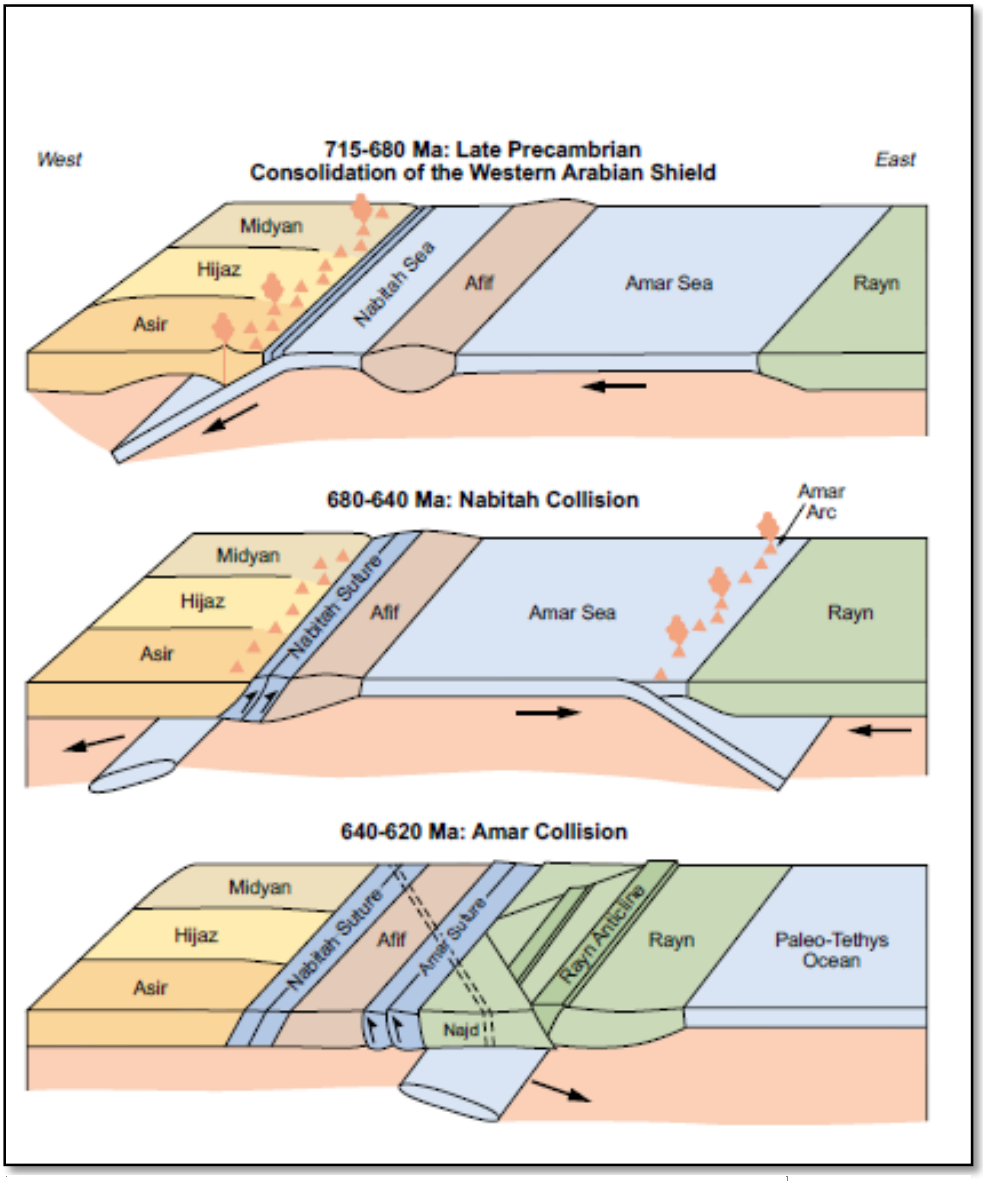

Figure 1.3 The accretionary evolution of Arabian Shield (Al-Husseini, 2000).

The north trend of the Arabian Plate arches and oil fields were interpreted to be surface reflections of the Precambrian basement configuration (Edgell, 1987). The major events

that shape this basement were the Ammar collision, the Najd fault system, Dibba Fault, the Oman Salt Basin and the Wadi Al Batin Lineament (Al-Husseini, 2000) (Figure 1-4). The intersection of the Precambrian structure produced jointed basement fabric, which was reactivated later by subsequent tectonics (Ziegler, 2001) (Figure 1-5).

The Arabian Plate has evolved through five tectonic settings or evolutionary phases. These phases are plate accretion, intracratonic, back-arc, passive margin plate setting, and active margin setting (Sharland et al., 2001). Currently, the Arabian Plate boundaries are characterized by numerous types of plate boundaries (Konert et al., 2001). In the north and east boundaries, collision with Eurasia occurred during the Late Eocene, followed by the opening of the Red Sea during the late Oligocene to form a divergent margin in the western part. This divergent margin translated to the transform fault of the Dead Sea and the Gulf of Aqaba in the northwest margin of the Arabian Plate during the late Miocene (Hughes et al., 1999; Konert et al., 2001; Ziegler, 2001).

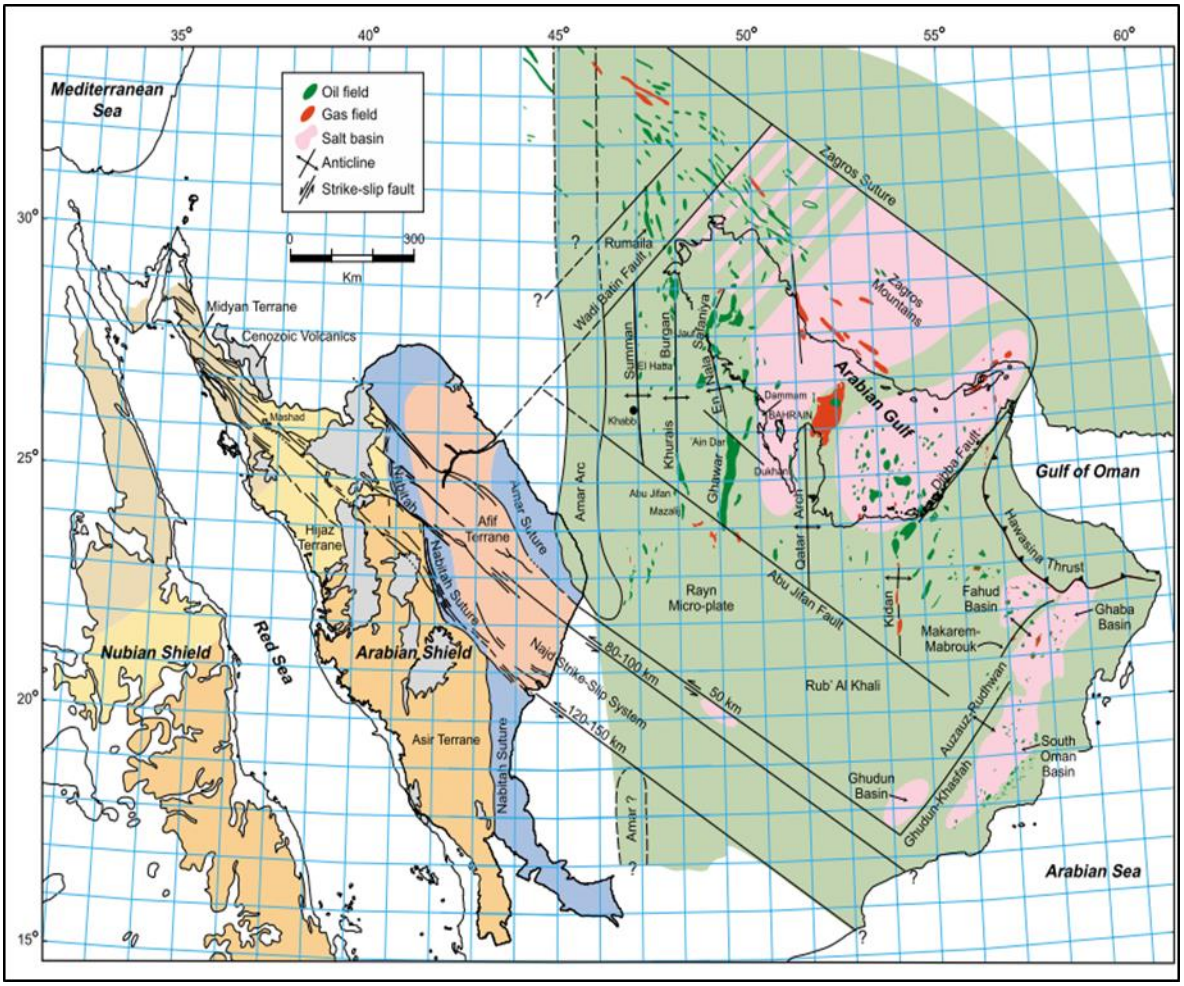

Figure 1.4 Geological map showing the configuration of the Arabian Shield's, the Arabian Arches, and the major fault systems that control the above sedimentary cover in the Saudi Arabia. Note the north trend of the Arabian arches which were controlled mainly by Ammar collision (Al-Husseini, 2000).

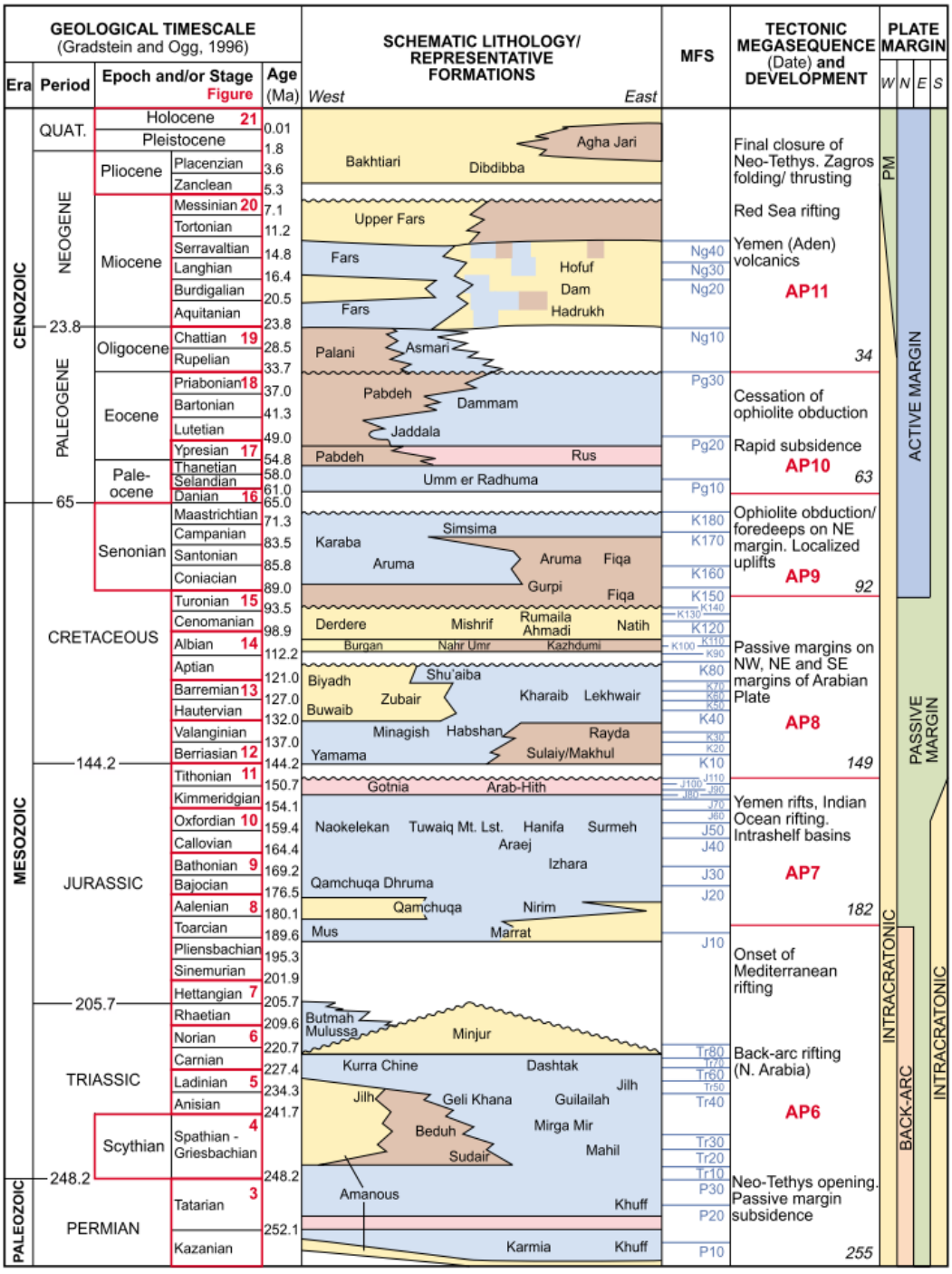

Figure 1.5 Stratigraphic column of the Arabian Plate from Late Permian to Holocene. Note that the Arabian plate had gone through different Plate boundaries during this time (Ziegler, 2001).

The Arabian Plate was located at different positions during the Precambrian and most of the Phanerozoic (Figure 1-6). According to Konert et al. (2001), the Arabian Plate was located close to the equator with an E-W orientation during the Precambrian. It started to move anticlockwise during the Early Paleozoic and reached the maximum south position by the Early Ordovician, the period of glacial deposits in the Arabian Plate. During the Silurian, a time of major transgression, the Arabian Plate moved clockwise towards the equator (Abu Ali et al., 1999).

In the region, another glaciation episode occurred from the Permian through the Carboniferous (Vaslet, 1989; Senalp and Al-Duaiji, 2001). The Arabian Plate was again located near the equator during the time of deposition of the Arab-D in the Late Jurassic. The paleogeography of the Arabian Plate during the Early to Late Jurassic was a warm, arid climate representing the southern margin of the Tethys Ocean (Murris, 1981; Le Nindre et al., 1987; Al-Husseini, 1997).

The Arabian Plate during Jurassic was occupied by a shallow marine carbonate platform (Al-Husseini 1997; Handford et al., 2002). Tectonic activity during that time created a number of intra-shelf basins in the carbonate platform (Ziegler, 2001). These intra shelf basins are the Arabian, Qotnia, and Al Rub Al Khali basins. During this period, a thick interval of carbonate succession was deposited, the Shaqra Group, which includes seven pure carbonate formations. Based on micropaleontological studies, Hughes (2004b) subdivided these Jurassic formation into three possible super sequences of formations that could be differentiated according to their paleoenvironmental setting.

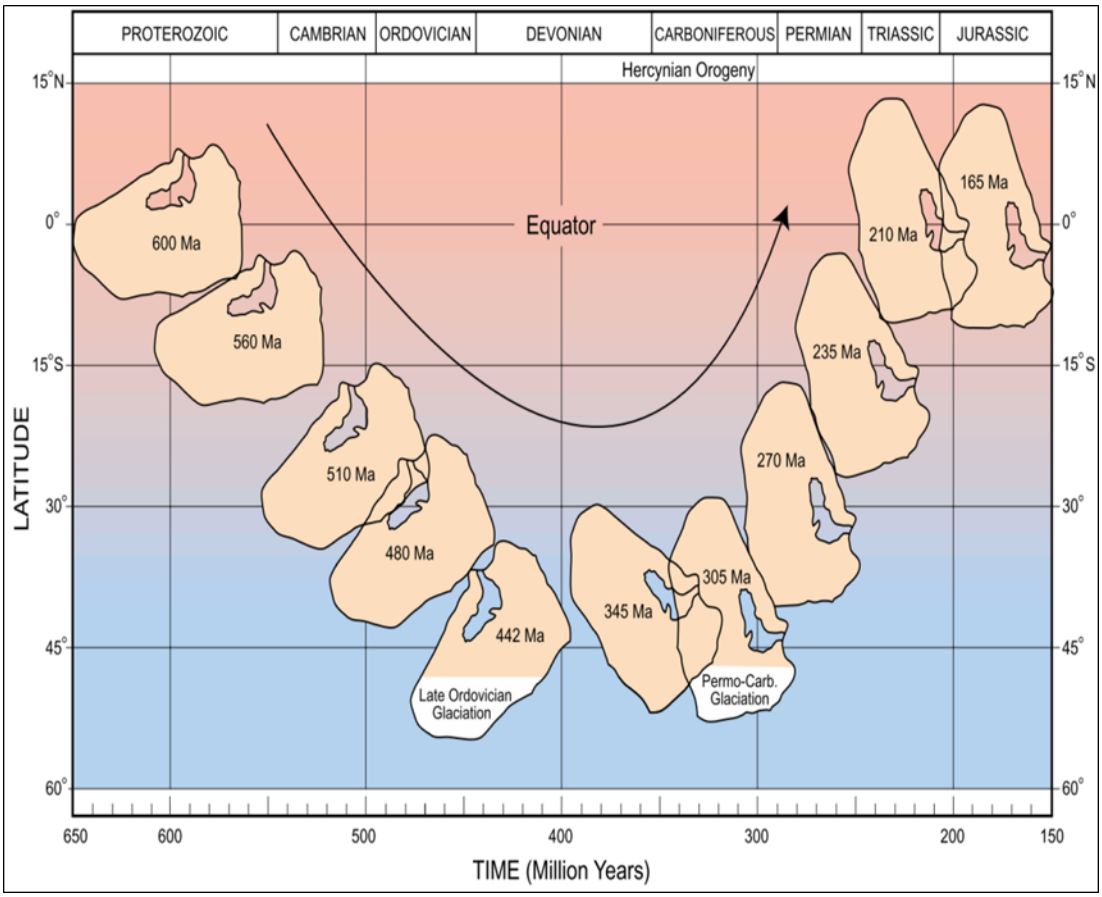

Figure 1.6 Paleolatitude positions of the Arabian Plate from Proterozoic to Jurassic. The Arabian Plate started to move anticlockwise to the south until it reached higher latitude in the Ordovician and Devonian. The plate was completely rotated and started to move north and reached close to the equator in the late Jurassic time (Konert et al., 2001).

1.5.2 Shagra Group

The Jurassic Shaqra Group (Le Nindre et al., 1987) is the most important stratigraphic unit in the Middle East. The sedimentology, stratigraphy, biofacies, paleoenvironment, and reservoir quality of this group have been studied since the middle of the last century (Steineke and Bramkamp, 1952; Powers, 1962; Powers, 1966; Wilson, 1981; Le Nindre et al., 1987; Mitchell et al., 1988; Vaslet et al., 1989; Enay and Mangold, 1994; Le Nindre et al., 1996; Al-Husseini, 1997).

This group comprises seven formations that are, from bottom to top, the Marrat, Dhruma, Tuwaiq Mountain, Hanifa, Jubaila, Arab and Hith formations (Figure 1-7). These seven formations host twelve major hydrocarbon reservoirs in Saudi Arabia; they are, from bottom to top, Marrat, Farida, Sharas, Lower Fadhili, Upper Fadhili, Hadriya, Hanifa, Arab-D, Arab C, Arab B, Arab A, and Manifa (Steineke et al. 1952; Powers et al. 1966; Powers 1968; Murris 1980; Ayres et al. 1982; Le Nindre 1987, 1990, Husseini 1997 and Hughes, 2004a).

In terms of lithostratigraphy, the onset of the Bajocian transgression, following the Aalenian hiatus, resulted in the deposition of the Dhruma and Tuwaiq Mountain formations marking a significant increase in sedimentation rate and increased tectonic subsidence (Le Nindre et. al 2003). The Callovian Tuwaiq Mountain Formation overlies the Dhruma Formation disconformably marking the Bathonian–Callovian boundary (figure 1.5) (Le Nindre 1990, Alsharhan and Nairn 1997).

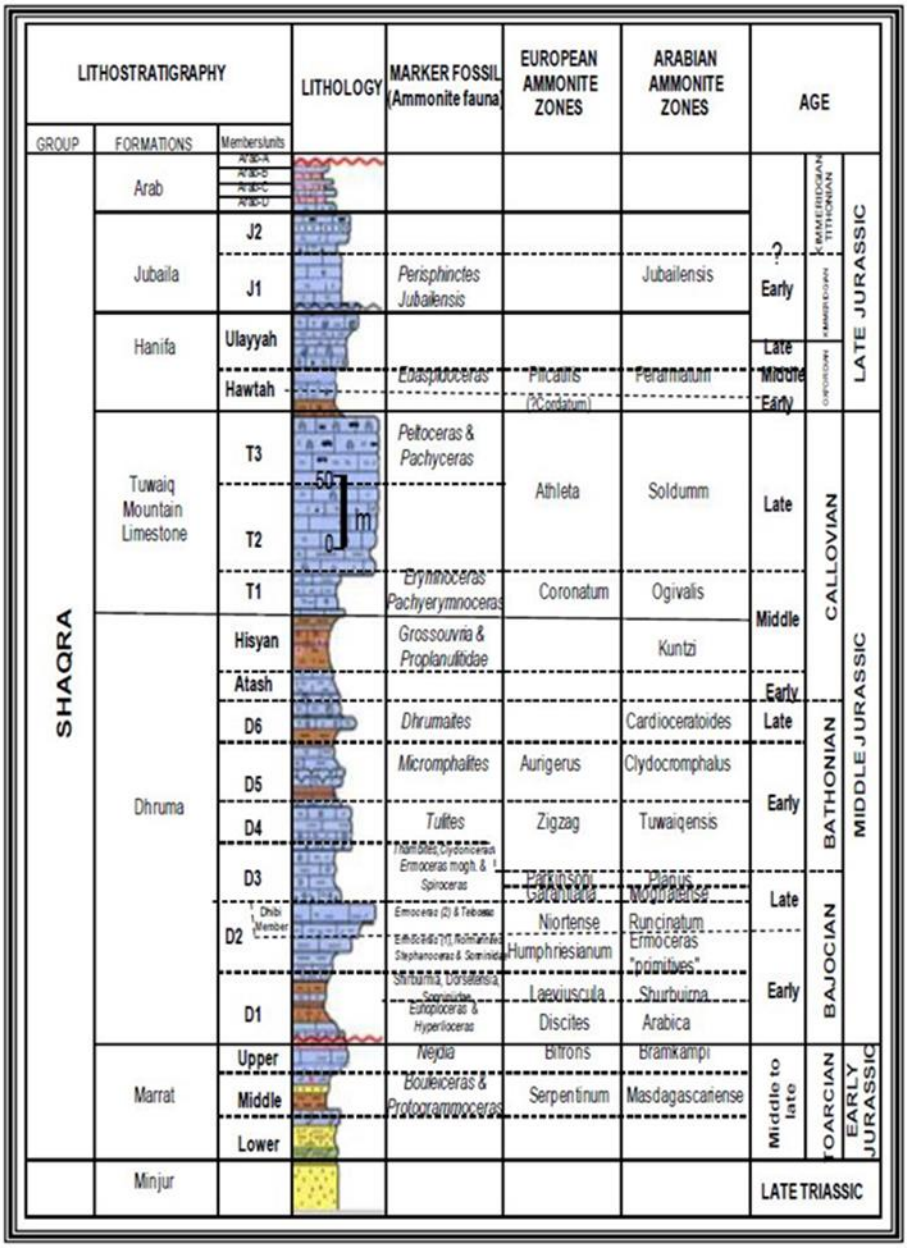

Figure 1.7 Stratigraphic succession of Shaqra Group. This group encompasses seven formation separated by six hiatus (Hughes, 2004a).

The Tuwaiq Mountain Formation is about 300 ft thick and comprises three members: the lower Baladiyah, the middle Maysiyah and the upper Daddiyah (figure 1-8) (Enay et al. 1987 cited in Hughes 1995, Powers et al 1966). During the late Callovian transgression, restricted water circulation of the developed Arabian intra-shelf basin led to euxinic

conditions which, coupled with high productivity, resulted in the deposition of organic-rich clay and mud-rich carbonates. The average TOC values for these units is about 3 wt. % but can be as high as 13 wt. % (Murris 1980; Carrigan et al. 1995). The marls pass transitionally upward into higher energy, open marine coral- and calcareous-algae-bearing facies corresponding to Upper Fadhili and Hadriya reservoirs (Powers 1968; Alsharhan and and Kendall 1986; Le Nindre 1990; 2003, Alsharhan and Nairn 1997).

The Oxfordian Hanifa Formation is underlain by the Tuwaiq Mountain Formation and is overlain by the Jubaila Formation. Vaslet et al. (1983) subdivided the Hanifa Formation into two members: the Hawtah and Ulayyah (Figure 1-8) (cited in Husseini et al 1996). Each member represents a shallowing upward high frequency sequence composed of several high frequency cycles and cycle sets (Mattner and Husseini 2000). The Ulayyah member contains the Hanifa reservoir which is composed of aggrading and prograding grainstones (McGuire et al 1993).

The Early Kimmeridgian Jubaila Formation rests unconformably on the underlying Hanifa Formation separated from it by a clear textural and color shift (Steineke et al. 1958; Powers et al. 1966; Powers 1968). The Jubaila records initial phases of transgression of the Jubaila-Arab-Hith 2nd-order supersequence. The Jubaila Formation is composed of organic-rich (0.5-3.5% TOC), subtidal, laminated wackestones and packstones that become increasingly bioturbated up-section with concommitent loss of organics (Wilson 1981, Meyer et al. 1996, Alsharhan and Nairn 1997).

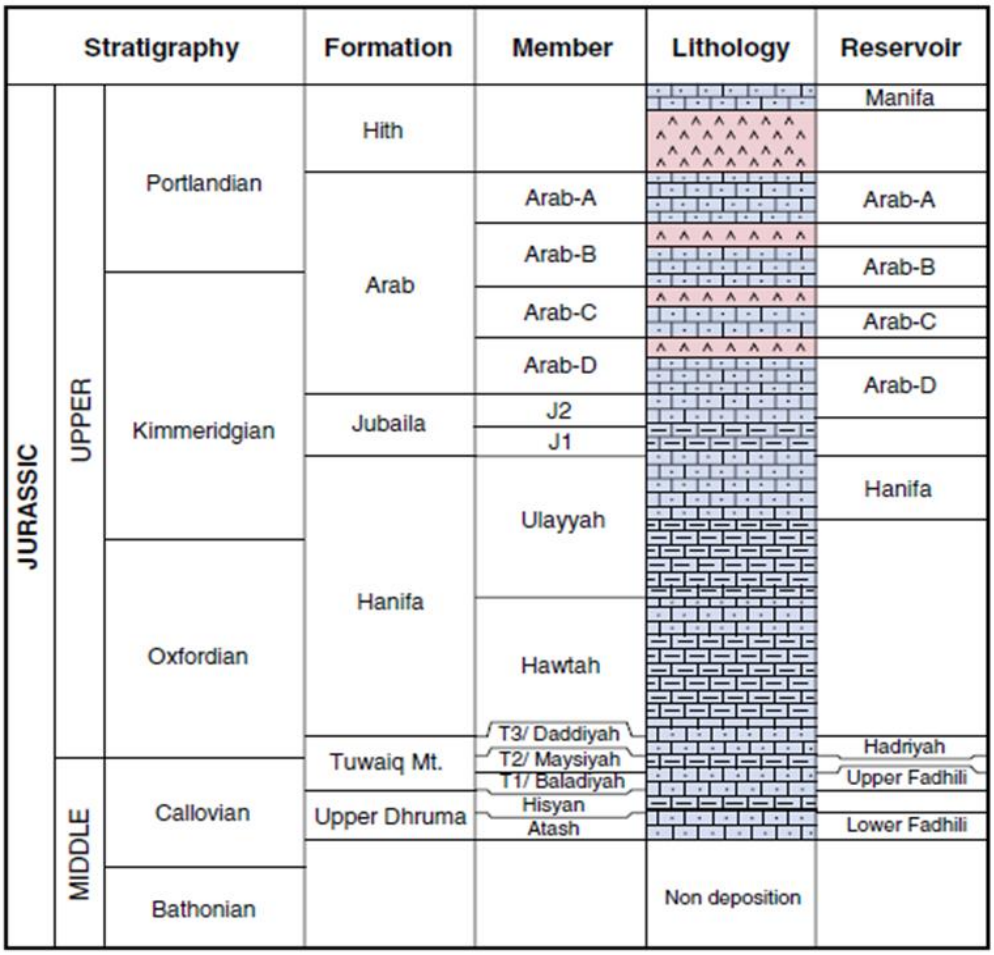

Figure 1.8 Lithostratigraphy of the AP7 megasequence (Sharland et al. 2001) of the Middle to Upper Jurassic showing the Upper Dhruma to Hith formations Modified from Hughes (1995) and Al-Husseini (1997).

The Arab carbonate-evaporite cycles represent transgressive-regressive depositional sequences of approximate 5 Ma duration (Sharland et al., 2001; Hughes 2010). These sequences were deposited upon a restricted platform. The more open-marine transgressive hemicycles are characterized by shallow-subtidal carbonates whereas the regressive late highstands are characterized by evaporites.

Based on exposure description by Enay et al. (1987), the Marrat Formation was interpreted as a shallow to moderately marine condition; the Dhruma Formation was moderately shallow to deep marine; the Tuwaiq Mountain Formation was deep marine to shoal setting;

the Hanifa Formation was back shoal to lagoonal; the Jubaila Formation was restricted lagoonal; the Arab Formation was a tidal flat; and the Hith Formation was a saline environment. It should be noted that east-ward of the outcrop belts described by Enay et al. (1987) intrashelf basins developed such as that described for Hanifa Formation by Hughes et al. (2008).

Based on their micropaleontological data, these formations have been subdivided into five groups (Hughes, 1996, 2004a 2004b, 2009). Each group has a unique biofacies assemblage that indicates a certain paleoenvironment. The sequence stratigraphy framework of the Upper Jurassic formations, including the Jubaila and Arab Formations, has been studied from different perspectives. Le Nindre et al. (1996) suggested a sequence stratigraphic framework based on the global sea level model of Haq et al. (1986) that was followed by Al-Husseini (1997), who established the sequence stratigraphic framework of the Gulf region. By applying the principles of sequence stratigraphy from Galloway (1989) using the maximum flooding surface, Sharland et al. (2001) subdivided the Upper Jurassic sequence into 9 maximum flooding-based stratigraphy (Galloway, 1989).

1.5.3 Paleogeographic Reconstruction

The Arabian Plate regional paleogeographic reconstruction for the Jurassic indicates that it was a stable, broad carbonate shelf, modified by the presence of the Arabian, Gotnia, and Rub' Al-Khali intrashelf basins (Figure 1-9). These basins and associated shallow ramp areas were controlled by structural lineaments set up by three tectonic phases (Al-Husseini, 2000). The Arabian Basin is the site where giant oil fields developed such as Ghawar, Khurais, Abqaiq and Qatif (Murris 1980; Ayres et al. 1982; Alsharhan and Kendall, 1986; Al-Husseini, 1997; Sharland et al., 2001). During the Jurassic the Arabian Plate was located

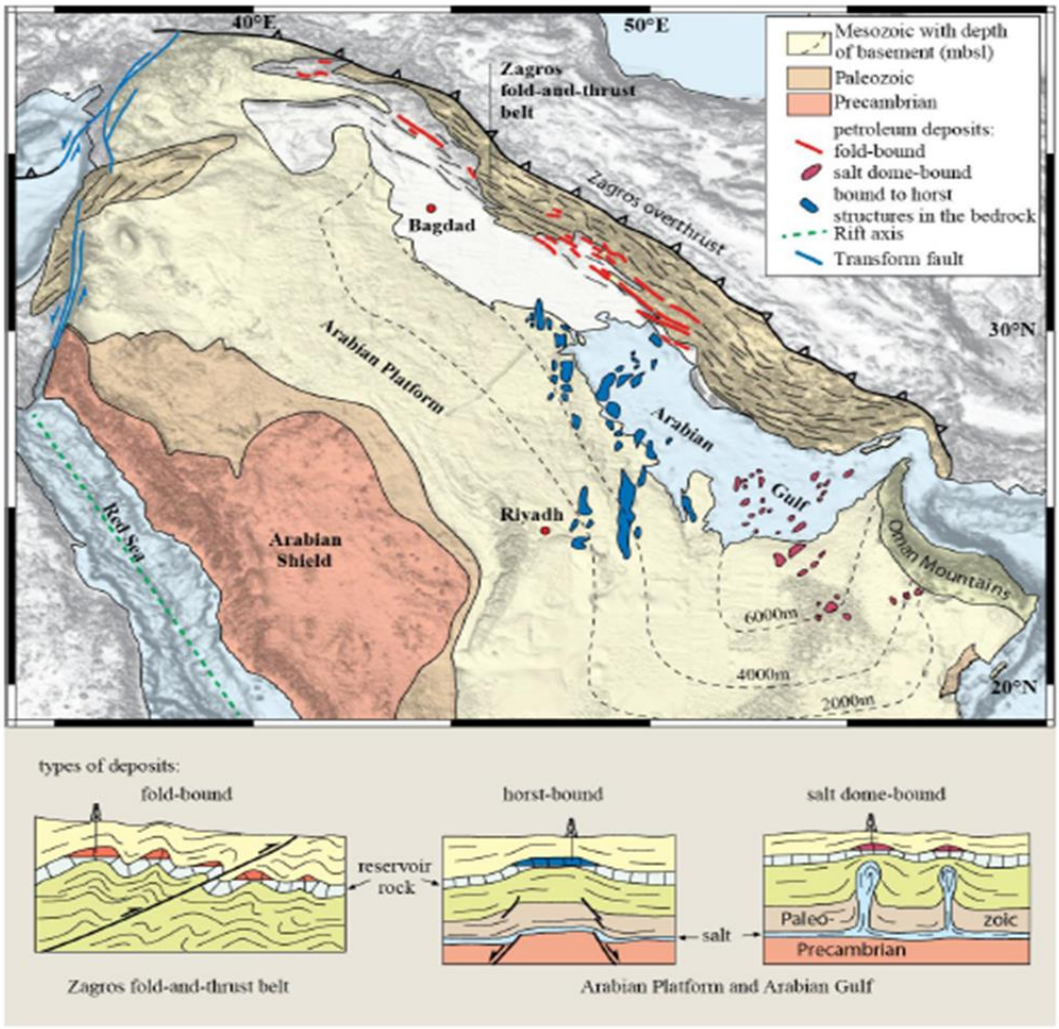

Figure 1.9 Map showing the Arabian Plate boundaries. The location of Zagros thrust belt is believed to represent the zone where the true margin of the Kimmeridgian ramp. The generalized cross sections represent the different trapping styles of the Jurassic petroleum traps between the Arabian platform and the Zagros thrust belt (modified from Frisch et al. 2011)

During the Toarcian, the post- rift thermal subsidence in the northern parts of the plate resulted in the creation of a deep water, intra-shelf Sargelu Basin. The Sargelu Basin differentiated, due to variable subsidence, into two intra-shelf basin. These are the Gotnia Basin and the Arabian Basin that were separated by the Bajocian Rimthan Arch (Figure 1-10) (Murris 1980; Ayres et al. 1982; McGuire et al. 1993;Al-Husseini 1997; Al-Husseini 2000; Sharland et al 2001).

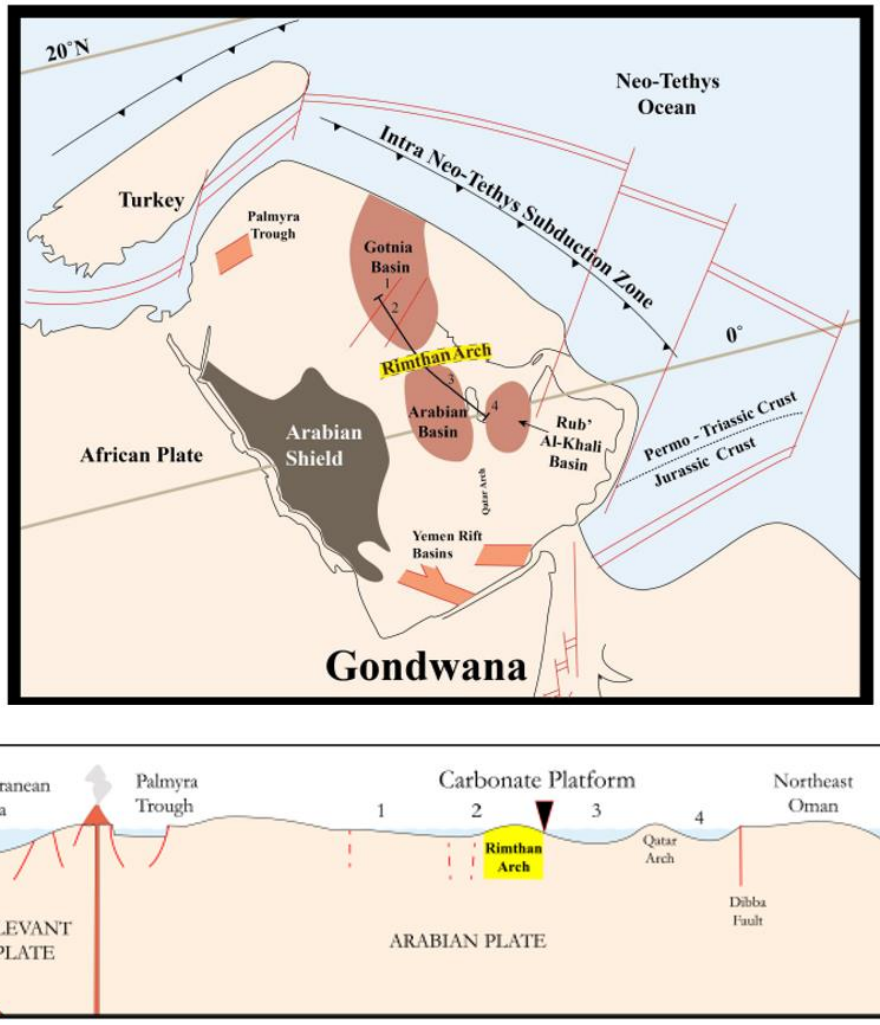

Figure 1.10 The paleogeographic location of the Arabian Plate during AP7 megasequence. Intrashelf basins were present in the Iraq-Kuwait (Gotnia), central Saudi Arabia (Arabian) and southern Gulf (Rub Al-Khali) areas and due to their nature of depth and restriction they were sites of source rock deposition. The location of the intrashelf basins was controlled by old structural lineaments such as Rimthan and Qatar Arches. The lower diagram displays a cross sectional view of the developed intrashelf basins including the Gotnia, Arabian and Rub Al-Khali basins.

During the Middle Jurassic, the Qatif Field was located on a broad stable, platform where carbonate sedimentation predominated (Murris 1980, Ayres et al. 1982, McGuire et al. 1993, Al-Husseini 2000; Sharland et al. 2001). However, during the Late Jurassic, the development of intra-shelf basins and arches placed the Qatif Field as part of the Arabian Basin developing on the south-facing limb of the NNW trending Rimthan Arch. During the Oxfordian-lower Kimmeridgian, the Hanifa Formation was dominated by low energy,

organic rich, euxinic carbonate sediments (Powers et al. 1966, Powers 1968, Alsharhan and Kendall 1986, Alsharhan and Magara 1994, Alsharhan and Nairn 1997). The Hanifa represents the major source-rock bed for most of the Jurassic reservoirs in Saudi Arabia. Hanifa strata were overlain unconformably by dolomites and mudstones of the Jubaila Formation (Powers et al. 1966; Powers 1968; Murris 1980; Alsharhan and Kendall 1986; Al-Husseini 1997). The Jubaila Formation passes conformably into four grainstone-dominated third-order sequences with basal carbonates and capping evaporites, known as the Arab D (oldest), Arab C, Arab B, and Arab A (youngest) (Alsharhan and Nairn, 1997). The Kimmeridgian Arab Formation carbonate members of the A, B, C and D sequences represent reservoir facies, whereas the capping evaporites are excellent seals (Steineke et al. 1952; Powers et al. 1966; Powers 1968; Murris 1980; Alsharhan and Kendall 1986; Alsharhan and Magara 1994; Alsharhan and Nairn 1997; Al-Husseini 1997).

1.5.4 Hanifa Formation (Early-Late Oxfordian)

Hanifa Formation was defined as outcrop in central Saudi Arabia by Max Steineke in 1937 as member of Tuwaiq Mountain Limestone. Hanifa was included also in the Tuwaiq Mountain group in 1945 by Bramkamp. Hanifa was retained at formational rank by Steineke, Bramkamp (1952b), formal publication of Arabian stratigraphic nomenclature (1954), Steineke and others (1958). Powers et al., 1966 named Hanifa Formation after the Wadi Hanifa where the type section was measured and described. The age, fossils, thickness, lithologic character and contact relationship with the overlying Jubaila Formation and underlying Tuwaiq formation were delineated by Powers et al. (1966) and Powers (1968). Vaslet et al. (1983), conducted geological mapping as part of the Saudi Arabian geological mapping project, divided the Hanifa Formation at the outcrop into two

members Hawtah and Ulayyah , this nomenclature of lithostratigraphy has been used in all successive publications at the outcrop within the Hanifa formation. Murris (1980) Moshrif (1984), Al-Husseini (1997) and Ziegler (2001) proposed a very limited regional palaeoenvironment map for Hanifa formation that shows an undifferentiated shallow with an approximation shoreline carbonate platform .(Figure 1-11).

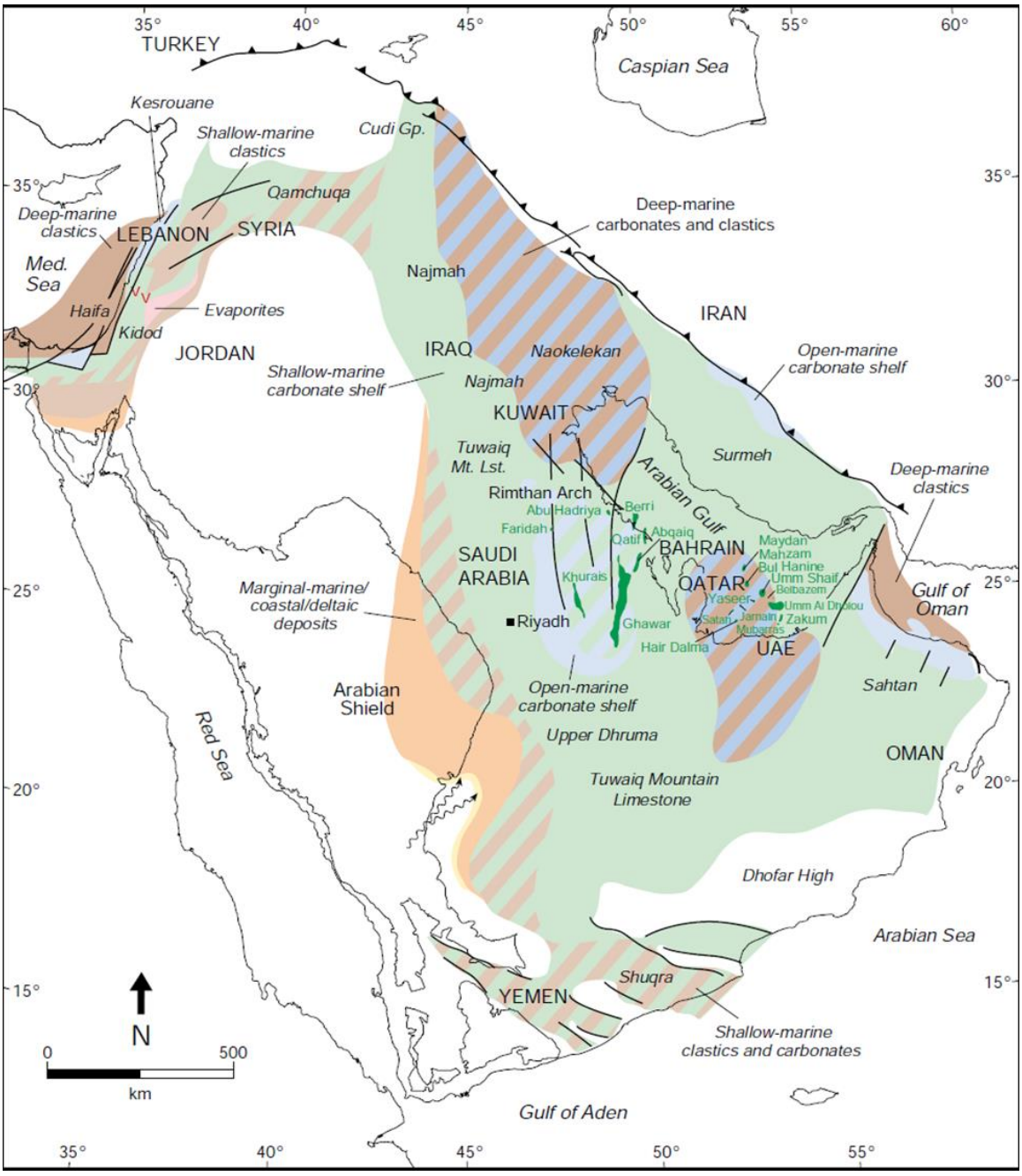

Figure 1.11 Callovian and Oxfordian times. Palaeoenvironment of the Arabian Plate (Ziegler, 2001).

A palaeogeographic map for the Oxfordian in the northern Arabian Gulf was provided by McGuire et al. (1993, and in Mattner and Al-Husseini, 2002) in which the influence of regional eustatic changes was considered, following Hallam (2001).Hanifa formation was

described in Qatar by Droste (1990) as characterize with the presence of organic-rich lime-mud, dark, basinal laminated intra-platform with local anhydrites. Alsharhan and Kendall (1986), McGuire et al. (1993), Luthy and Grover (1995), de Matos and Hulstrand (1995), Alsharhan and Nairn (1997), Al-Naji (2002) and McGuire (2003) described Hanifa formation based on Lithology , stratigraphy (Figure 1-12) and palaeoenvironment aspects. The Arabian Platform regional sea level fluctuation chart was presented by Haq and Al-Qahtani in 2005. All Jurassic sections in Saudi Arabia were studied based on biofacies zones, biostratigraphy and palaeoenvironments (Figure 1-13) by Hughes (1996, 2004a, b, c, 2006) and Hughes et al. (2008). The Sequence stratigraphic framework of the Jurassic succession was done by Le Nindre et al. (1990a, b) Hughes (2004a, b, c; 2006; 2007) and Sharland et al. (2001).

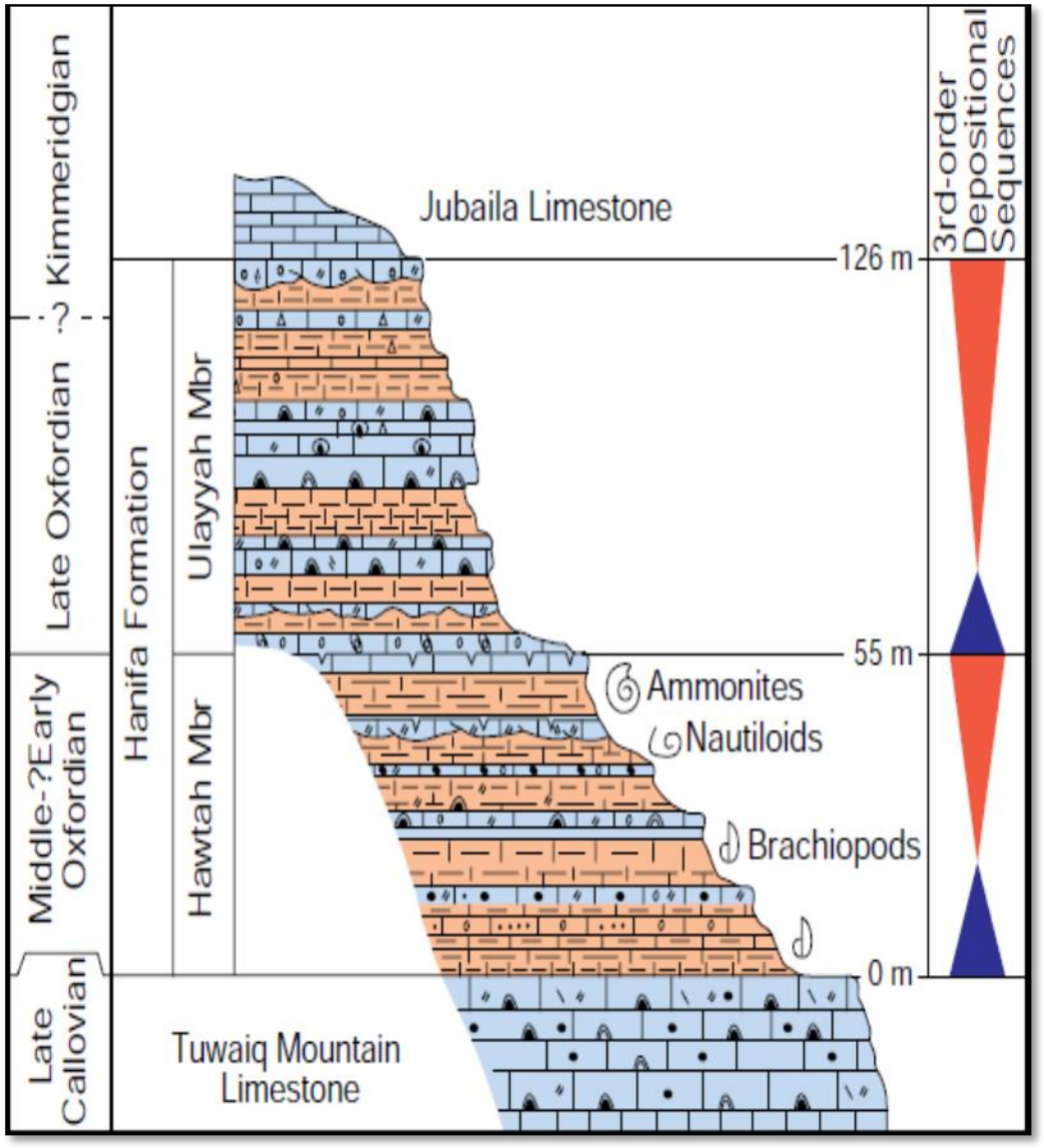

Figure 1.12 lithostratigraphy and chronostratigraphy of the Hanifa Formation (Hughes, 2008).

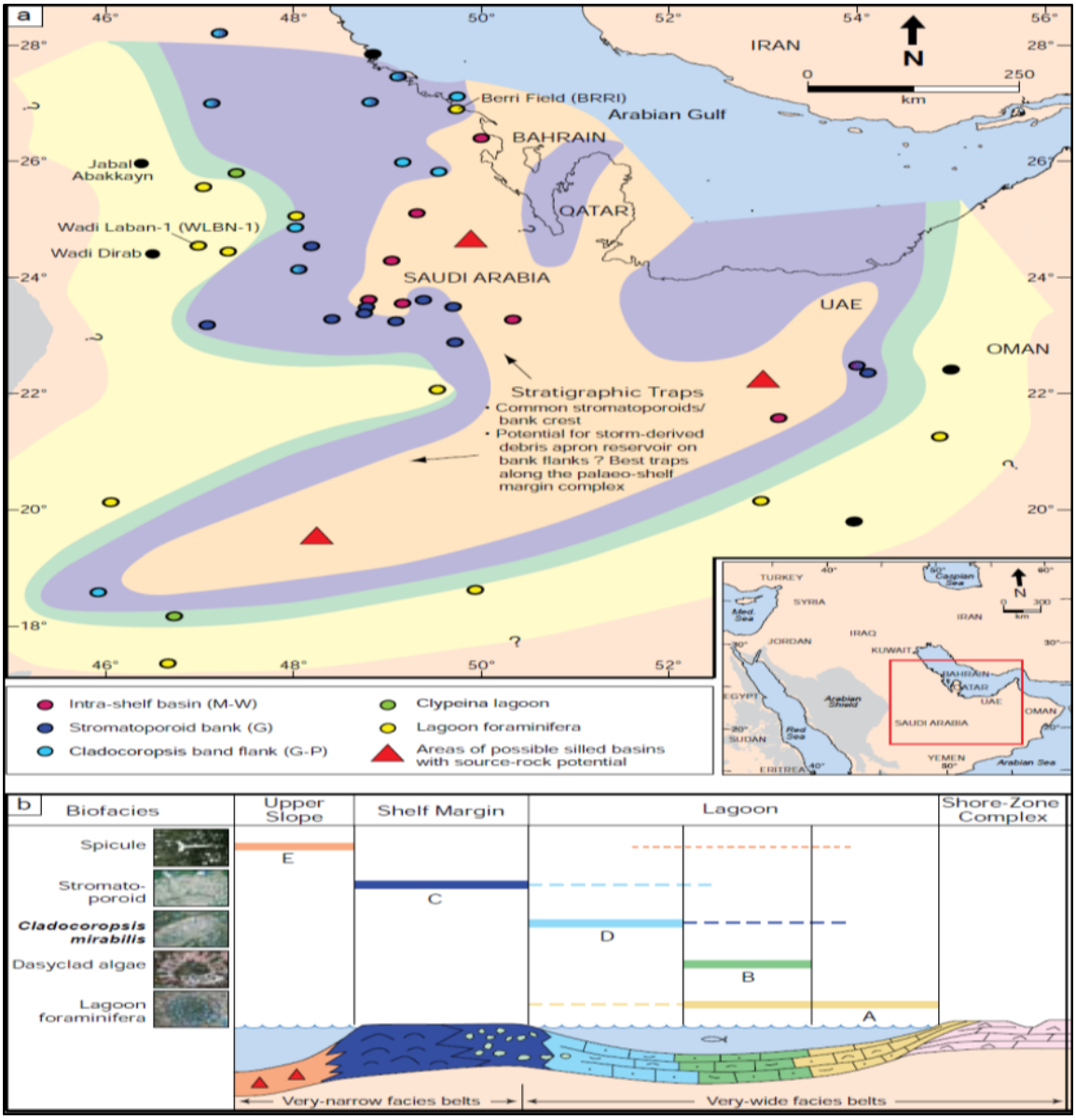

Figure 1.13 Depostional Environment Model of intrashelf Hanifa Formation (Hughes, 2008).

Hawtah Member (Erly-middle Oxfordian)

The Hawtah Member is early Oxfordian (? Cordatum zone) at the base, based on brachiopods (Boullier, in Manivit et al., 1990). The middle and upper parts of the Member

are middle Oxfordian (Plicatilis zone) according to the *Euaspidoceras* ammonite fauna (Enay et al., 1987), nautiloids (Tintant, 1987) and nannoflora (Manivit, 1987).

Ulayyah Member Reservior Equivalent (Late Oxfordian)

The Ulayyah Member is late Oxfordian in its basal part, based on the occurrence of foraminifera *Alveosepta jaccardi* (Andreieff, in Manivit, 1990), and brachiopods (Boullier, in Manivit, 1990). The upper part of the Member yielded echinid faunas (Clavel, in Manivit et al., 1990) that suggest an early Kimmeridgian age (? Hypselocyclum zone).

1.5.5 High Resolution Sedimentlogical Analysis

The establishment of a high resolution sedimentology model improves predictivity of: (1) the distribution of reservoir and source rocks, (2) their geometrical characteristics and internal heterogeneities, and (3) the diagenetic alteration patterns. Significant progress in understanding ancient carbonate platform facies architecture has been made based on analysis of outcrops. Models derived from outcrop analysis are useful in many ways, some of them are great scientific and economic importance. However, it is also true that many outcrop interpretations are highly model driven, and this can be a limiting factor in expanding understanding of how platforms work. Simply describing an outcrop in terms of current models may achieve little because often there is no good test to validate models, so it is difficult to improve the models using this method. Sequence stratigraphic interpretations of platform strata often fall into this trap. The sequence stratigraphic model has many implicit assumptions, many of which are untested, and some highly questionable.

1.5.6 Gamma Ray Spectrometry

Gamma ray (GR) spectrometry measures the total gamma radiation and the individual contribution from the three main radioactive isotopes elements: thorium (Th), potassium (K) and uranium (U). This technique, when associated with the direct analysis of the rocks (biostratigraphy, sedimentology, petrography, and geochemistry) can be a very helpful and important tool for basin analysis, particularly in sequence stratigraphic studies (e.g., Catuneanu, 2006) lithostratigraphic characterization (e.g., Raddadi et al., 2005)and correlation with subsurface data (e.g., Aigner et al., 1995; Leslie et al., 1993). Gamma Ray data are also used to characterize the radiometric signature of the different lithologies and lithostratigraphic units in outcrop .The SGR log provides significant rocks component information (Slatt, et al ., 1992) .This information is widely used for lithofacies correlation and sequence stratigraphy . GR spectrometry in wells and outcrops can be integrated with geochemical analysis. This provides delimitation of the order Regressive- Transgressive cycle of facies (R-T), identification of maximum flooding intervals (maximum flooding surfaces in Galloway, 1989) depositional environment in terms of water depth ,oxygen water condition and terrigenous input .This might help understanding the pattern of lithofacies and consequently provides higher resolution order for reservoir unit characterization . In carbonate sequences, the K and Th isotops are mainly concentrated in the minerals that constitute the insoluble residue (e.g., Lucia, 2007). The U also occurs in the detrital clay fraction however, and unlike Th, it is also partly carried in solution as uranyl carbonate complexes (UO2 (CO3)2) (Langmuir, 1978). Under oxygen depleted conditions, it may precipitate to enrich the sediment in authigenic (nondetrital) U, fixed at

the sediment-water interface accumulating together with the organic matter (Wignall and Myers, 1988).

1.5.7 Reservoir Quality

Carbonate reservoir rocks contain more than 60% of the world's oil reserves and 40% of its gas reserves. The evolution of the reservoir quality, i.e. their porosity and permeability, is for a large part controlled by the sedimentary facies and their digenetic features. The evaluation of reservoir potential and attributes within depositional and stratigraphic trends provide insight to how reservoir quality and distribution are related to those aspects in Ulayyah Member reservoir. If relationships can be determined between depositional and reservoir aspects, then depositional facies and the established vertical stacking pattern of facies can be used in conjunction to provide a more robust understanding of the spatial distribution of reservoir quality in subsurface. Quantifying, predicting, characterizing of carbonate reservoir quality are considered some of the main challenges of reservoir characterization. Recognizing the critical link between reservoir quality and the rock fabric are considered the key to understand carbonate reservoirs.

Porosity and permeability (i.e., reservoir quality) are direct functions of pore architecture, which again is tied to primary depositional facies and/or position within a sequence stratigraphic framework. Reservoir quality has a direct correlation with primary depositional facies. Because of this, the predictability of reservoir distribution, both laterally and vertically, may be enhanced by the development of a sequence stratigraphic framework. Porosity and permeability measurements are important to characterize the geobodies or reservoir units which are relatively highly porous and permeable. The integration between the microfacies analysis from the thin sections and the petrophysical

analysis will result in an interpretation for the heterogeneity within the reservoir units. There are numerous studies that have been conducted to link the concepts of high resolution stratigraphy to reservoir quality I will only discuss some of them:

Koehrer et al., (2009) constructed a high resolution sedimentological and stratigraphical model based on outcrop mapping to follow the high lateral continuity of facies distribution and to delineate, evaluate the reservoir quality .They concluded that finely crystalline lagoonal dolo-mudstones can be considered the best reservoir unit with micro-intercrystalline and vuggy porosity (mean: K = 37.8 mD; Φ = 20.2%), of the 3rd-order cycle in the upper regressive portion the most porous dolomite occurred.

Aigner et al,. (2012) pronounced the hierarchy of stratigraphic cycles Based on outcrops, gamma ray (GR) logs and thin sections. The reservoir facies consists of skeletal and oolitic carbonate grainstones (Φ max 23%, *K* max 700 mD) reservoir properties show gradual lateral changes. Vertically, in contrast, the properties change commonly on a decimetre scale and are largely controlled by stratigraphic cycles. Petrophysical modelling enhanced the understanding of key factors and processes controlling reservoir quality.

theAigner et al., (2007) focussed on the architecture, sedimentology, and petrophysics of carbonate sandbodies in outcrop analogues in the Triassic Muschelkalk. The petrophysical data shows that the reservoir quality is not only driven by depositional facies, but by a combination of facies and pore type, i.e. diagenesis.

1.5.8 Geostatistical Model

The study of outcrop modeling provides the opportunity to investigate and quantify the geometry and the distribution of sedimentary bodies along a depositional profile. Field-based, 2-D and 3-D geological data play an essential role for the characterization of sub-

surface reservoir properties, which cannot be accessed using geophysical imaging tools and wells (Kerans et al., 1994; Grammer et al., 2004; Jones et al., 2008). Whereas outcrop modeling studies have been intensely performed on clastic sediments "e.g. Miall and Tyler, 1991; Bryant and Flint, 1993", the scientific interest on the 3-D modeling of ancient carbonate systems, has drastically increased during the last ten years "Verwer et al., 2004; Adams et al., 2005; Aigner et al., 2007; Qi et al., 2007; Kenter et al., 2008; Phelps et al., 2008; Verwer et al., 2009; Koehrer et al., 2010; Palermo et al., 2010; Tomás et al., 2010). Various simulation techniques and strategies have been generated (Adams et al., 2005; Sech et al., 2009) and constantly improved (Gringarten and Deutsch, 2001; Zappa et al.,; Tolosana-Delgado et al., 2008; Koehrer et al., 2010) in order to capture the geological heterogeneity observed in the sedimentary record and turn it into an outcrop model. The prevalent modeling technique is called stochastic facies modeling, which applies simulation algorithms to populate facies between data points (White et al., 2003; Aigner et al., 2007; Koehrer et al., 2010). The flexibility to match data input, the relatively short time required for each simulation, and the opportunity to establish a fully automated modeling workflow make stochastic modeling the privileged technique for outcrop and sub-surface case studies. Despite considerable effort devoted to the improvement of stochastic simulation (e.g. Coburn et al., 2006), the experience and knowledge of the modeler still play a crucial role in the quality of the final model (Falivene et al., 2007). The establishment of a suitable modeling strategy designed to reveal the geological heterogeneity observed in the sedimentary record remains challenging for the building of a realistic 3-D geological model for carbonate deposit

CHAPTER 2

Methodology

I described, measured, and sampled several stratigraphic sections sedimentologically.A sedimentary log for each section was established and sampled for each bed to ensure high resolution for the facies model.

The methods used in this study will be separately discussed for field work (data collection) and laboratory work.

2.1 Field Work

2.1.1 Filed Investigation for Sedimentology and Stratigraphy

Detailed sedimentological and stratigraphic investigations were conducted at the Ulayyah Member outcrop analog. Field investigation includes a description of the outcrop facies and the subdivision of the outcrop into beds, bed sets and high-frequency sequences. This step also includes the classification of rocks as reservoir or non-reservoir. The description includes; lithology, thickness, sedimentary structures, lateral continuity and spatial remarks. Then, a sample from every bed was taken for further investigations in the lab. Also, a detailed drawing and photos were made in the field for each sections been used to capture small features that helped in descriptive interpretation.

2.1.2 Sampling

The sampling strategy was dependent on the bed thickness, which could ranges from 10 to 30 cm in the thinner beds in the outcrop and from 60 to 100 cm in the thicker ones. A single

sample was collected from beds less than 30 cm thick. For beds thicker than 30 cm, samples was collected at 30 cm intervals. This sampling system has been conducted to get full coverage of all facies types present in the study area.

2.2 Laboratory Works

During laboratory analysis, all collected samples were slabbed and redescribed for sedimentological investigation. All samples were preserved for thin section analysis and for further microfacies identification. In order to differentiate between carbonate minerals types, thin sections were stained using alizarin red (Dickson, 1996). Interpretation of the depositional environments were based on field and laboratory observations. palaeoenvironmental analysis of macro- and microbiofacies of the outcropping succession of the Ulayyah Member was based on the works Hughes (2004a, 2004b, 2009).

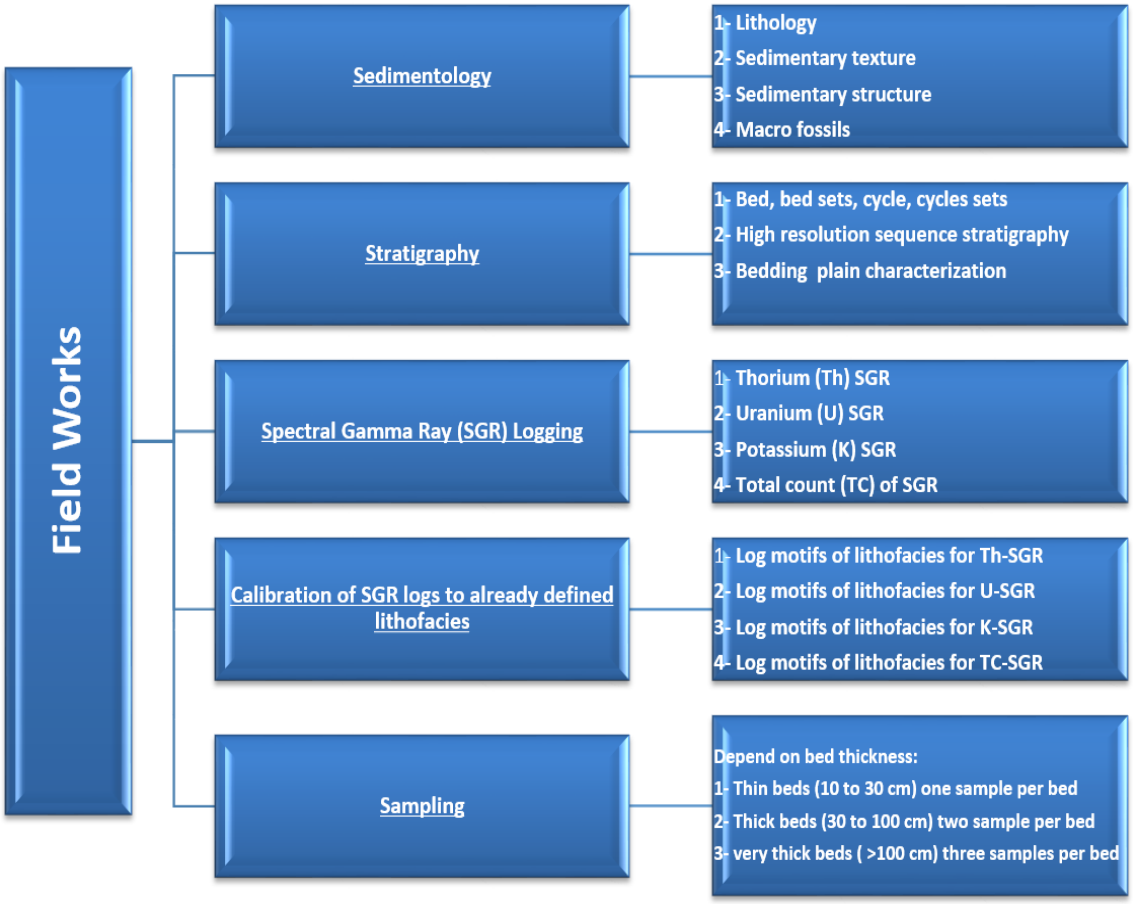

Figure 2.1 field investigation for sedimentology and Stratigraphy.

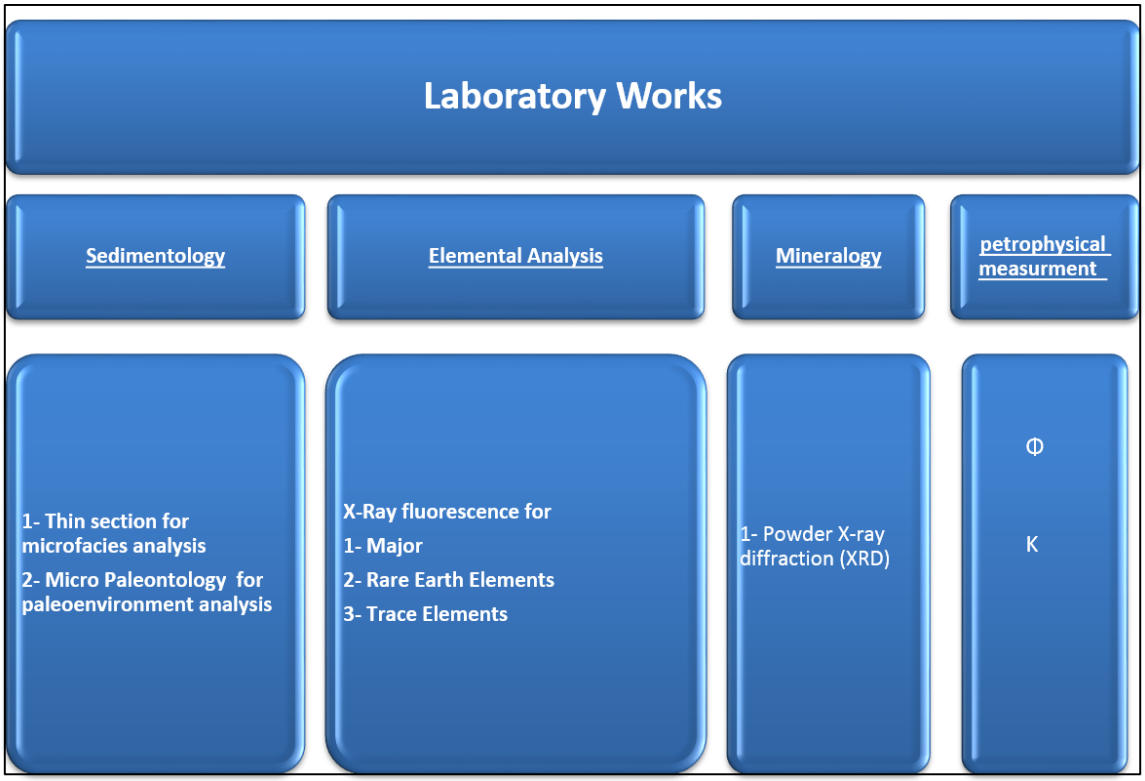

Figure 2.2 Laboratory work flow.

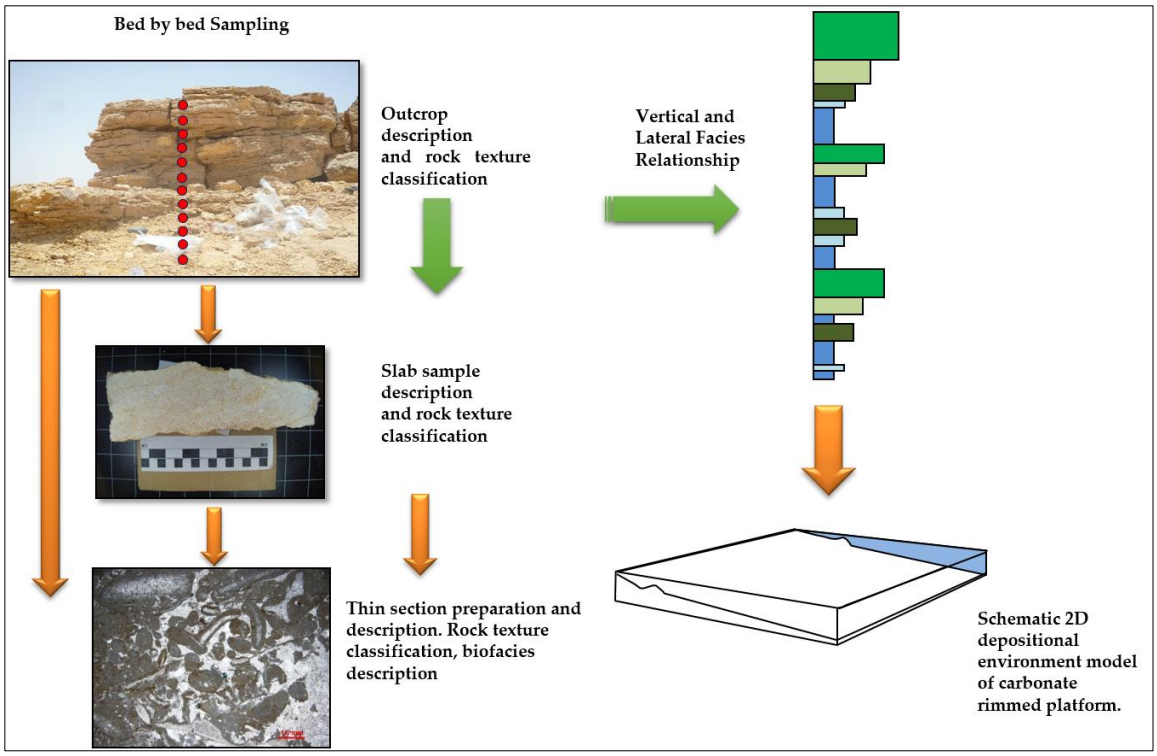

Figure 2.3 Work flow of Lithofacies and depositional environment model based on field and laboratory work.

2.3 Spectral Gamma Ray (SGR) Logging

A spectral gamma-ray (SGR) spectrometer was used to measure the total gamma-ray emissions and the individual levels of uranium, thorium and potassium for each measured sections. The SGR logs for each stratigraphic section been calibrated to lithofacies to develop SGR log motifs for each facies.

The radiation was measured in the field using geophysical 1024-channel gamma-ray spectrometer with BGO detector (Gamma Surveyor)

The SGR readings were collected vertically every 20 cm up the face of the outcrop for each stratigraphic section. The sampling time window was selected after measuring the same point 33 times for durations of 10, 20, 30, 60, 120, 180, and 300 seconds to evaluate reading variability among these time windows. This study used 33 measurements because

populations with 30 samples represent the boundary between small and large samples and have statistical parameter values with low variability that are reasonably representative of the whole population .Among these measurements, the 180-second reading showed the least variability; however, from a practical viewpoint, a minimal sampling time with an acceptable variability is needed.

For this purpose, 3 min were measured per meter along 14 m of the outcrop face for each sampling time. The challenge of proper time window for Gamma Ray measurements in outcrop studies has been discussed by many authors. (Table 2-1).

Figure 2.4 Geophysical 1024-channel gamma-ray spectrometer with BGO detector (Gamma Surveyor).

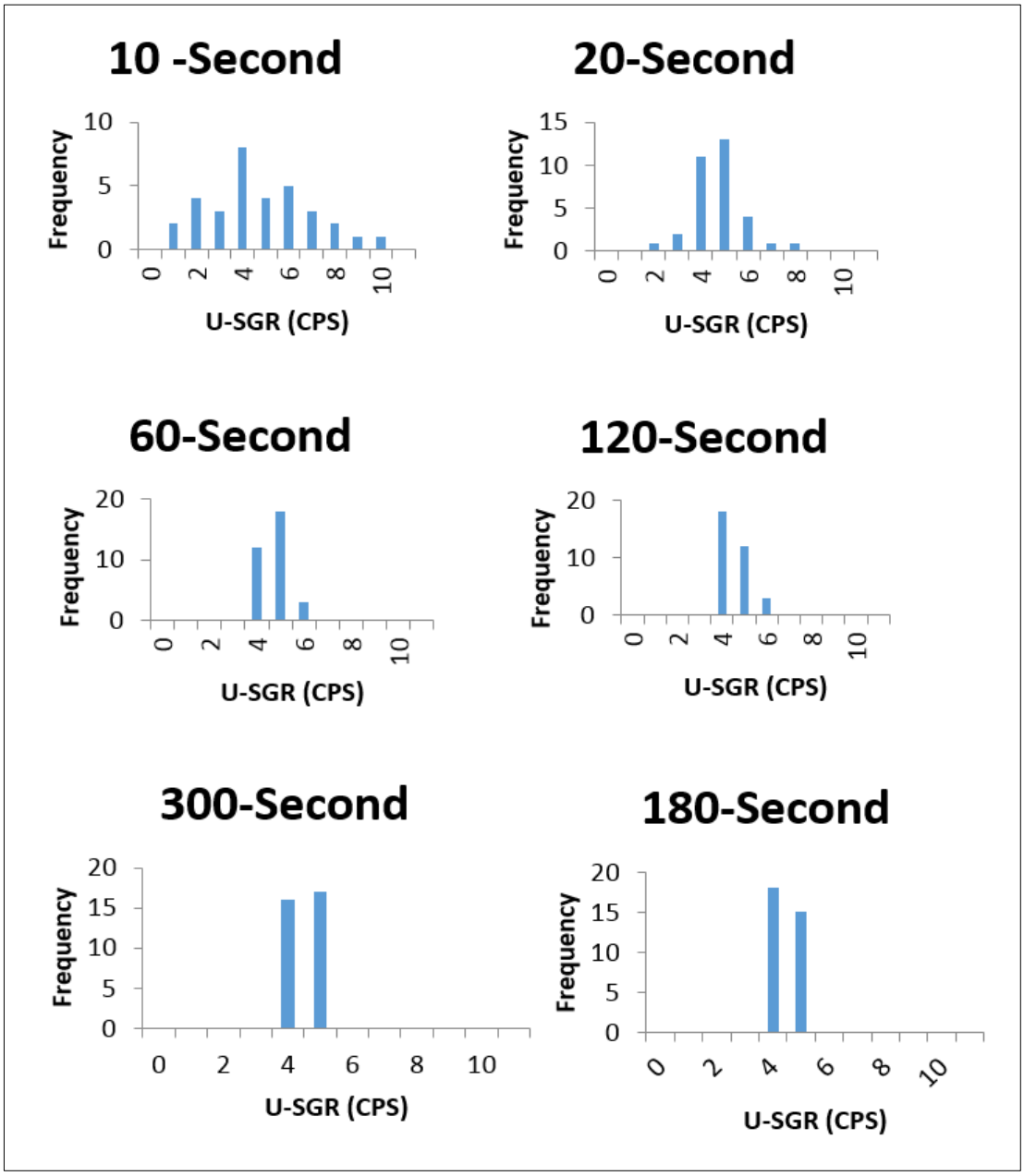

Figure 2.5 Histograms for single-point U-SGR readings using different sampling time windows.

Table 2.1 Literature Summary of Outcrop SGR Logging Validation

	Author-Date	Logging interval (centimeter)	Total interval (meter)	Time Window (Second)
1	Šimíček et al. (2012)	50	20 to 50	120
2	Aigner et al. (1995)	10	36	1,5, and 10
3	Krystynlak (2003)	50	26,64 and 71	60
4	Ridgley et al. (2000)	30	30	90
5	Hladil et al. (2011)	50	280	240
6	Kalvoda et al. (2011)	50 to 100	190	240
7	Svendsen and Hartley (2001)	20	68	120
8	Schnyder et al. (2006)	25-50	107	*
9	Evans et al. (2007)	50	50	1 and 10
10	Collins et al. (2006)	100	100	ni
11	Koptíková et al. (2010)	25	125	120
12	Koehrer et al. (2010)	50	350	15
13	Michael et al. (2012)	50	350	15

2.4 Geochemical Analysis

Out of the 150 samples collected from the study areas, I selected 80 representative samples for geochemical analyses based on bed by bed sampling. These samples represent 6 outcrop profiles in which complete individual sections were sampled and logged by full SGR spectrometry. The samples were selected to cover the whole range of lithofacies in the study area. Specifically the following analyses were conducted

- 80 samples covering 2 stratigraphic sections were studied petrographically
- 80 samples were taken for XRF analysis
- 10 samples were analyzed by Energy Dispersive Spectroscopy (SEM-EDS), and powder X-ray Diffraction (XRD).

2.5 Petrophysical Properties

For all the samples from the outcrop (total number 75), horizontal and vertical plugs were prepared in the laboratory. Each plugs were examined in the saturation apparatus assembly and benchtop liquid and TKA-209 gas permeameter systems to measure their porosity (Φ) and permeability (κ) respectively. Porosity and permeability measurements are important to characterize the geobodies or reservoir units which are relatively highly porous and permeable. The integration between the microfacies analysis from the thin sections and the petrophysical analysis will result in an interpretation for the heterogeneity within the reservoir units. Porosity and permeability were determined for each core plug using the water saturation method. Core porosity was calculated by measuring the weight of dry samples and subtracting the measured value from the weight of the wet samples. Samples are placed in water with known density under vacuum to make sure all the pores are filled with water. Permeability was also measured using the water saturation method by injecting

the water with known properties through the core and measuring the amount of water that goes through the core in different time intervals

Figure 2.6 A, B shows benchtop liquid and TKA-209 gas permeameter for porosity and permeability measurement

2.6 Geostatistical Outcrop Modeling

The geostatistical model was built following the standard surface-based modelling work (Pringle 2006). The model was constructed using 6 stratigraphic sections

A geocellular outcrop model of the study area was build using the data of the Ullayah reservoir analog (e.g. mapped stratal horizons, thickness of layers and sedimentary logs). The stratigraphic sections were assigned to their geo-reference locations, the geographical coordinates for each outcrop section were generated according to the reference GPS data coordinates. Preliminary analysis was conducted on the facies, the petrophysical parameters logs of the outcrop were tested for test normality and other statistical parameters.

the following steps were used are: 1) picking stratal horizons; 2) generation of three-dimensional key surfaces using the interpreted stratal horizons to attain a stratigraphic modelling framework; 3) construction of three-dimensional stratigraphic-structural grid for the geocellular outcrop model; 4) import and upscale sedimentary sections as pseudo well data; 5) populate the geocellular model in the facies modelling .I used Petrel software to construct the Sequential Indicator simulation (SIS) for facies model and Sequential Gaussian Simulation model (SGS) for the property model.

I started creating the final output models of SIS and SGS 20 realizations of porosity and permeability data with importing the $logk$ values into Petrel software in the form of well log data (.ASCII extension), immediately after the top and bottom horizons were determined for the data in relation to each pseudo well depth.

Next step was Gridding; I chose (50*50) for the x and y Directions cells (top, mid and bottom Skeletons). After that I designed the model zones, and suggested 40, 25 and 15 layers for each 3 lithofacies association depending on the sedimentological profile of the outcrop.

The last step was to import the semivariogram parameters to generate SIS and SGS models, then I selected (30912) as a seed number to define the path of realizations in order to generate the models of in Sequential Gaussian Simulation.

Since infinity many of models can be generated I will be showing only the 20 most reliable models in the results section based on their statistics when compared to our data set.

To evaluate the spatial variability of the data one needs to construct an experimental semivariogram which is the basic tool to analyze spatial variability and statistical anisotropy. It is measures the of spatial correlation between data values separated by a

given distance, and reflects the intuitive idea that data values are generally more correlated for short distances than for long distances Spatial analysis was conducted using semivariograms, which were constructed in different directions to determine the major and minor trends of the data variability. The search radius of the semivariograms was one half of the data domain size to minimize the edge effect. Using the resulting semivariograms, a geological interpretation was performed regarding isotropy versus anisotropy, continuity and the internal variability , However, to allow direct hard data conditioning and to include the spatial analysis results (indicator semivariograms for each of the lithofacies types) a SIS modelling method was utilized to model the three-dimensional facies distribution of the Ullayah reservoir analog. In the facies modelling process various methods can be used to generate facies distribution models, such as Sequential Indicator Simulation (SIS) by using indicator variogram.in the property modeling Sequential Gaussian Simulation (SGS) was used with 20 number of realizations.

Figure 2.7 Base map shows the location of outcrop section

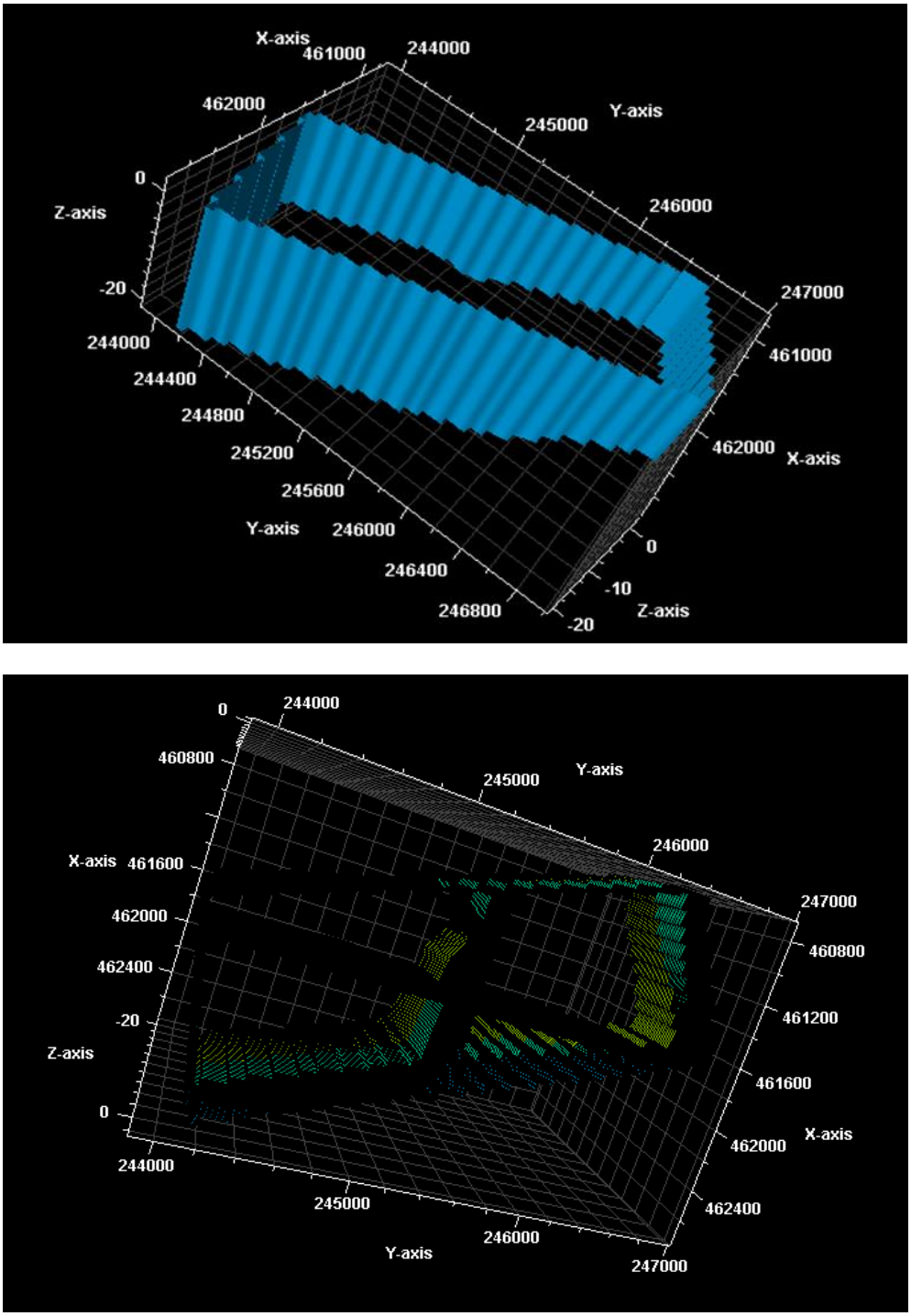

Figure 2.8 The polygon structure (Edges) of our data set models (Different views).

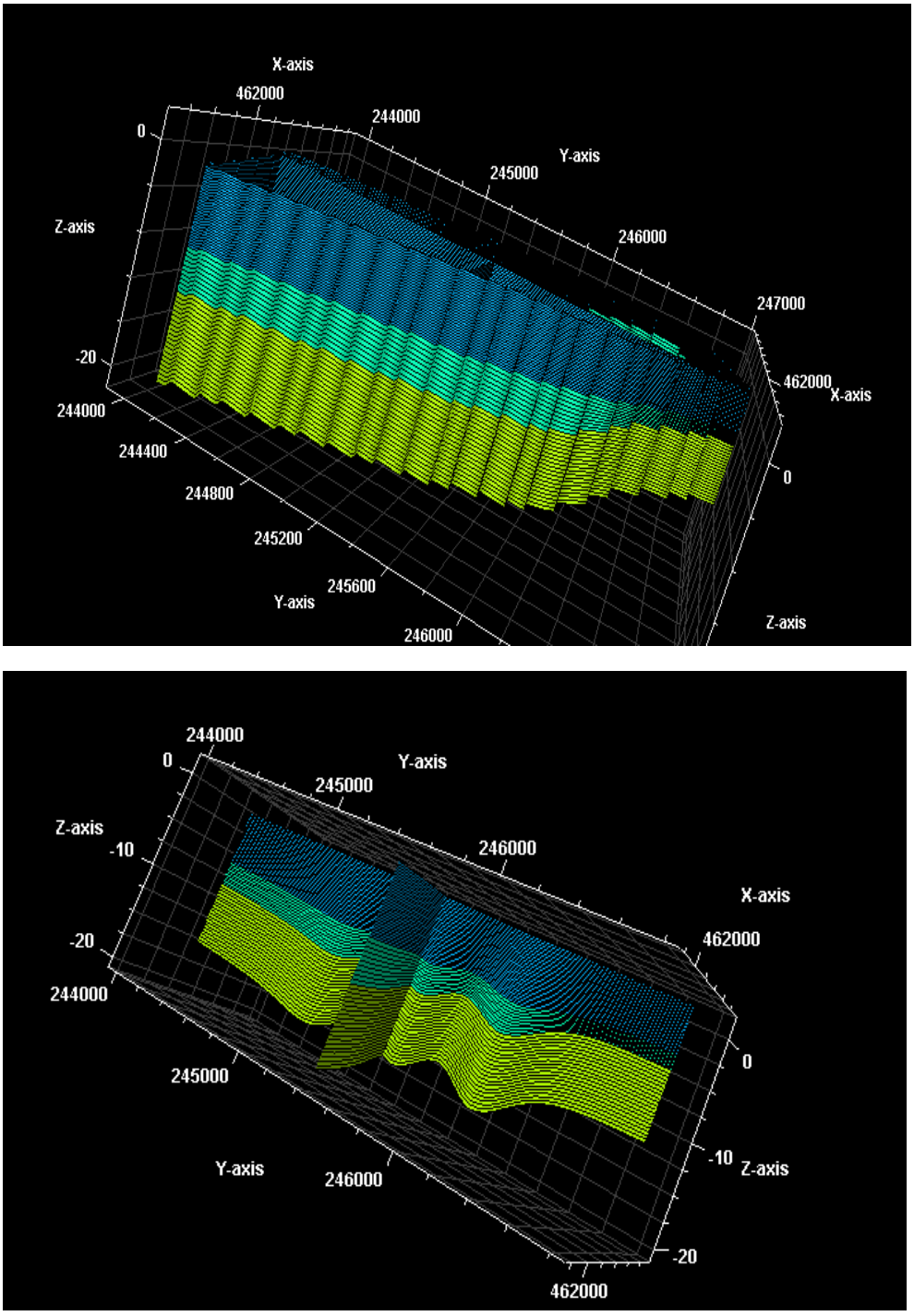

Figure 2.9 Three-dimensional stratigraphic-structural grid for the geocellular outcrop mode

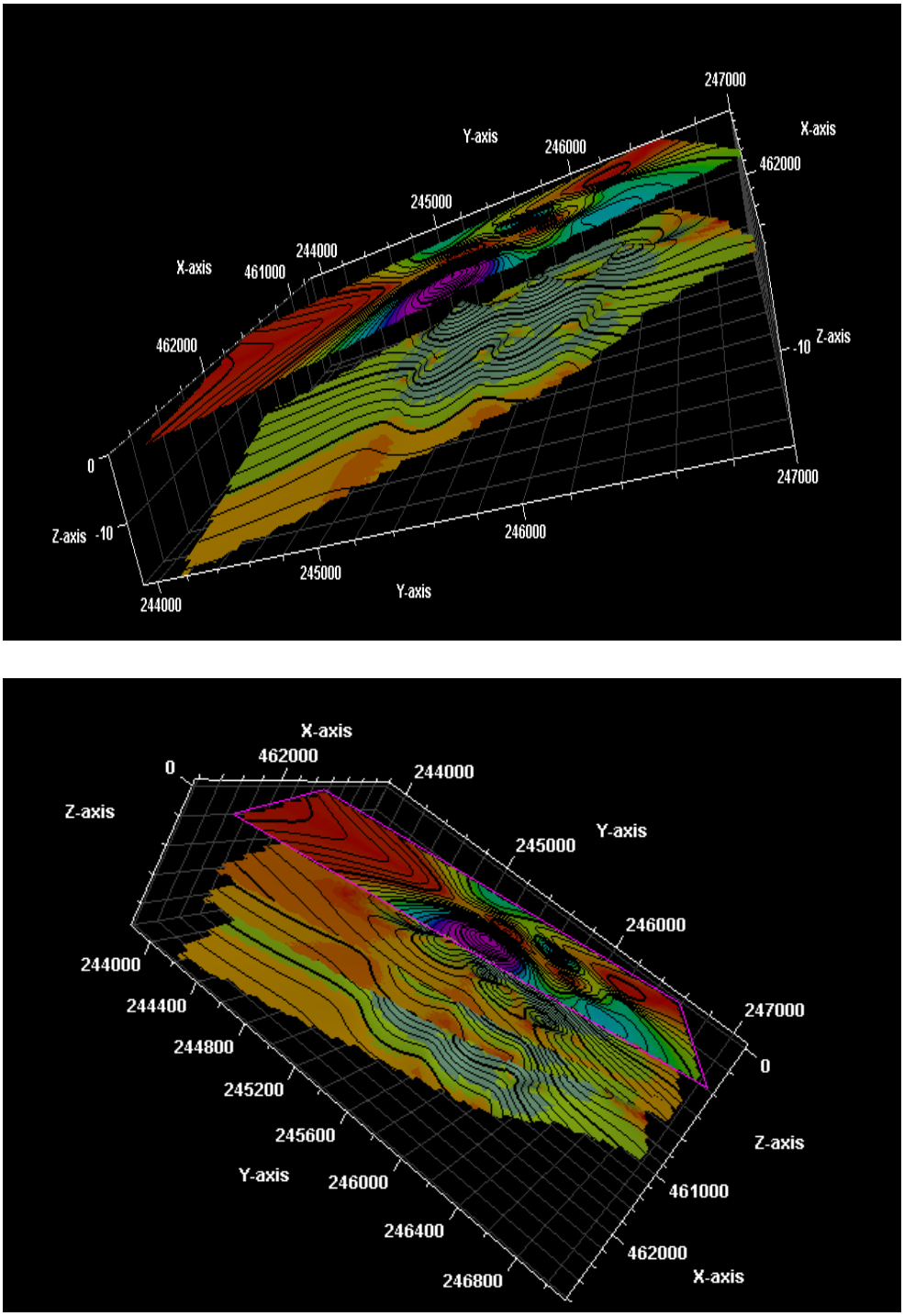

Figure 2.10 The designed top and bottom surfaces of the models

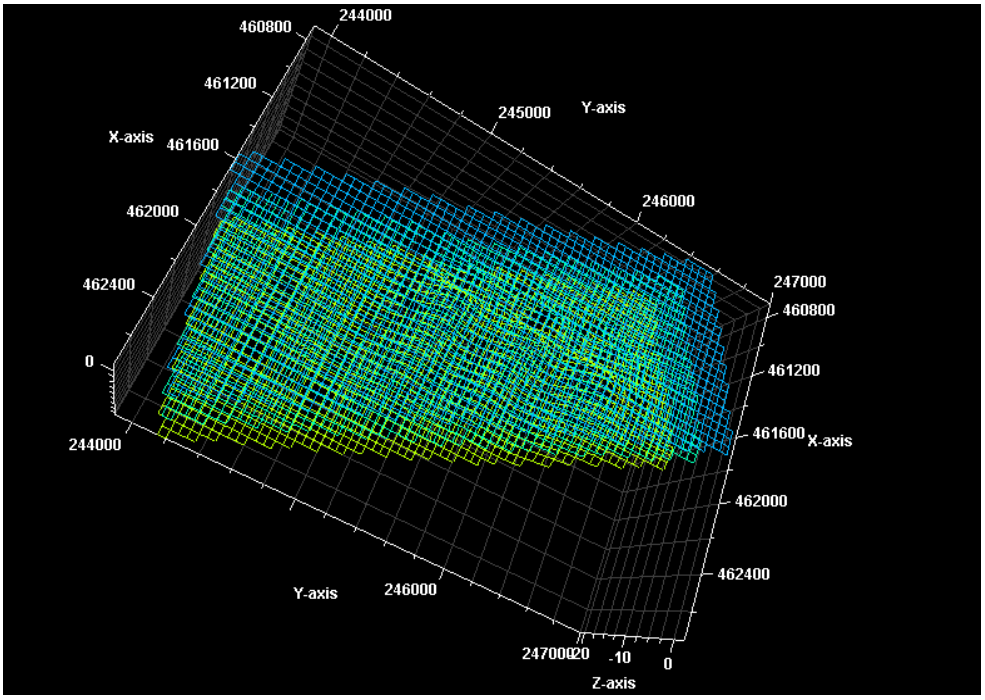

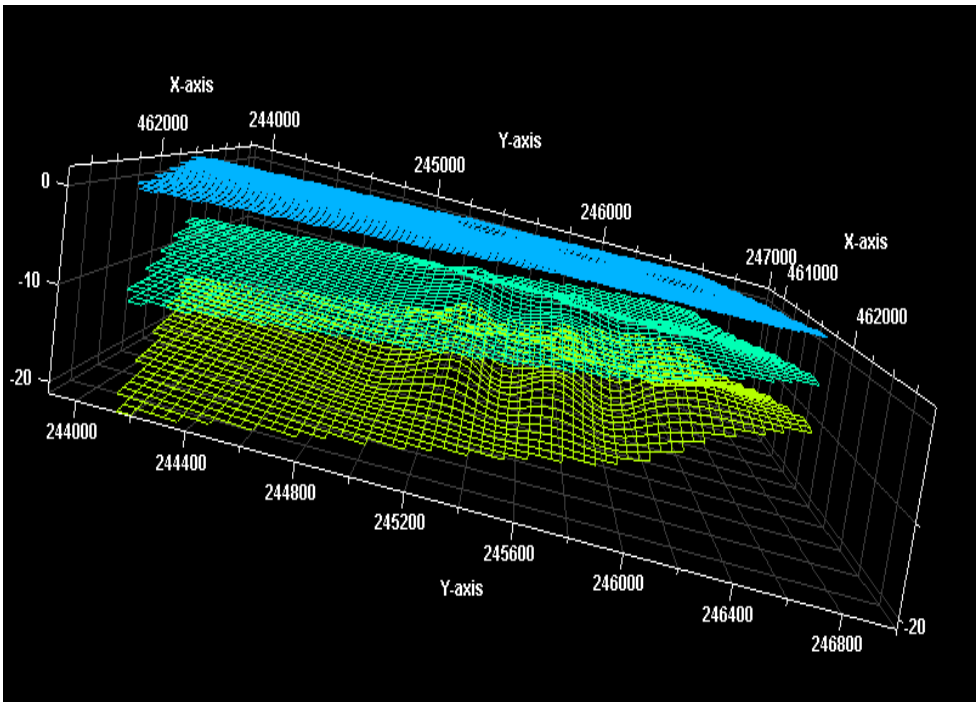

Figure 2.11 The skeleton gridding surfaces of outcrop model (50 × 50) in x, y directions

CHAPTER 3

SEDEMENTOLOGICAL ANALYSIS

3.1 Lithostratigraphy Terminology

The lithostratigraphic units represent the sedimentary strata that conform to Steno's Law of Superposition which states that sedimentary layers are deposited in a time sequence, with the oldest on the bottom and the youngest on the top). The lithostratigraphic units include lithofacies, vertical facies successions and lithofacies tracts that make up the basis of the chronostratigraphic units (Kerans and Tinker, 1997).

3.1.1 Lithofacies

Lithofacies represent three-dimensional rock units recognized for a distinctive set of characteristics such as mineral composition, sedimentary structures, bedding characteristics, allochem types and indicator fossils (Kerans and Fitchen, 1995; Kerans, 1995; Kerans and Tinker, 1997). Each lithofacies includes all the features that reflect specific environmental conditions including, but not limited to, types of carbonate-producing organisms, water depth, water chemistry, latitude, temperature, water circulation, turbidity, sunlight intensity, ρCO_2, nutrient supply and salinity (Wilson, 1975; Hallock and Schlager, 1986; Kerans and Fitchen, 1995; Schlager, 2000, 2003; Pomar and Hallock, 2008).

3.1.2 Vertical Facies Succession

Vertical facies successions represent the typical repetitive, upward-shallowing succession reflecting the filling of the accommodation space created during cycle-scale sea-level rise (Kerans and Tinker, 1997). The described sections of the upper Ullayah Reservoir in terms of high-frequency sequences in the Jabal Abakkayn illustrate the repetition of upward-shallowing cycles where subtidal deposits are capped by shallower subtidal, intertidal strata .Thus, each cycle records the filling of accommodation created during a low-eustatic-amplitude greenhouse Milankovitch setting. Despite the limited evidence, the cycles are capped by exposure surfaces that become conformable when correlated to relatively deeper parts of the succession zone between sea-level and the base of fair-weather wave, can be characterized by skeletal-peloidal shoals, oolitic shoals and/or cryptalgal laminites. Thus, the suite of these facies can be termed as ramp-crest lithofacies tract.

3.2 Lithofacies Description

The fundamental first step in the modern carbonate reservoir characterization workflow is to describe depositional lithofacies and to develop a depositional model for the given stratigraphic/structural setting. As a result, the interpretation of the depositional paleoenvironments has been complicated locally. However, the presence of specific faunal assemblages and preserved sedimentary structures from detailed field (bed by bed) description of 6 sections are sufficient to allow for construction of a detailed depositional model. Below I will detail the key attributes of the depositional lithofacies with brief interpretations of the depositional environments for each

Table 3.1 Summary table of Upper Ullayah Reservior carbonate facies

Facies	Lime-Mudstone	Ooids Grainstone	Massive ,Skeletal Grainstone	Foraminiferal –Grainsone	Peloid grain – Packstone and Grainstone	Strmatoporoid Wackestone/ Packtone	Spiculitic Wackstone	X-bedded sandy greenstones	Fine laminated sandy grainstone
Color code									
Depositional environment	Deep lagoon	Shallow lagoon	Shallow lagoon	Outer lagoon	Shallow lagoon	Outer Lagoon	Restricted Basin	Sand shoal margin	Beach Ridge
Rock type (modified Dunham)	Mudstone	Grainstone	Grainstone	Grainstone	Packstone	Wackstone and Packstone	Wackstone	Grainstone	Grainstone
Mineralogy	argillaceous lime mudstone-calcareous fissile shale	Limestone	Limestone	Limestone	Limestone	Limestone	Limestone	Limestone	Limestone
Grain Type	Pellets , Intraclast mud and peloids	Peloids, Fine ooid, skeletal fragment	Coated grain , peloid , skeletal fragment	Skeletal fragment, Intraclast ,ooids and peloids	peloid , skeletal fragment	Peloid , Stromatopor-oid	Pellets and peloids	Skeletal fragment, Intraclast ,ooids and peloid	Intraclast, fine ooids, skeletal fragment
Fossils	Bivalve ,gastropods ,echinoderm	-	Bivalve , foraminifera	Foraminiferal assemblages	*Thalassinoides* burrows	Cladocropsis , Stromatopor oid	Monaxon and tetraxon	Skeletal fragment dasycladac ean algae (*Clypeina*	Skeletal fragment
Sedimentary Structure	Burrower and mud cracks	Laminated	finely laminated, low angle	-	Burrower, massive	Burrower	-	High angle x-bed	Laminated
Grain Size	Clay – silt	Fine – medium	Fine-medium	Medium – coarse	Medium-coarse	Fine – Medium	Fine	Coarse – medium	Medium - fine
Color	White, gray, tan to dark olive	Light -gray	Tan-gray	Tan	Tan	Tan	Grey-tan	Light -gray	
Reservoirs Quality	None	Inter-skeletal, medium permeability	High interpartical porosity and medium permeability	High interpartical porosity and high permeability	Intra, Microporosity , low permeability	Inter-skeletal ,Moldic Micoporosity , low intrpartical and fair permeability	interpartica l porosity	High interpartical porosity and high permeability	Moldic porosity , micro porosity and high permeability

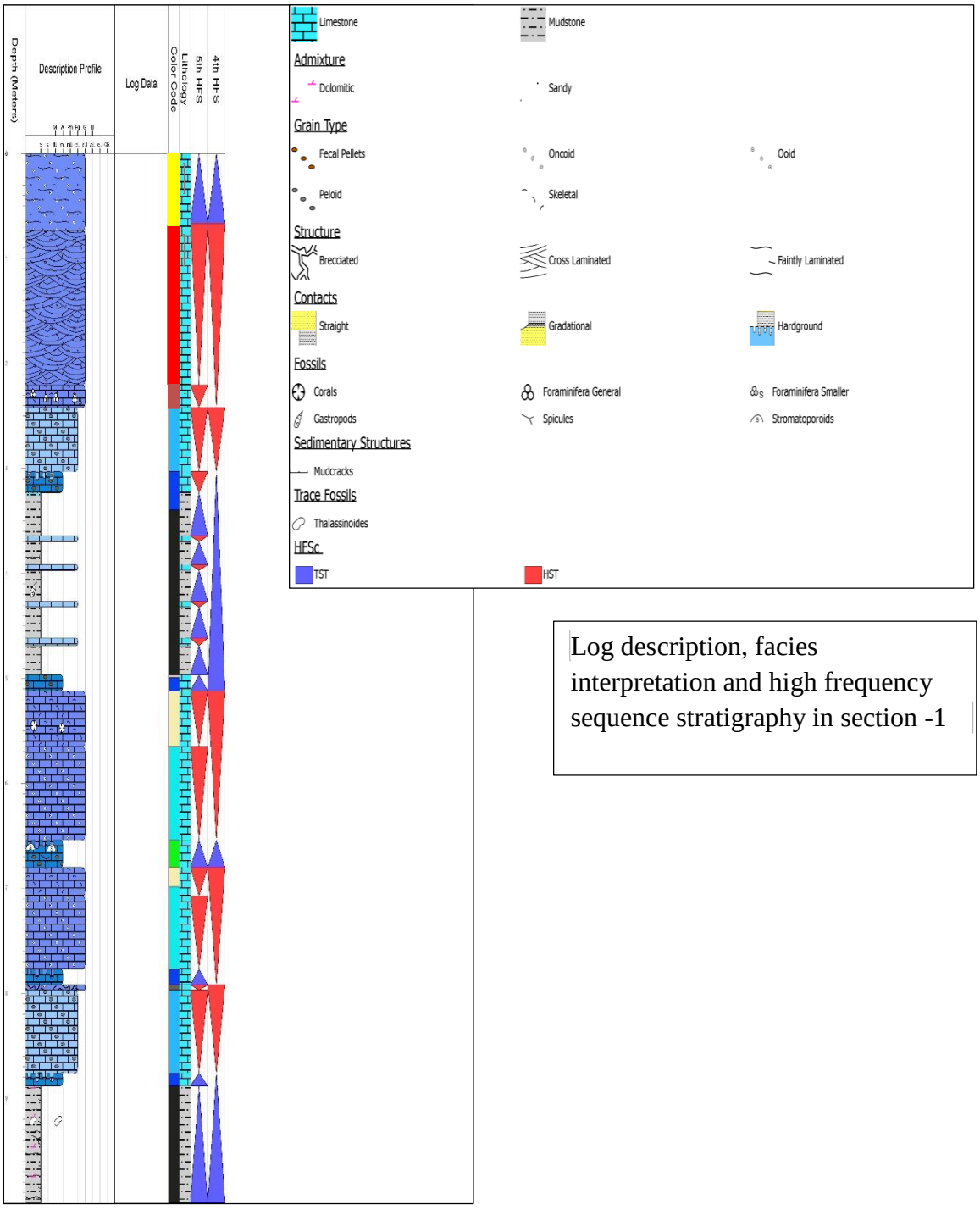

Log description, facies interpretation and high frequency sequence stratigraphy in section -1

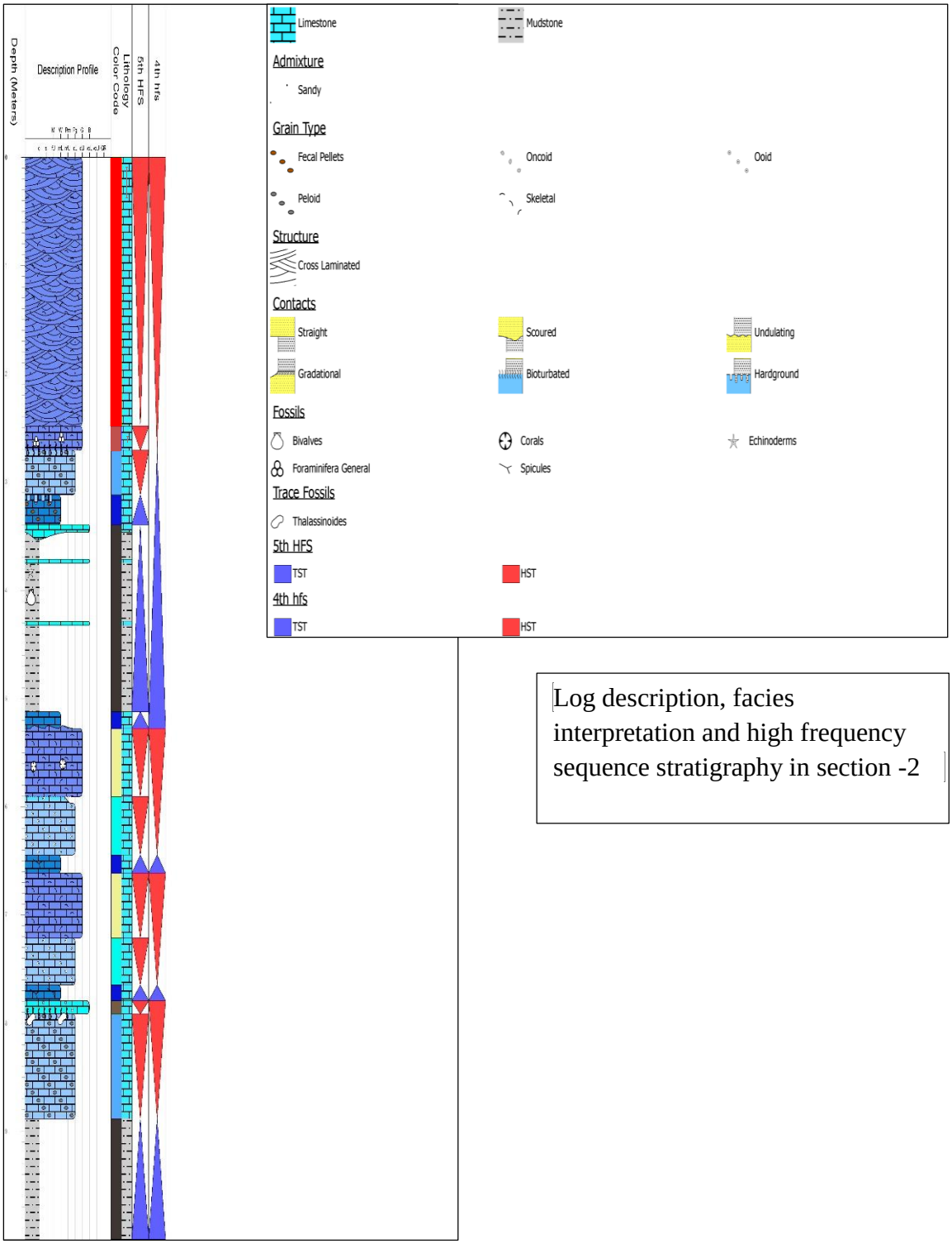

Log description, facies interpretation and high frequency sequence stratigraphy in section -2

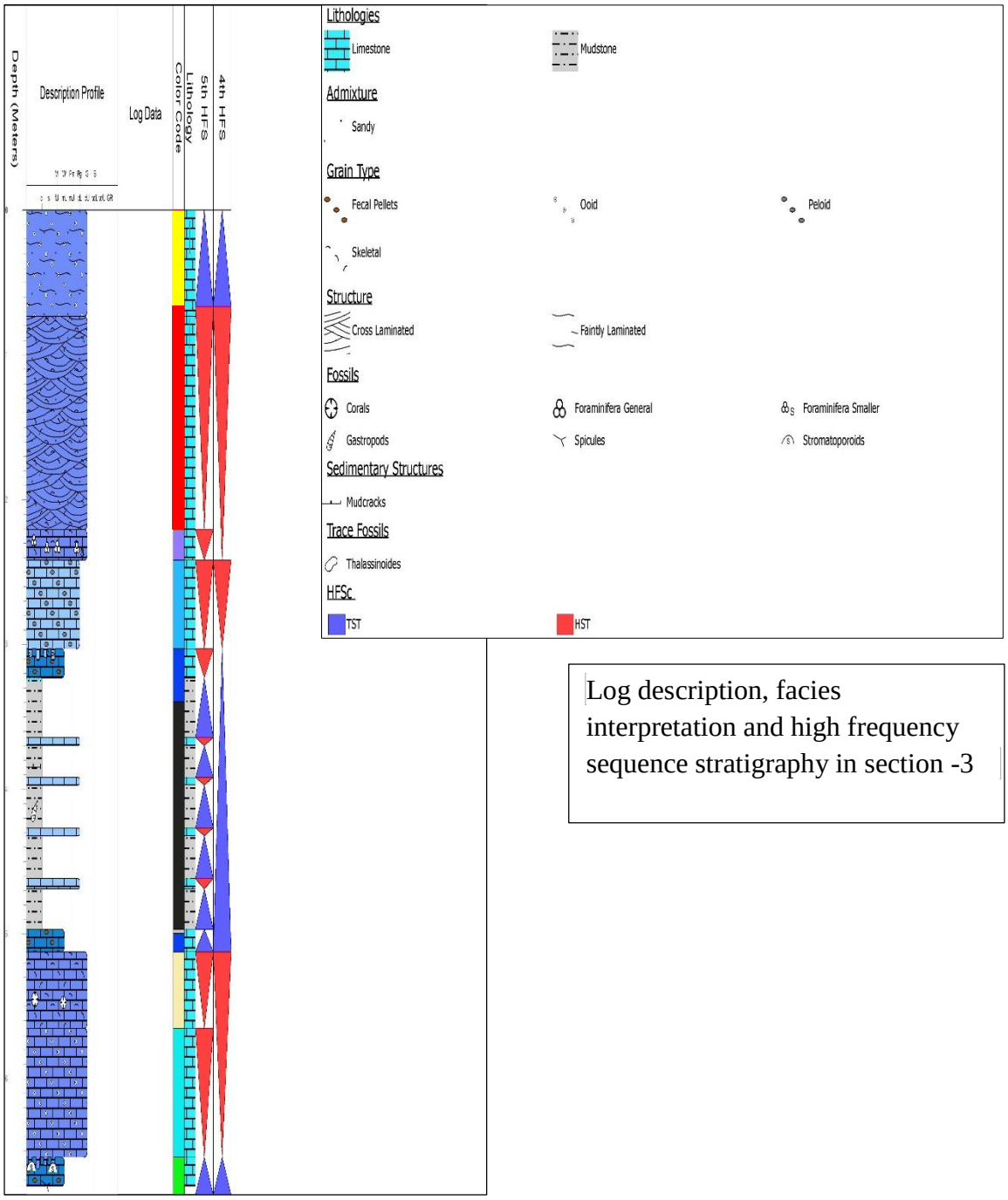

Log description, facies interpretation and high frequency sequence stratigraphy in section -3

3.2.1 Lime mudstone argillaceous calcareous shale

The lime mudstone Lithofacies is present within HFSc-1 and HFS-4 in the upper part of Ullayah Reservoir equivalent, In addition to lime mud, the components of this lithofacies include micritized pellets; brachiopods, bivalves; foraminifera and rare reddened and/or blackened peloids and/or pellets. Bed thickness ranges from 30-200 cm with mostly sharp hardground or firmground caps. This lithofacies is characterized by heavy bioturbation that, generally, churns the sediment and becomes more distinct, filled with grainier sediment infills, and preferentially dolomitized toward the hardground caps.

When this lithofacies is not interrupted by bioturbation, original horizontal to slightly inclined to undulated laminations, commonly attributed to the size difference between mud and micro pellets are preserved. Rare hummocky cross-stratification (HCS) to swaley bedding marks this lithofacies. This facies also shows rhythmic succession of calcareous fissile shale graded to argillaceous lime mudstone and ended by pebbly large grain intraclast mud. The shales also shows shrinkage mud cracks and discontinuous layer of diagenetic gypsum.

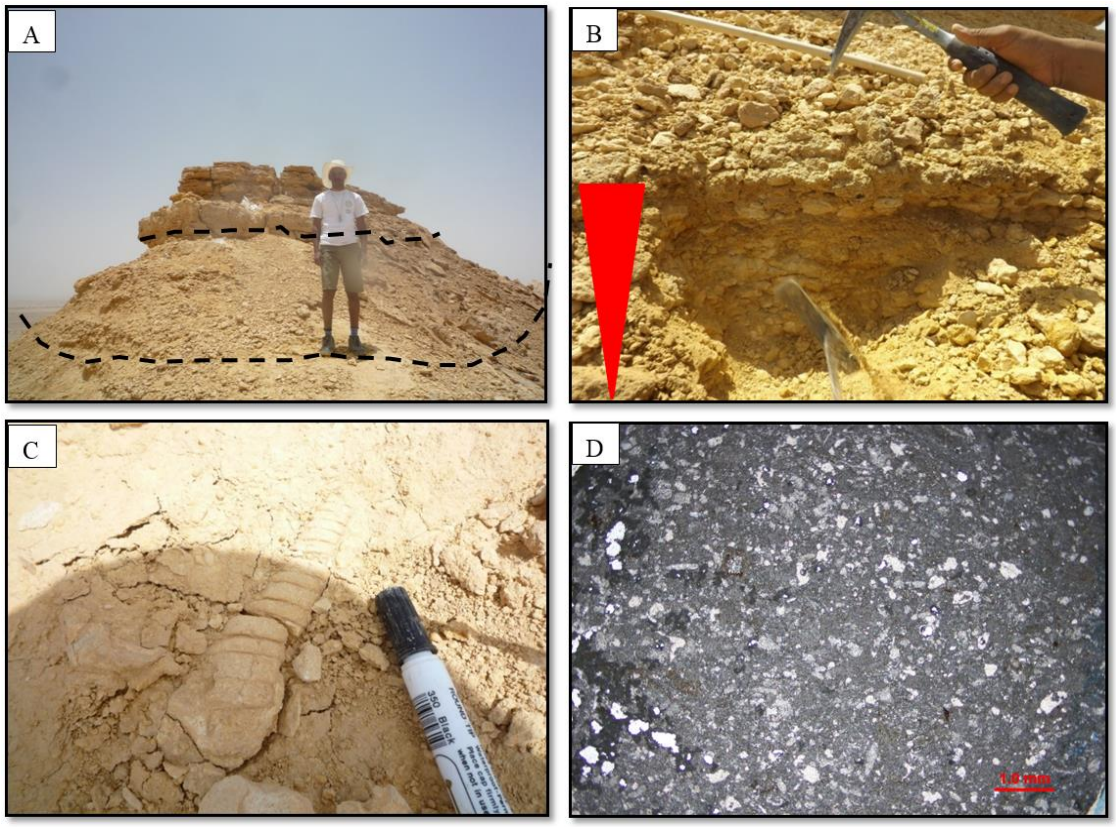

Figure 3.1 (A) The outcrop photograph is typical of the lime mudstone lithofacies (B) rhythmic succession of calcareous fissile shale graded to argillaceous lime mudstone and ended by pebbly large grain intraclast with mostly sharp hardground or firmground caps and transitional bases.This lithofacies is characterized by heavy bioturbation that, generally, churns the sediment and becomes more distinct, filled with grainier sediment infills, and preferentially dolomitized toward the hardground caps. Some large fossil have been documented as (C) bivalve, brachiopods and echinoderm .the microphotograph (D) shown mm scale lamination with no porosity.

3.2.2 Burrowed skeletal wackstone

The spiculitic wackestone forms thin (5-60 cm) beds of homogeneous grey-tan color. The spiculitic wackestones typically form the base of the Upper Ullayah Reservoir Equivalent shallowing succession and are then succeeded by burrowed skeletal packstone. The main allochems within the spiculitic wackestone are 45-125 μm monaxon and tetraxon sponge spicules of siliceous Demospongia (Clarkson, 1998; Flugel, 2004; Hughes, 2004). The silica is commonly dissolved leaving moldic porosity (2-8%) which later may be cemented by blocky calcite.

The predominance of mud and a monospecific faunal assemblage is indicative of a stressed, low energy setting interpreted here to be a restricted environment. A distinct subfacies of the spiculitic wackestones is represented by thin (5-20cm) beds of darker, skeletal wackestone that is most obvious on the wireline logs as distinctive 5-40 cm thick high API gamma count intervals. These beds are highly traceable and appear to represent short-lived anoxic events within the overall disaerobic deeper water section. These beds combined with the more abundant spiculitic wackestones may represent productivity cycles in the deeper lagoon environment. These lithofacies shows horizontal, non-branching burrows *Planolites* in association with the absence of other open marine faunal assemblages suggests that these lithofacies were deposited in a stressed environment deep lagoon where circulation was diminished, likely resulting in elevated salinities and reduced oxygenation. *Planolites* wackestones are interpreted as cycle-scale flooding events and result in a significant increase in gamma ray response (Raspini, 2001)

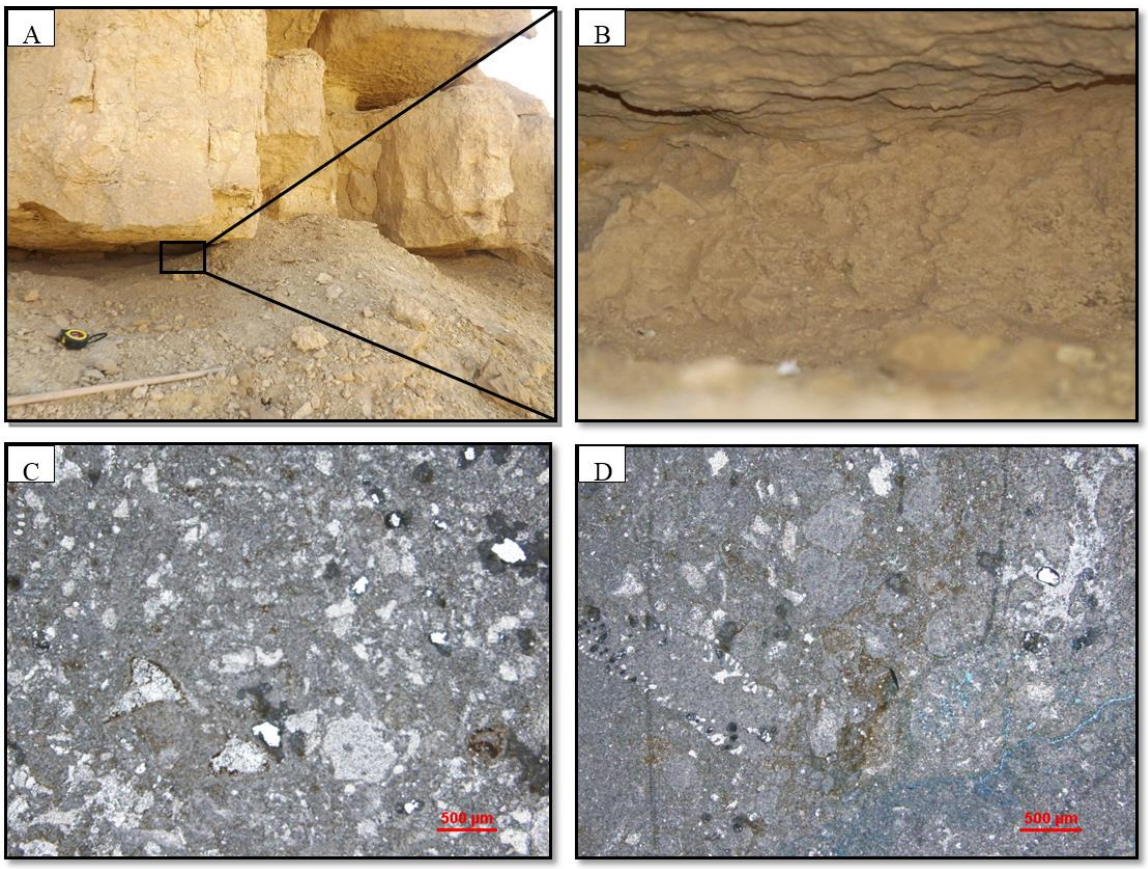

Figure 3.2 (A,B) the outcrop photo is typical of this lithofacies and shows spiculitic wackestone .The photomicrographs C and D shows dissolve Tetraxon (T) and Monoxon (M) crated moldic porosity that may be filled with calcite ,kurnubia (K) and Lenticulina (L) indicative deep water condition

3.2.3 Burrowed skeletal peloidal packstone

The burrowed bioturbated peloidal mud dominated packstone consists of 135- 150 cm thick coarsening upward beds where *Thalassinoides* burrows are found at the base. The peloidal packstone lithofacies is differentiated from the overlying skeletal grainstone by the absence of current stratification and from the underlying wackestones by the predominance of peloids. Both the upper and the lower contacts are gradual, where the upper contact marks the base of wave influence and the lower contact marks the increase of environmental stress indicated by the monospecific sponge fauna. The decrease in mud content and the increase of faunal diversity from the underlying beds are indicative of a relatively higher energy

depositional setting. In addition, the higher energy, associated with the increase of open marine fauna and *Thalassinoides* burrows, suggest a better oxygenated shallow marine environment, and it is thus interpreted as shelf lagoon open circulation deposits within the fair-weather wave base (Pemberton et. al, 1992; Taylor and Gawthorpe, 1993). These distinct burrows, associated with hardgrounds, are subsequently referred to as hardground burrows. The hardground burrows are sometimes outlined with oxygenation halos and occasionally are dolomitized. In addition, due to their development in the seaward of shelf crest, they are protected from storm influence and hence the absence of any tempestite. The base of peloidal lithofacies is marked by a distinctive gamma ray log response with a consistently higher API reading compared to the overlying skeletal grainstone.

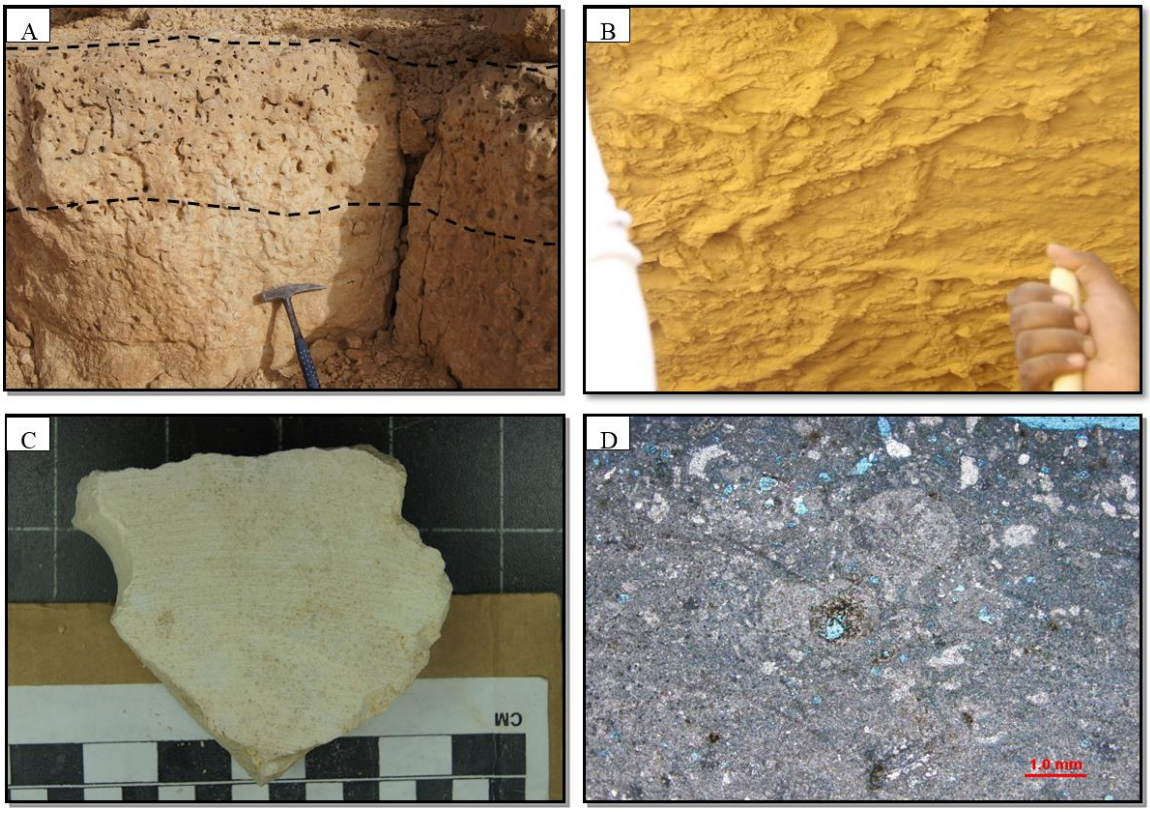

Figure 3.3 (A) Outcrop photograph of is typical of this litofacies shows the firmgrounds that are characterized by color alterations and terminated burrow tops against the firmground surface. Angular to subangular mudclasts rest on top of the hardgrounds. Other sedimentary structures include (B) burrowing (Thalassinoide) at the base, graded bedding, (C) horizontal laminations, and rare hummocky and/or swaley cross-stratifications. (D) The porosity types present in this lithofacies are interparticle, intraparticle, and microporosity.

3.2.4 Oncloid fossiliferous intraclast grainstone

The brownish to yellowish color, calcurdite, skeletal-oncolitic-intraclastic grain-dominated packstone lithofacies overlies the skeletal fragment highly pored grainstone lithfacies with sharp boundary. Bed thickness ranges from 30-40 cm with sharp hardground or firmground bases. This facies is present in the lower part of Upper Ullayah Reservoir Equivalent and is composed of oncolitic and/or intraclastic rudstones and floatstones with matrix textures ranging from wackestone to grain-dominated packstone. The components in this lithofacies are extremely poorly sorted and include angular to subrounded intraclasts, oncoids (marked by coating development around intraclasts and skeletal fragments)

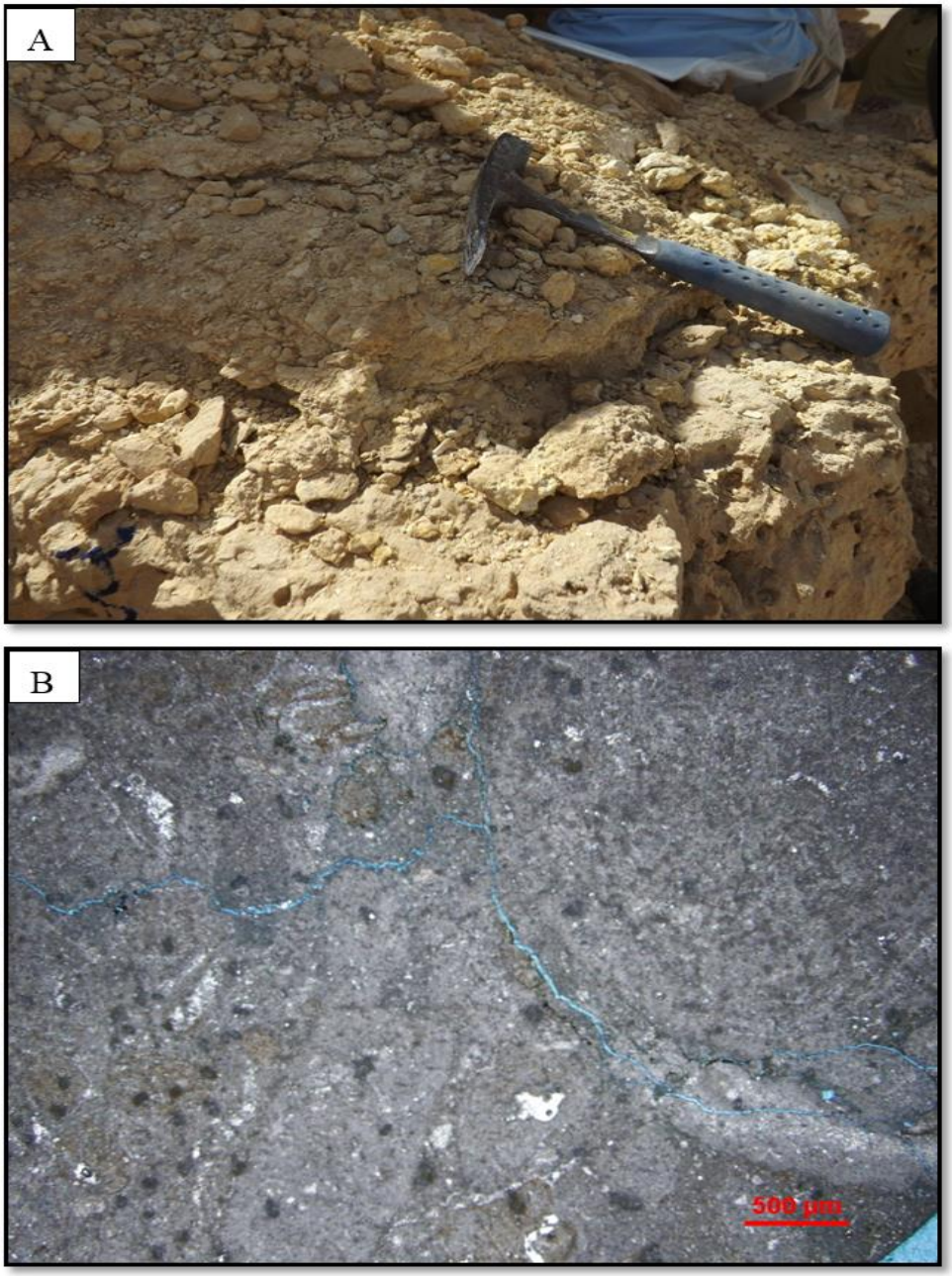

Figure 3.4 (A) Typical outcrop lithofacies highly pored grainstone lithfacies with sharp boundary.(B) thin section shows large skeletal peloidal with grain dominated packstone

3.2.5 Fine grain oolitic skeletal dominated grainstone

The skeletal fine grain-dominated grainstone consists of 40-45cm thick units that are planar stratified but weakly bioturbated. The upper contact is gradational with overlying massive coated -skeletal grainstones, bioturbation is reduced significantly; while the basal contact of this lithofacies with the wackstone lithofacies is recognized by increase of current stratification, marking the lower limit of fair-weather wave base. This lithofacies is composed of abundant shallow marine skeletal allochems, includes rare echinoderms, bivalves and brachiopods, up to 10% lime mud, fine grain ooids (15-40%) represent the dominant non-skeletal allochem. The gamma ray log response shows slightly higher API readings compared to the overlying skeletal grainstone especially if they are representing flooding events marking the base of depositional cycles.

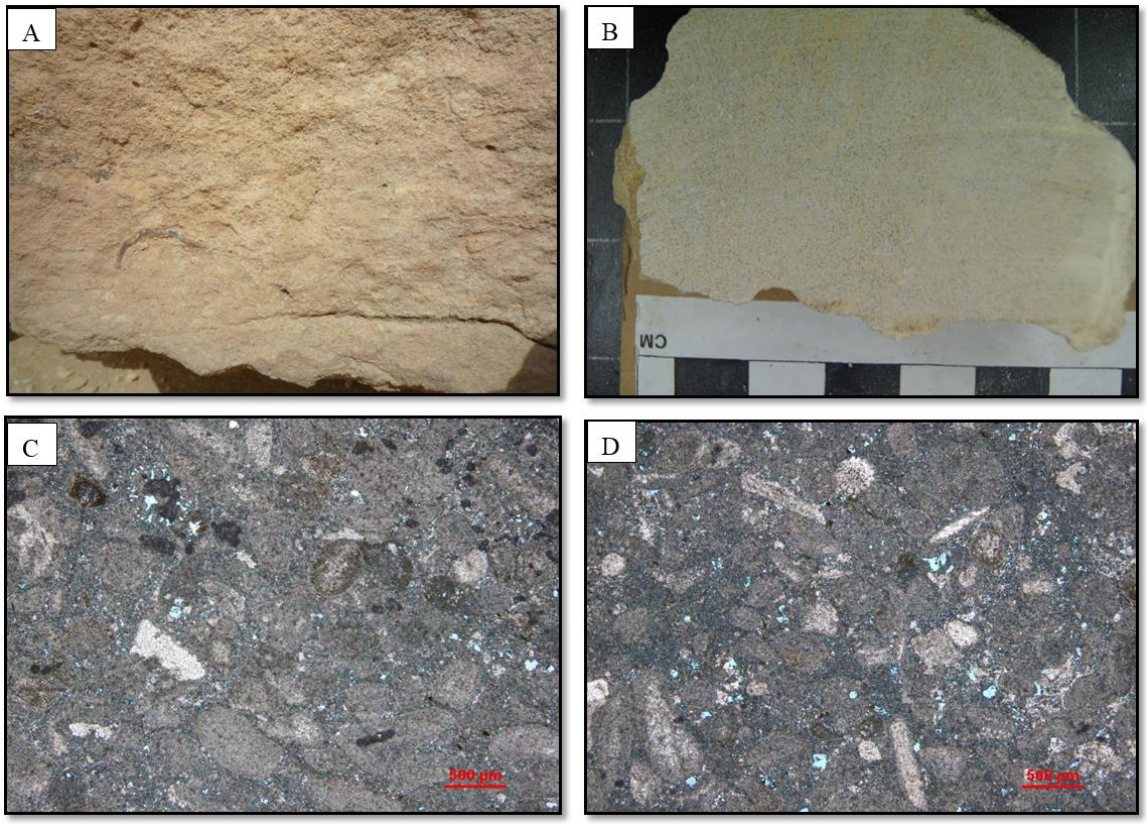

Figure 3.5 The skeletal fine ooid grainstone is composed of abundant open marine skeletal allochems, include rare echinoderms, bivalves and brachiopods. While the fine grainstone lithofacies constitutes peloids (15-40%) represent the dominant non-skeletal allochem

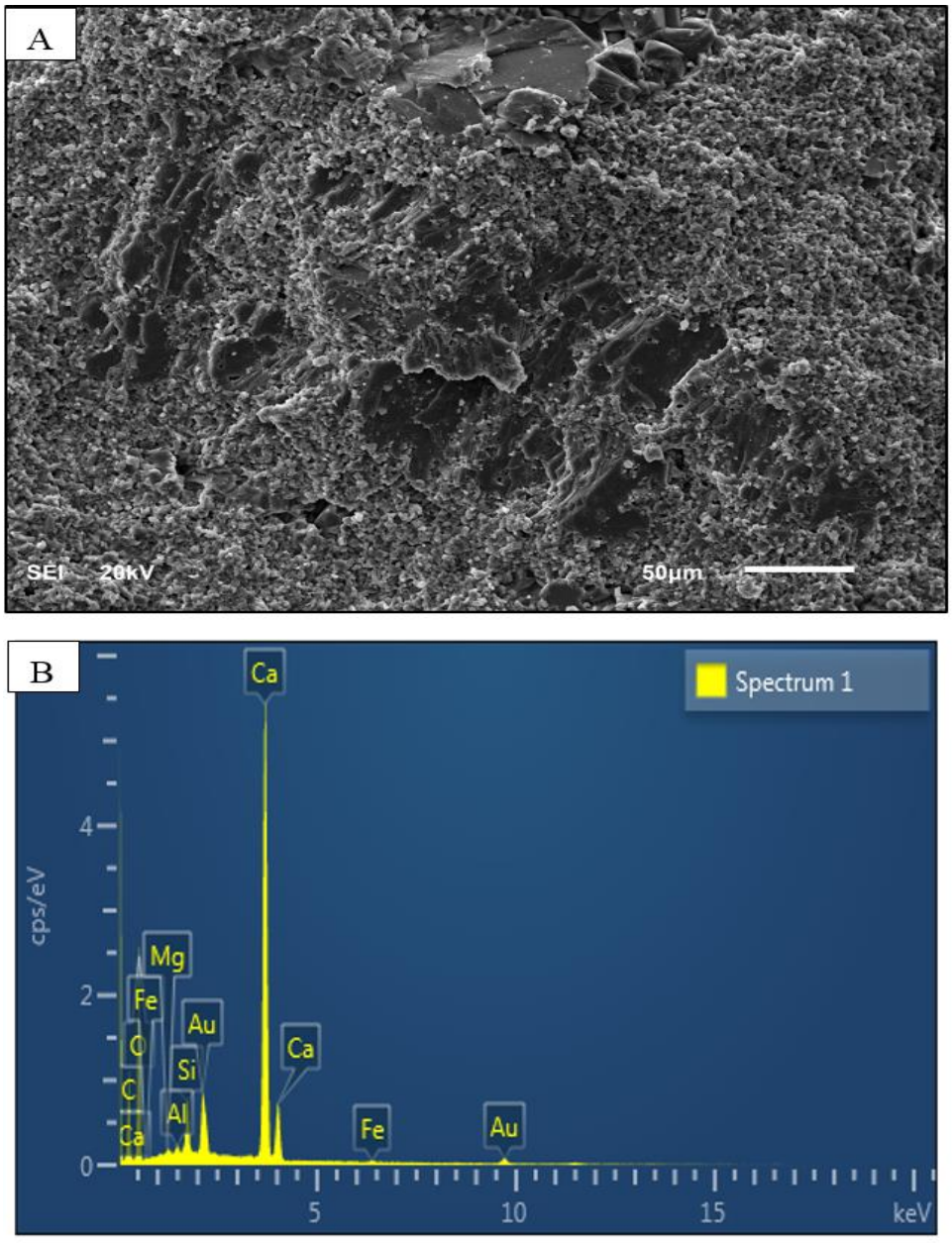

Figure 3.6 SEM and EDS of the oolitic skeletal grainstone

3.2.6 Massive skeletal intraclast grainstone

This facies consists of white to tan gray calcarenite massive unstratified beds, horizontal lamination, low-angle cross-stratification, bioturbation, medium to coarse grain-dominated intraclast packstone, and grainstone .Grain types include coated-grains, peloids, and was

partially cemented with early marine isopachous cement and is composed of medium sorted, well-rounded to rounded, fine to medium grained skeletal-peloidal, grain-dominated grainstone .These can form in beds from 45 to 80 centimeter thick. Bivalve fragments, fragmented micritized, and foraminifera are among the components present in this lithofacies

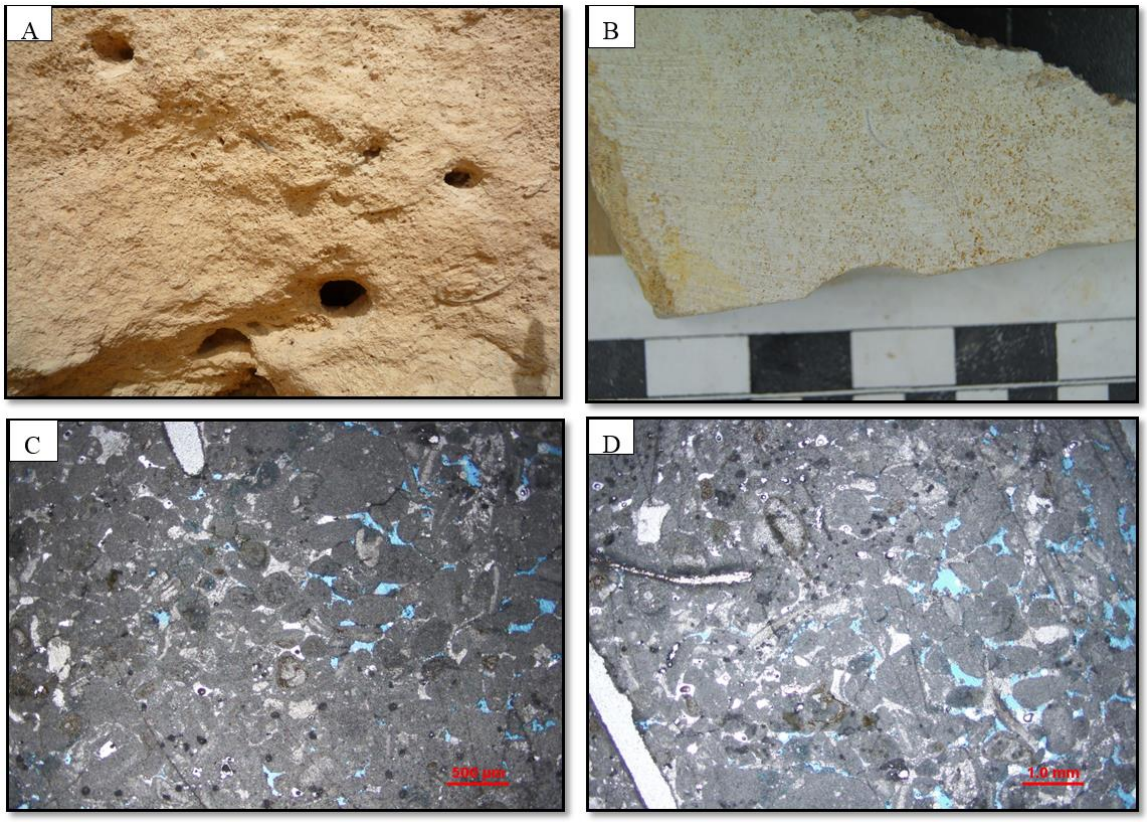

Figure 3.7 (A)Low-angle cross-stratifications, rounded, sorted, and winnowed components (B) skeletal fragments and intraclast that are characteristics of the massive skeletal lithofacies indicate an increase in hydrodynamic energy and an increase in sorting and abrasion ability as the lithofacies belts continue shallowing toward the shoreline.(C and D) microphotograph showing good inter particle porosity cemented partially by isopachous cement.

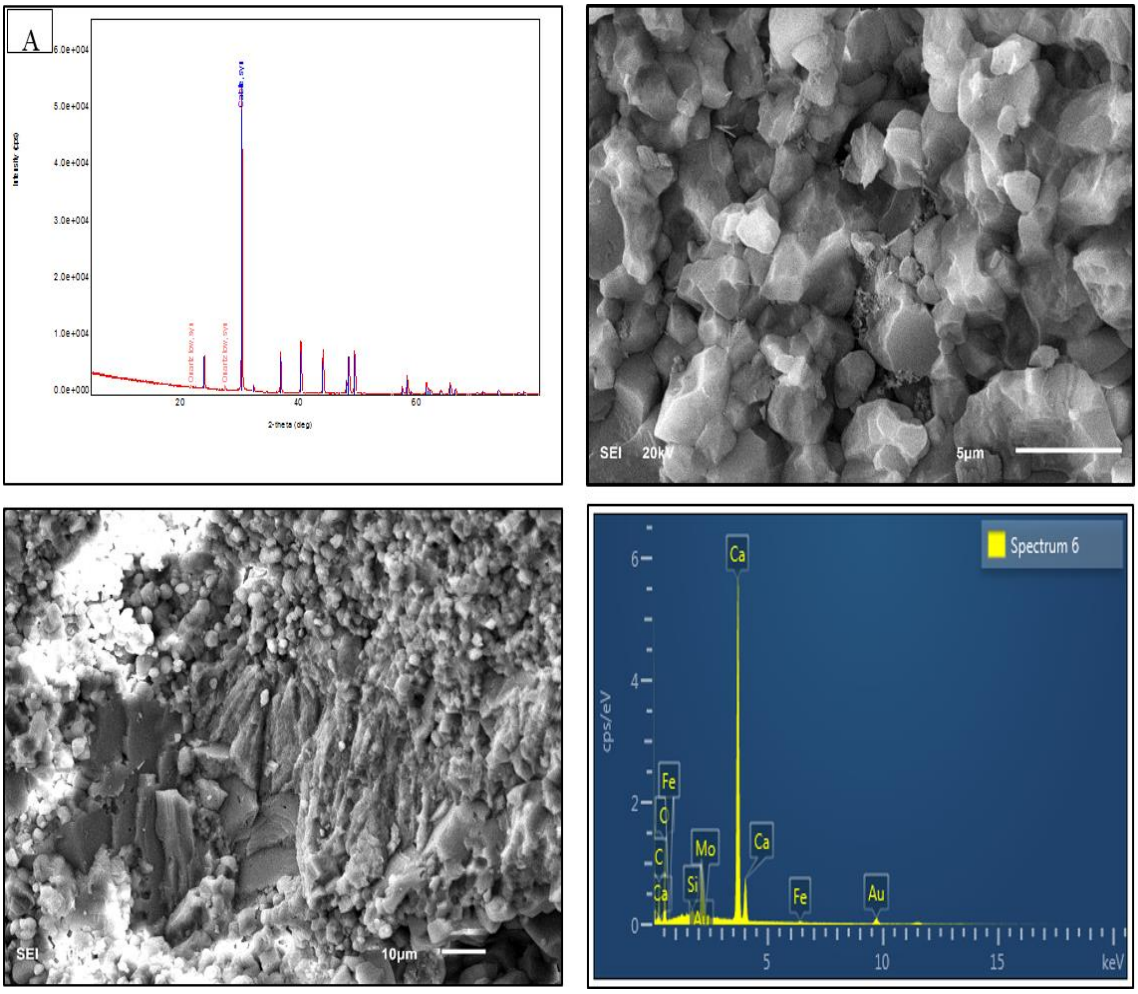

Figure 3.8 shows XRD, SEM and EDS of massive grainstone lithofacies

3.2.7 Stromatoporoid-Cladocropsis wackstone/packstone

These are highly weathered friable, strucureless, whitish to tan colored and are composed of *Cladocoropsis* and encrusting stromatoporoid, batches of scattered of coral reef with less common sponge spicules. The underlain contact of this facies is erosive with collapse and talus of poorly sorted calcareous lime interbedded with carbonate argillaceous lime mudstone and cut by scoured channeled of heavy pored skeletal calcarenite intraclast. These facies are generally 50-70 cm thick and are composed of floatstones and rudstones with matrix textures ranging from wackestone to mud-dominated packstone. The

components of this lithofacies are very poorly sorted, with a wide range of grain sizes from fine sands to pebbles. The components include mostly displaced domal and encrusting stromatoporoids with little of pellets, peloids and intraclast. The lithofacies contains scattered stromatoporoid fragments that are not build up, suggesting that the depositional setting of the stromatoporoid is storm reworked mounds and not an in-place reef, this lithofacies occurs at the mid of HFSc-4 and underlies the massive grainstone section.

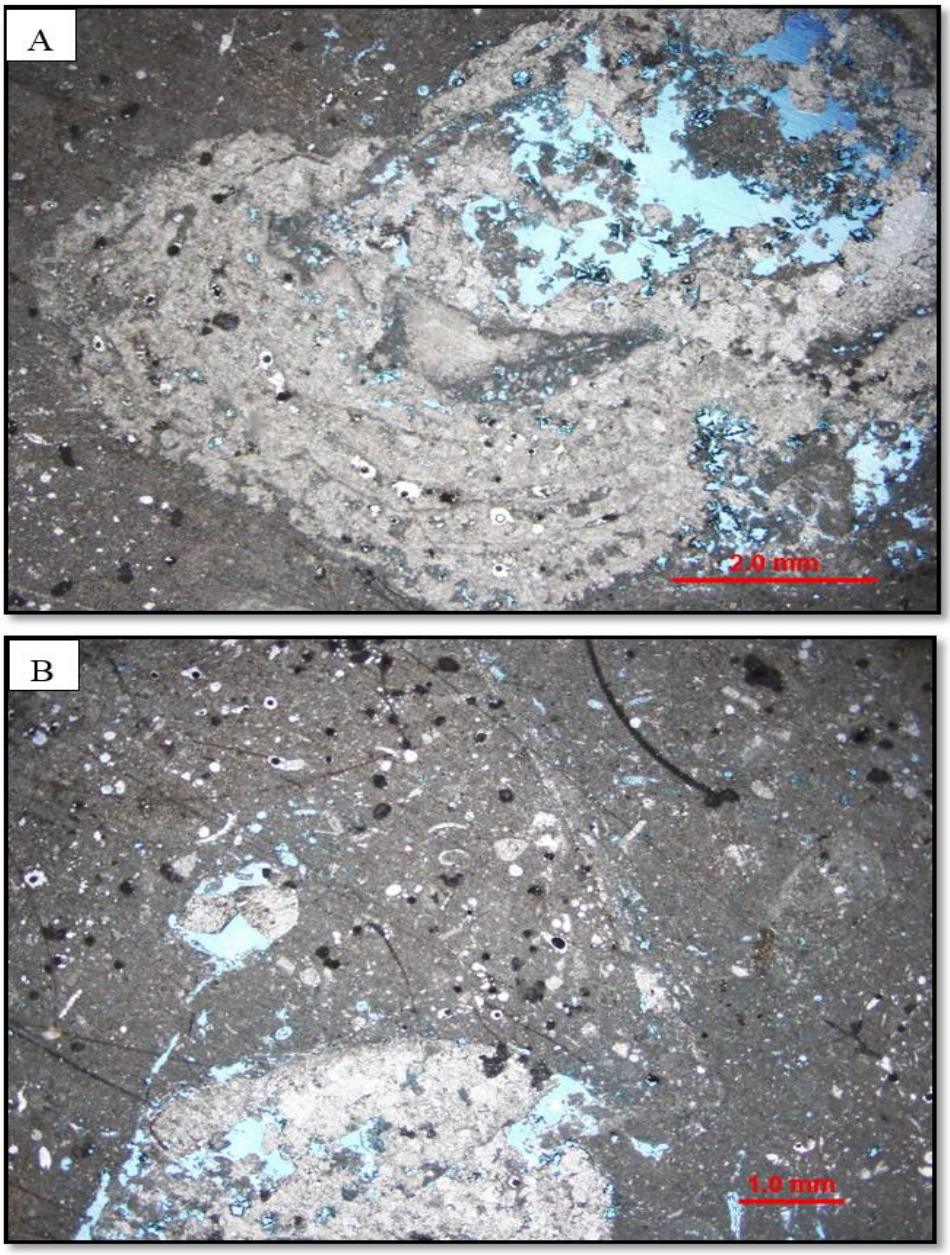

Figure 3.9 (A)Cladocoropsis and encrusting stromatoporoid lithofacies .(B) The components of this lithofacies are very poorly sorted, with a wide range of grain sizes from fine sands to pebbles nodular and dendroid Cladocoropsis (calcified sponge) mud-dominated packstones andwackestones in addition to floatstones

3.2.8 Foraminiferal skeletal grainstone

Units of the peloid-skeletal grainstone lithofacies range in thickness from 60-80 cm and represent the most abundant shallowing setting among the lithofacies. These grainstones display bioturbation and burrowed fill with coarse material. The upper contact of the grainstone lithofacies with the x-bedded skeletal grainstone is gradual, reflecting progressive shallowing and restriction. Also, the lower contact of the skeletal grainstone is gradational but it is characterized by gradual loss of energy with an underlying unit of Stramatoporoid wack/packstone.The main non-skeletal allochems in the peloid-skeletal grainstone are peloids (30-50%), with accessory ooids (<8%).These grainstones contain a diverse assemblage of skeletal allochems including common foraminifera (*Pfenderina, Redmondoides, Valvulina, Mangashtia, Nautiloculina, Miliolid*) dasycladacean algae (*Clypeina and Salpingoporella*) and *Thaumatoporella*. Accessory skeletal grains include echinoderms, bivalves and brachiopods.Several diagenetic overprints including, cementation, dolomitization and compaction may significantly decrease the original depositional porosity.

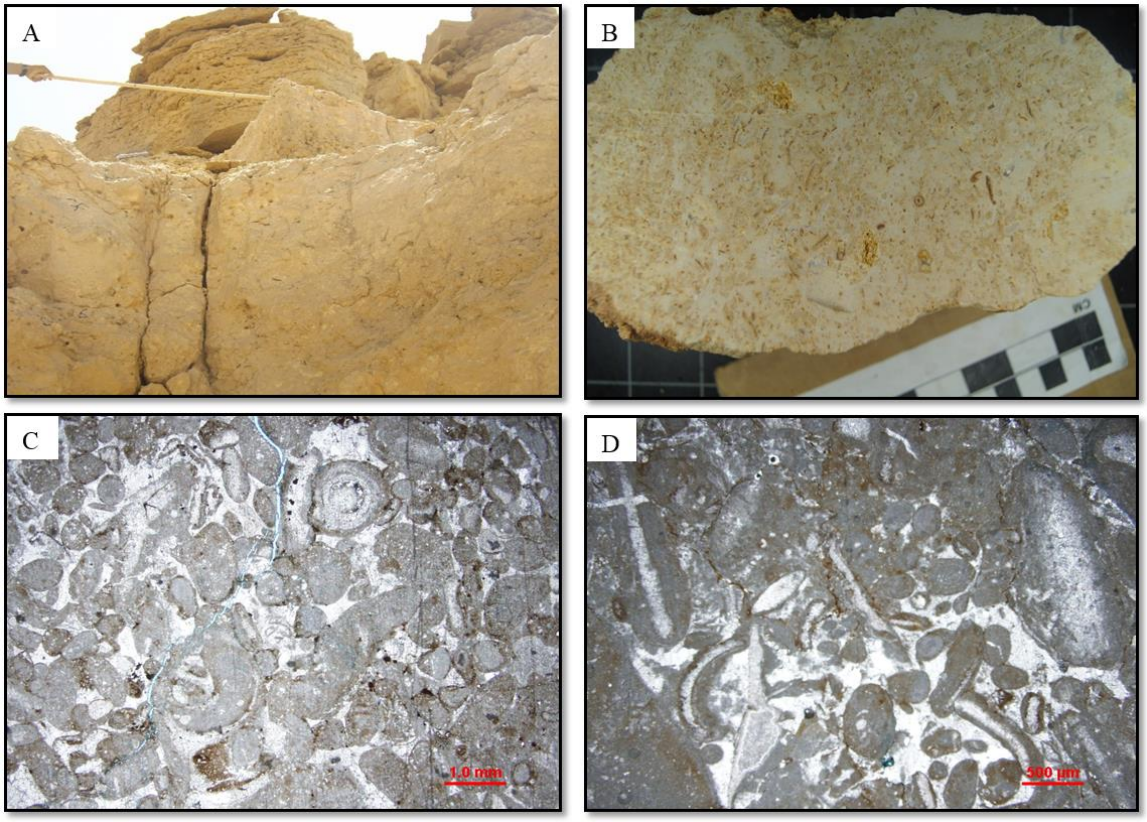

Figure 3.10(A) The field photograph is typical of this lithofacies (B) the slap section shows mm scale reflecting the bioturbation and macro skeletal component which include skeletal fragment , coated grain and a little intraclast grain, the black arrows shows coarse material filling (Firmground) indicate evidence of burrowing in a high energy setting , (C ,D) microphotograph medium to coarse grain size with cemented peloidal and skeletal grain , the arrows shows coated grain including common foraminifera assemblages .

3.2.9 X-bedded skeletal sandy grainstone

The lithofacies of skeletal sandy grainstone is present in the upper part of the Upper Ullayah Reservoir Equivalent and is composed of very well-sorted, well-rounded, medium grained ooids, bivalves, and foraminifera.

Oolitic grainstones are whitish to brownish color cross bedded at the top massive beds at the bottom with erosive base. The thickness of this lithofacies ranges from 80 to 200 cm and 100 to 320 for the stacked bed sets. Grains are dominated by well sorted, fine to medium ooids with intraclasts and scattered skeletal fragments. High- and low-angle cross-stratification, reactivation surface, herringbone (tide dominated), local burrows, and skeletal peloidal intraclast are the dominant sedimentary structures present.

Cross-bedded, well-sorted oolitic grainstones beds at the top interval represented by this lithofacies are interpreted to have been deposited in a high energy shoal or shoal bars. The massive oolitic grainstones at the bottom of the lower portion of the lithofacies are interpreted as shoal and carbonate sand bank representing mega ripples of shallow water high energy conditions. Aigner (1982), Koehrer et al.(2010a) ,Pérez- López(2001) discussed the presence of similar sedimentary features in modern and ancient analogs which are similar to this lithofacies

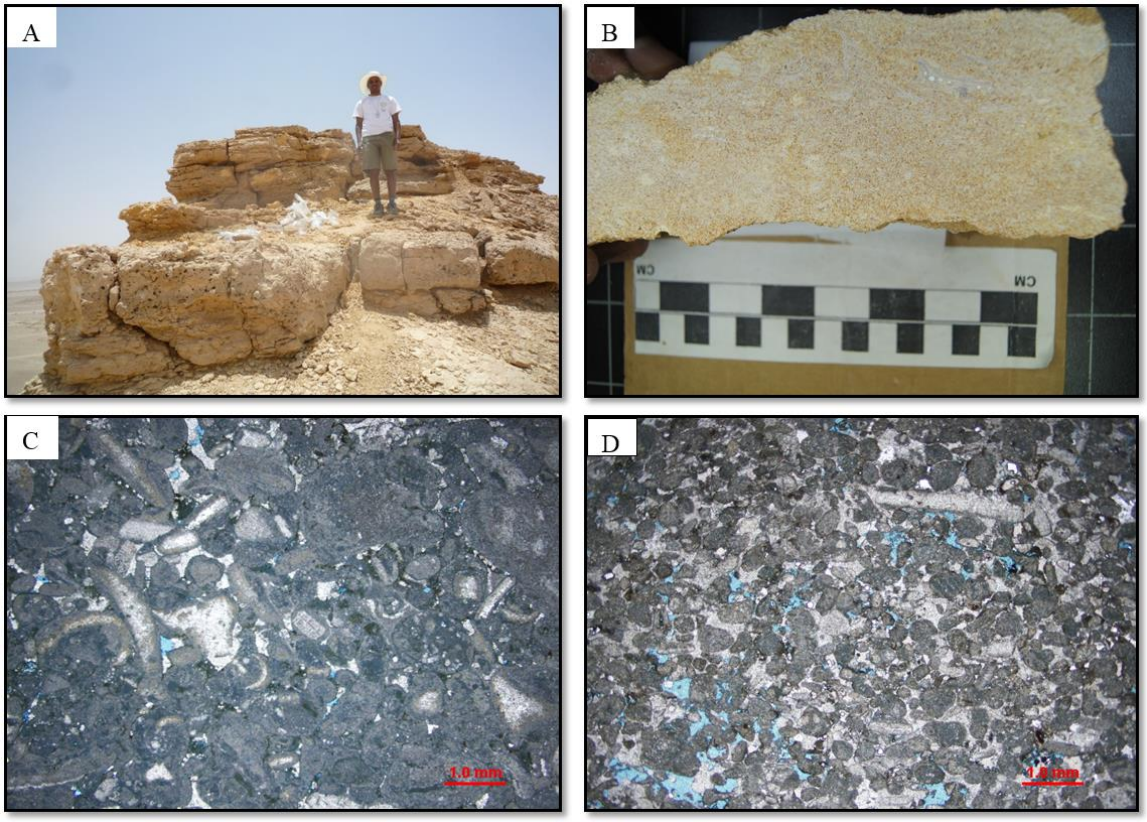

Figure 3.11 (A)Typical outcrop photo of this lithofacies The well-rounded,well-sorted,well-winnowed depositional texture of oolitic lithofacies and its cross bedded structure suggests a further increase in hydrodynamic energy, as the lithofacies belts continue shallowing to agitated water conditions, with (B) ooids, intraclasts and scattered skeletal fragments ,(C and D) microphotograph showing skeletal ooids grainstone , foraminiferal echnoids with coated ooids and peloid and good interparticle porosity.

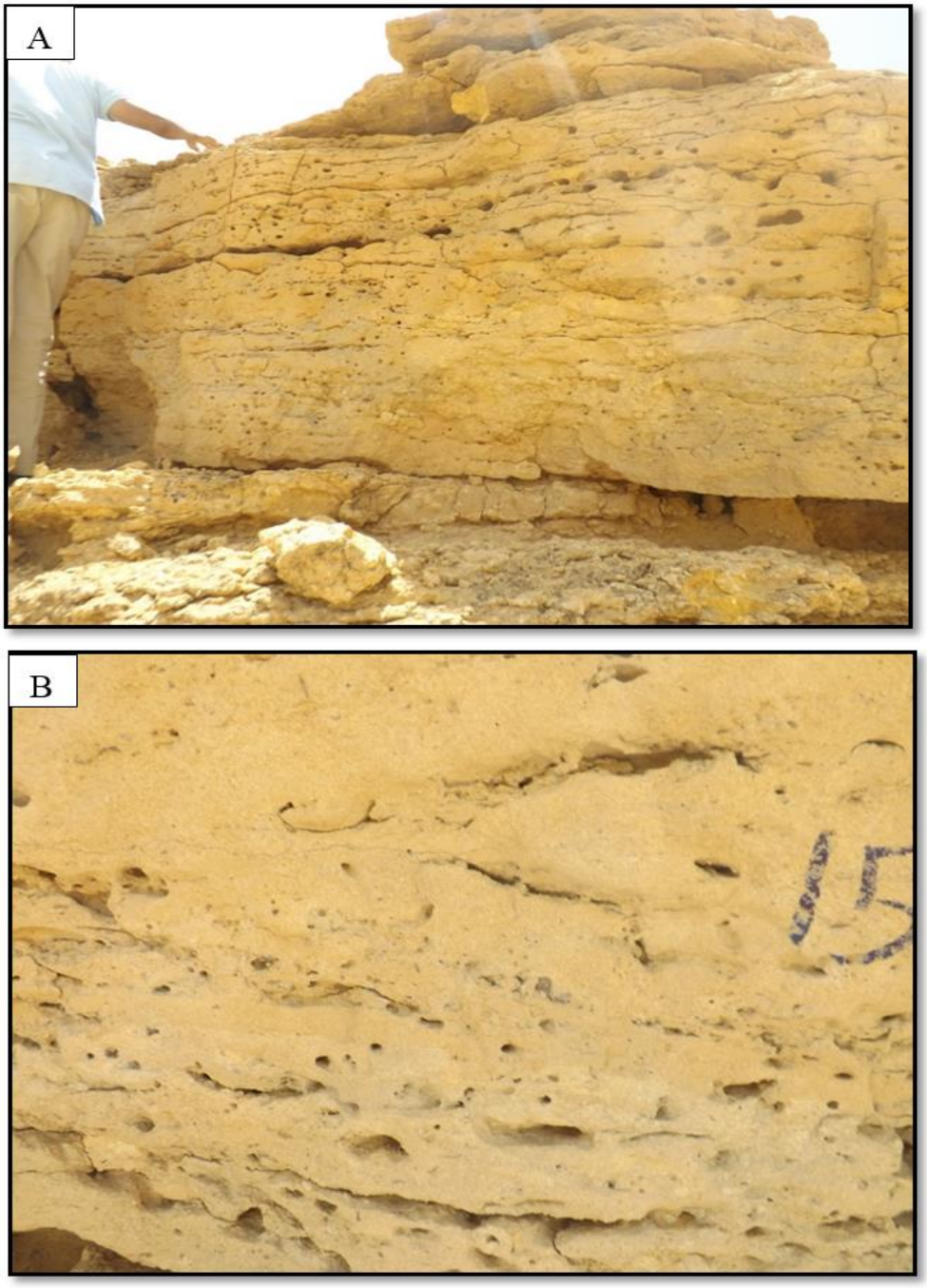

Figure 3.12 (A)The outcrop pghotograph is typical of this lithfacies shows Stacked, skeletal, intraclas and stratified oolitic grainstone, (B) Fine grain, herringbone, and reactivation surface (Tide dominated) grainstone

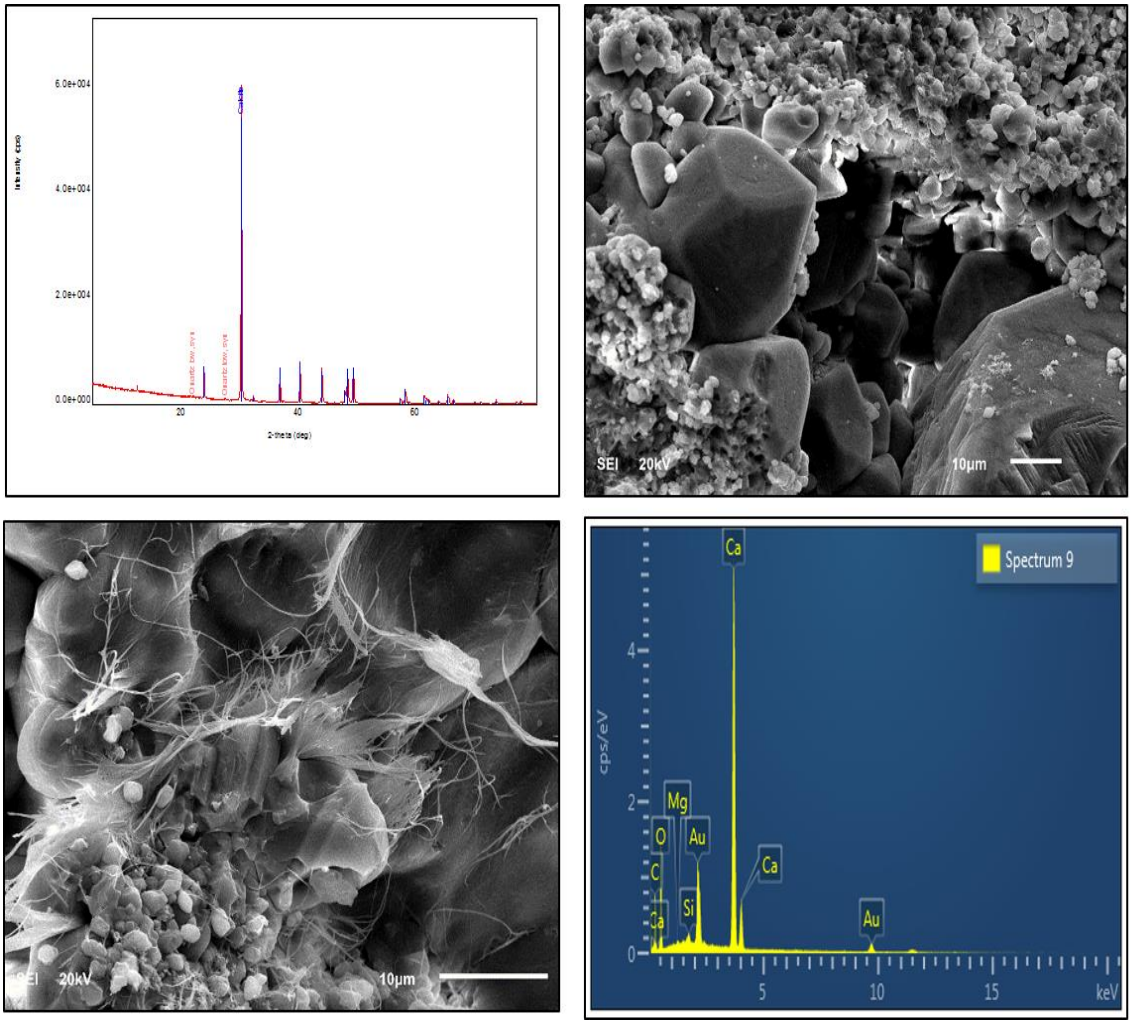

Figure 3.13 XRD, SEM and EDS of cross-bedded grainstone lithofacies

3.2.10 Laminated skeletal sandy grainstone

Graded bed grain dominated packstones to fine grainstone lithofacies in the outcrop occurs as reddish to light beige beds. The beds thickness ranges from 50 to 70 cm and stacked beds set ranges from 100 to 120 cm. The bed sets are separated by erosive marl fill surface and are laterally amalgamate. The dominant sedimentary structures are horizontal lamination, low angle trough cross-bedding, climbing wave ripple lamination, and hummocky cross stratification .The dominant grain types are very fine to fine ooids and detrital peloids. The sedimentary structures along with the grain size of this lithofacies indicate low to moderate depositional energy of storm sheets below fair-weather wave base and above storm wave base

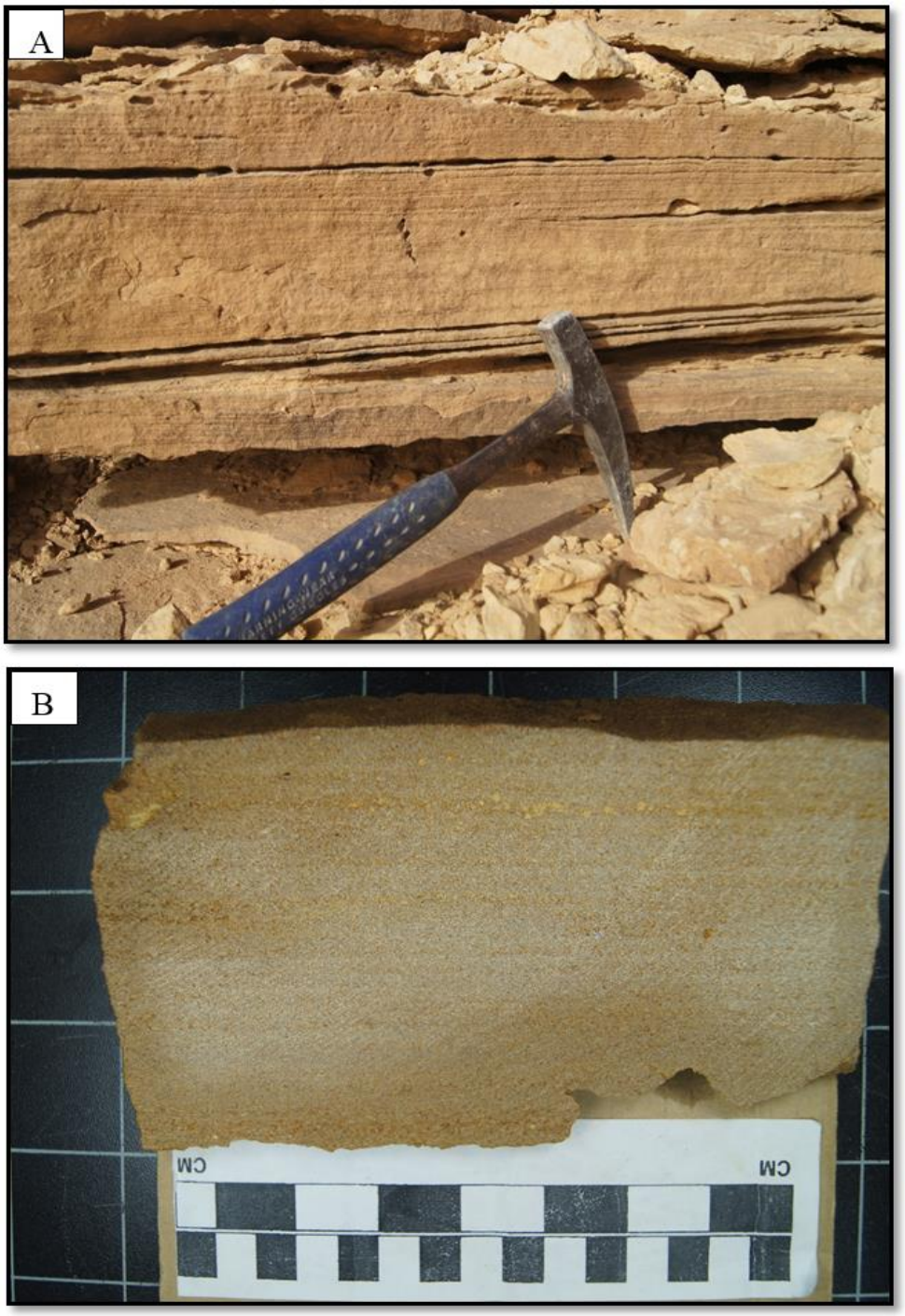

Figure 3.14 outcrop photo is typical of this litho facies shows continuous horizontal laminarion with (B) mm scale low angle cross bedding

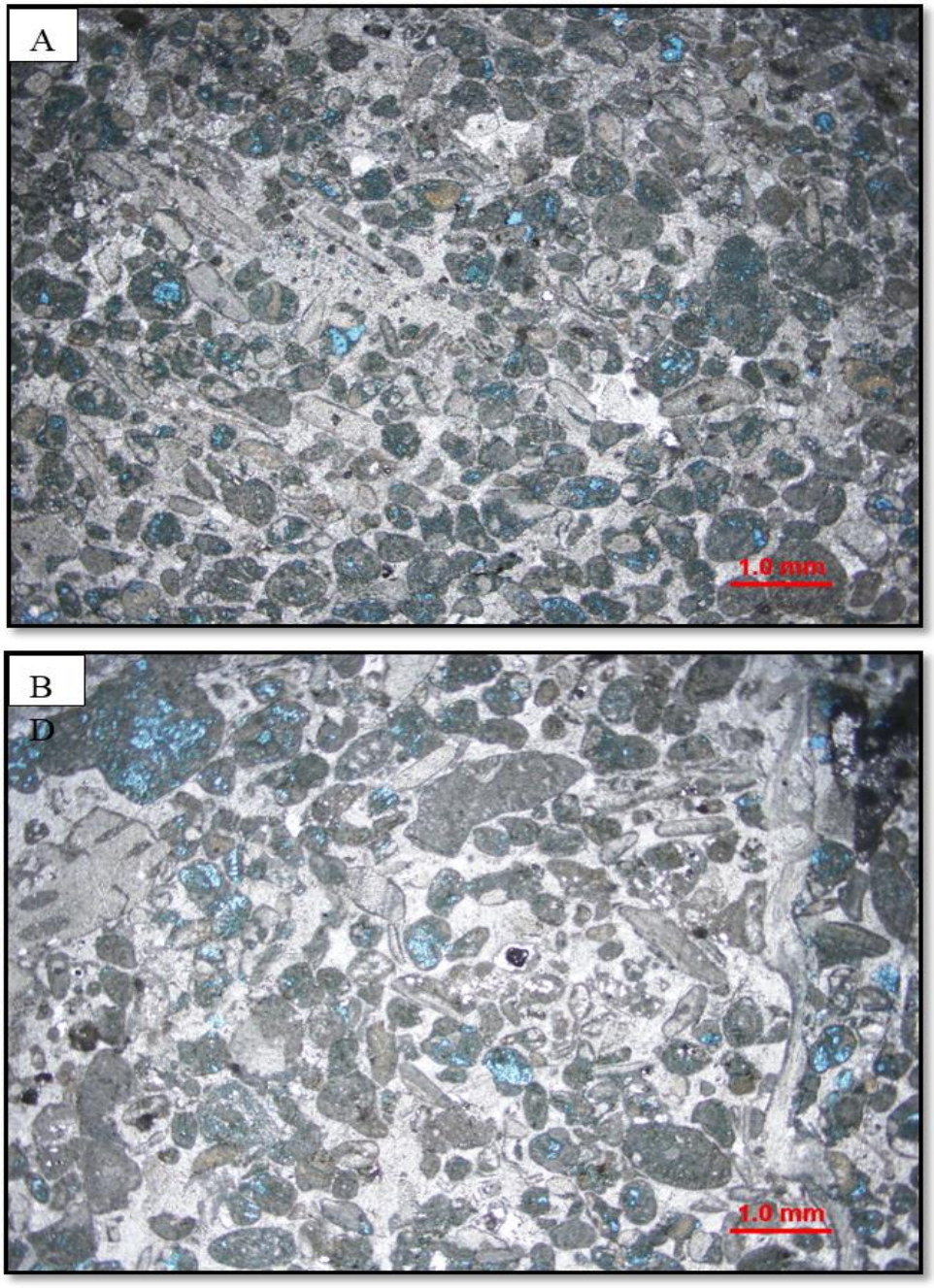

Figure 3.15 Photomicrograpph of laminated skeletal grainstone lithofacies displaying (A) peloidal preferred orientation coincides with lamination included reworked brachiopods, Thaumatoporella , echinoderm , Clypeina Jurassica and foraminifera everywhere. Deformation of grains during diagenesis makes their identification cumbersome.

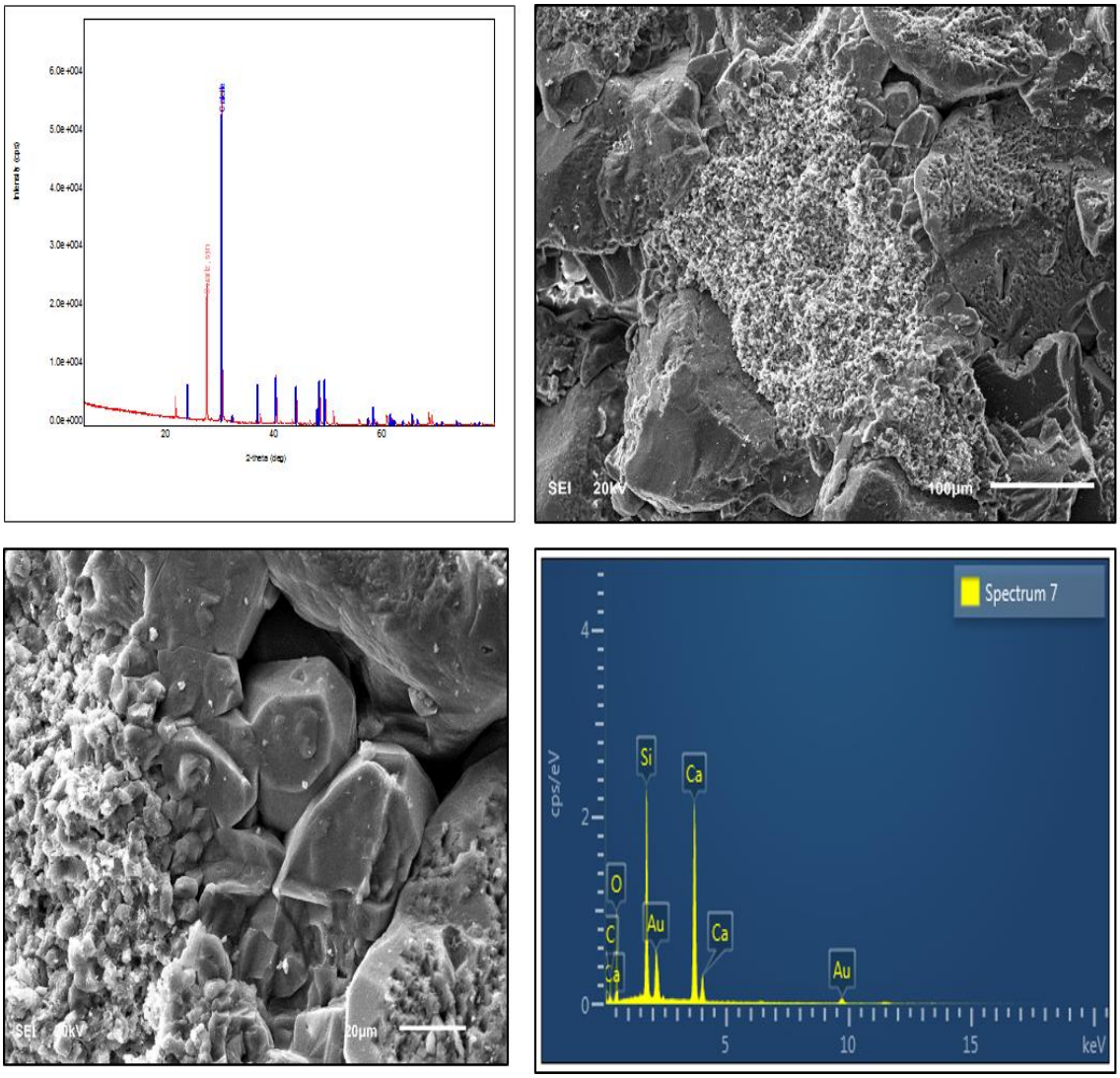

Figure 3.16 XRD,SEM and EDS of laminated grainstone lithofacies

Figure 3.17 Boundary between Hanifa formation and Jubaila formation shown by the presence of association of (A) Iron stained surface and (B) an oyster-encrusted one

3.3 Depositional Model

The Upper Ullayah Reservoir Equivalent at Jabal Abkyan is composed of 10 depositional facies that can be arranged spatially in several 2-dimensional models recording the gradual shoaling and restriction of the shallow rimmed setting. The lithofacies types reflect a range from high energy to low energy hydrodynamic conditions related to gradual increase in water depth. The lithofacies types and their equivocal interpretation of depositional environments are based on stratal context and related facies succession.

I constructed this model by defining the recognized lithofacies components, their stratigraphic positions in outcrop , the nature of their boundaries and sedimentary structures, their bedding thickness trends, in addition to integrating my finding with Hughes' (2004, 2009) published micropaleontological analysis of Hanifa formation.

On the basis of detailed facies analysis, the vertical and lateral distribution of the facies types, the lack of distinct bathymetric changes I propose a rimmed model for the carbonate deposits in the study area.

Based on lithology, sedimentary structures, textures, and the presence and proportion of skeletal (mainly foraminifera bivalves, corals, calcareous sponges, gastropods, and echinoids) and nonskeletal (peloid, ooid, intraclast and oncoid) grains, the depositional environment as recognized from the previously described depositional lithofacies of the studied strata is marine and it includes deep lagoon, shallow lagoon, and barrier shoal basin for all Ullayah member while the Upper Ullayah Reservoir Equivalent was deposited during shallow lagoon to shoal environments.

These are described and interpreted basinward as follows:

In the lower part of Ullayah member the semiarid climate and restricted water circulation led to partly hypersaline conditions with a restricted fauna (Flugel 2010). The very common lime mudstone intercalated with calcareous shale and skeletal wackstone indicate widespread low-energy, somewhat restricted deep lagoon environments punctuated only episodically by high-energy events such as storms and spring tides.

The textural characteristics and dominance of miliolids, bivalves and in places gastropods, the absence of larger foraminifera, textulariids, algal fragments, open marine fauna and the presence of some micritized grains and intraclasts suggest a very shallow-marine backshoal environment. It represents a semi-restricted lagoon in close vicinity of tidal flats with relatively low currents (e.g., Geel 2000; Romero et al. 2002; Vaziri-Moghaddam et al. 2006; Badenas and Aurell 2010) where large fluctuations in salinity and temperature may have occurred (Martini et al. 2007).

In fact, the Cladocoropsis presence behind the reef could have further reduced energy and enhanced mud deposition as its dendroid form would have baffled wave energy. Storm activity in the lagoon is manifested in the Cladocoropsis dendritic or branching form, which is a morphologic adaptation known to flourish in abrasive settings, as it is capable of substantial sediment shedding that is beneficial in keeping up with high sedimentation rates (Toland, 1994).

Last, the Cladocoropsis and dasyclad lithofacies that intermix and variably overlie the stromatoporoid lithofacies suggest a random distribution of the Cladocoropsis within the lagoon instead of its existence in a specific zone or belt as suggested by Hughes (2004) and Lindsay et al. (2006).

Grain-support and the low biotic diversity of fine oolitic facies indicate that these sediments were deposited in protected, restricted, well-oxygenated, shollow lagoon environments (Wilson 1975; Buonocunto et al. 1994; Martini et al. 2007; Flugel 2010).The abundance of micritized grains suggests occasional breaks in sedimentation (Hips and Haas 2009).

Oncoidal limestones are best related to a back barrier, shallow, open-lagoonal and (to a minor degree) closed-lagoonal facies (Wilson 1975; Alesi 1984; Aigner 1985; Schauer and Tebingen 1997).According to Wilson (1975) and Flugel (2010), oncolytic wackestones are typical of shallow, relatively quiet back bank environments where they form at the margins of ponds and channels subjected to intermittent current activity and relatively low sedimentation rates, indicated by micritic envelopes (Palma et al. 2007; Papaioannou and Kostopoulou 2008; Kavoosi et al. 2009; Brigaud et al. 2010; Wilmsen et al. 2010). A warm, euphotic environment is also supported by the very low proportions of bryozoans, corals, and encrusting sramatoporoid.The skeletal peloidal shows a significant increase in mud content, deterioration of sorting and flourishing of *Thalassinoides* burrowing suggest a better oxygenated shallow marine environment, and it is thus interpreted as shelf lagoon open circulation deposits within the fair-weather wave base. Low-angle cross-stratifications, sub rounded, medium sorted, and winnowed components that are characteristics of the massive skeletal lithofacies indicate an increase in hydrodynamic energy and an increase in sorting and abrasion ability as the lithofacies belts continue shallowing toward the shoreline.

Moreover, the lagoon sediments associated with bioherms reveal an open marine fauna indicating moderate to good living conditions.

The well-rounded, well-sorted, well-winnowed depositional texture of sandy grainstone lithofacies and its cross bedded structure suggests a further increase in hydrodynamic energy, as the lithofacies belts continue shallowing to agitated water conditions.

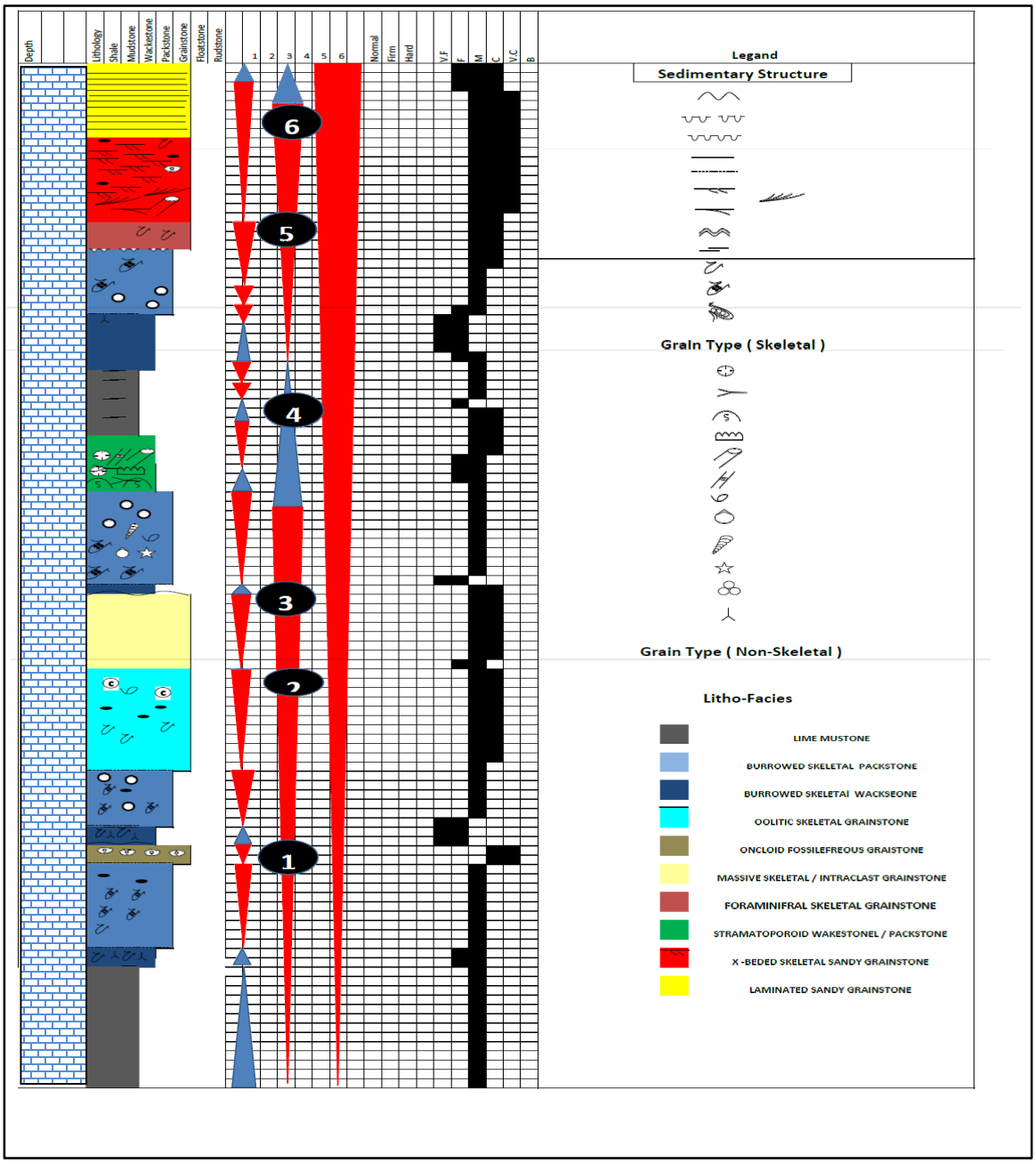

Figure 3.18 Composite sedimentological section representing the lithofacies association in upper Ulayyah Reservoir of Hanifa Formation

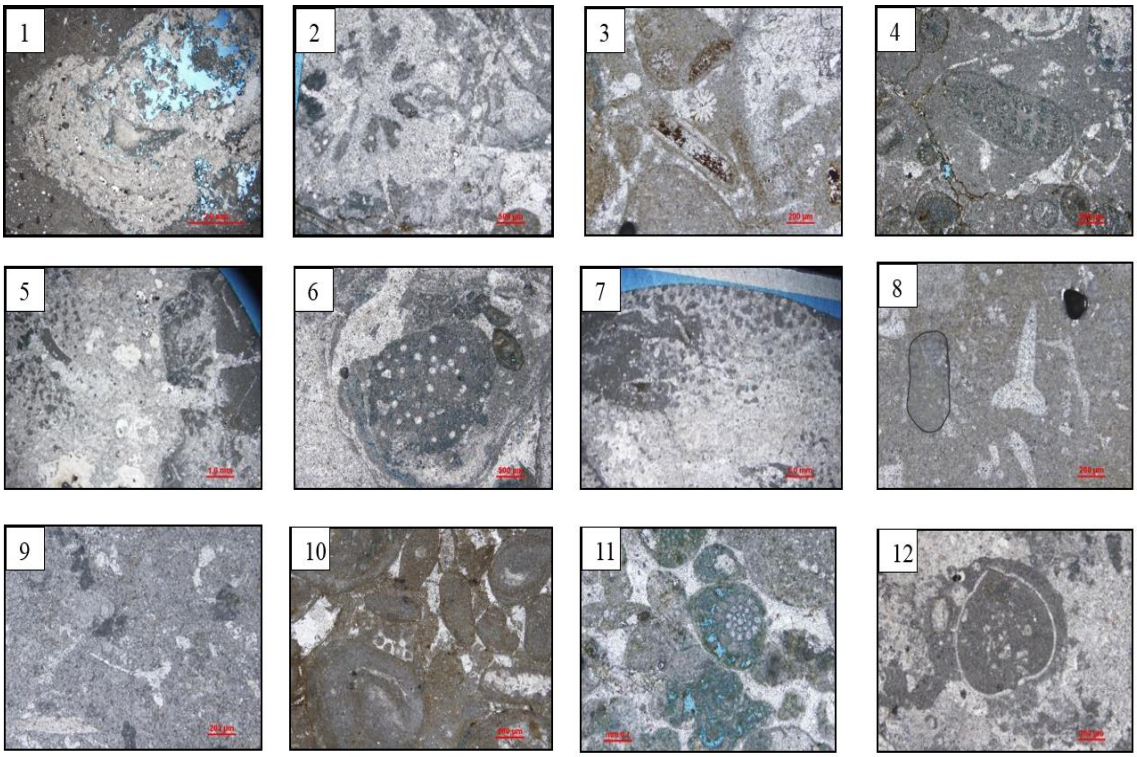

Figure 3.19 Bio-facies components in Ullayah reservoir member.(1) Stromatoporoid, (2,3)coral fragments and (4,5) Cladocoropsis mirabilis are restricted to Upper Ulayyah member This assemblage indicates open marine unrestricted regime (Hughes, 2004a, 2004b, 2009). The possible palaeoenvironment in the studied outcrop succession is open marine.

Pseudocyclammina lituus (6), (7) Thaumatoporella with Gastropods, Ostracod dominated in the Upper Ulayyah . This assemblage indicates shallow to very shallow lagoon setting.

Triaxon sponge spicules (8,9) indicate faunal assemblage is indicative of a stressed, low energy setting interpreted here to be a restricted environment. Dasyclad algae (10) indicate deep restricted lagoon environment.

Nautiloculina oolithica (11, 12) Kurnubia palastiniensis, Echinoid fragments, Brachiopod fragments distributed in the upper Ulayyah . These could either have a very wide paleoenvironmental tolerance (Hughes, 2004a, 2004b, 2009) or transported by channelized flow

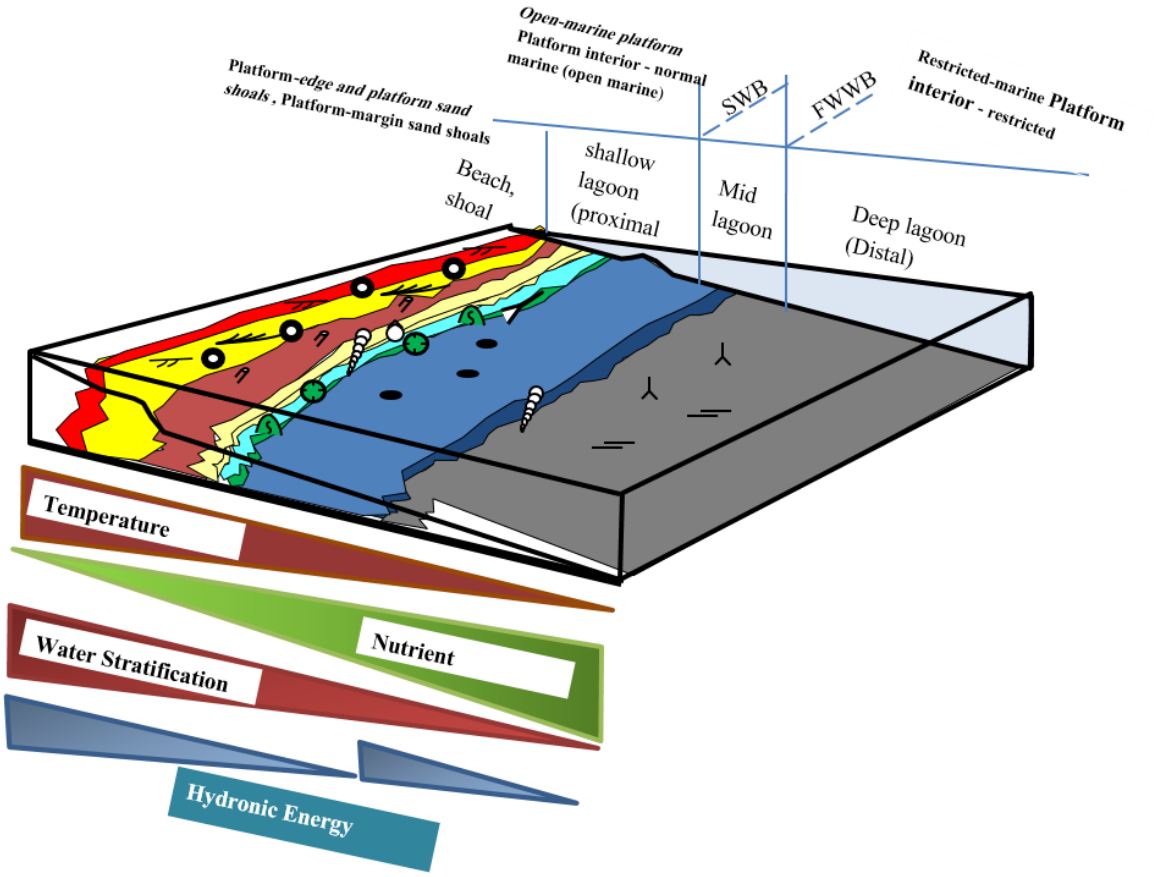

Figure 3.20 Schematic depositional model. The model is of a prograding, rimmed shelf, shallow, gently sloping, batches arid stromatoporoid reef. The hydrodynamic energy increased up to the reef, decreased by reef resistance to waves in the lagoon, and increased back up to shoal environment. The arid climate probably overheated the nearshore waters as shown by the temperature gradient. This overheating inflicted a corresponding vertical water stratification gradient. Lime mudstone, spiculitic wackstone that represent the quite deep lagoon environment was followed by peloidal and foraminiferal grainstone shallow lagoon environment. Cladocoropsis and dasyclad lagoon that was protected by arim by stromatoporoid reefs with small-scale population. These were followed by x bedded and fine laminated sand grainstone with high energy non well developed shoal sandy limestone environment. The controlling factors on the sedimentation pattern and geometries are: (a) relative sea-level variations, at different scales: third order of eustatic/tectonic origin, fourth order and fifth order of eustatic/climatic origin (Milankovitch type) (b) input of siliciclastic sands from local high shield area. Size, morphology and reproductive characters of grainstone seem to be directly related to changes in water depth (accommodation).

3.4 Chemostratigraphy

Chemostratigraphy, the study of the variation of chemical compostion in sedimentary sequences, has also been utilized to meet this objectives of in this study. The geochemistry of sedimentary rocks is the result of their provenance, depositional setting, and their diagenetic history (Andrew et al., 1996), and such analyses of mudrocks are indispensable

to detect subtle differences during deposition (Algeo et al., 2003; Rimmer et al., 2004; Rowe et al., 2008). The study of the variations in major and trace element abundances in sedimentary rocks, chemostratigraphy utilizes major and trace elements to characterize and sub-divide geochemically distinct units, for regional (or global) correlation of strata (Andrew et al., 1996). Major elemental variations indicate changes in mineralogy, and are used to differentiate lithology changes in the stratigraphic zone, and thus can help in correlation.

Changes in major oxides concentrations are mainly related to changes in minerals content, and so, could be very useful tool in lithostratigraphic separation and correlation. Broadly, major elements oxides in the studied section show two different geochemical zones; having separated approximately at the mid of the studied section. All oxides show some fluctuation in the lower part of the section and, generally, more steady concentrations through the subsequent upper samples, with exception of SrO which shows a reverse trend. Through the shallow lagoon environment the zone shows clear depletion in, Mgo, Al2O3, SiO2, Fe2O3 and K_2O associated with sharp sudden increase in Cao and SrO. In facies of open marine environment SiO_2, Al_2O_3 and Fe2O3 reveal part of their higher percentages through the whole section, in a blocky log motif pattern, whereas MgO, CaO and SrO2 show the complete reverse to the previous oxides pattern. All oxides have their least lowest values in the studied section, except of CaO, which assume there its highest value. SrO concentration in this facies is distinctive, showing a highly fluctuating curve. I will consider SiO_2 and $Fe2O3_2$ as continental detrital indicators while Al_2O_3 will be interpreted as proxy for clays. The moderately high percentages of CaO, SrO & MgO go parallel with the slight decrease in all clay components (SiO_2, Al_2O_3, Fe_2O_3, and K_2O). The chemical profiles

defined the regressive and transgressive phases and reflect cyclic depositional patterns within in the Upper Ullayah reservoir member. The geochemical data show marked differences in character and distribution of different lithofacies, which might help in defining reservoir zonation.

Open marine lime mudstone dominated has high values of clay mineral components in blocky log motif similar to the associated U & Th logs in gamma ray log. All previous observations infer to a continental detrital clay layer. The high concentration of Al_2O_3 associated with rises of SiO_2, Fe_2O_3 and K_2O, in addition to the great depletion in the CaO, MgO & SrO strongly infer, geochemically, to the existence of detrital clay minerals. This proposition is strengthened by the sharp rise in Th & U concentration values in the SGR.

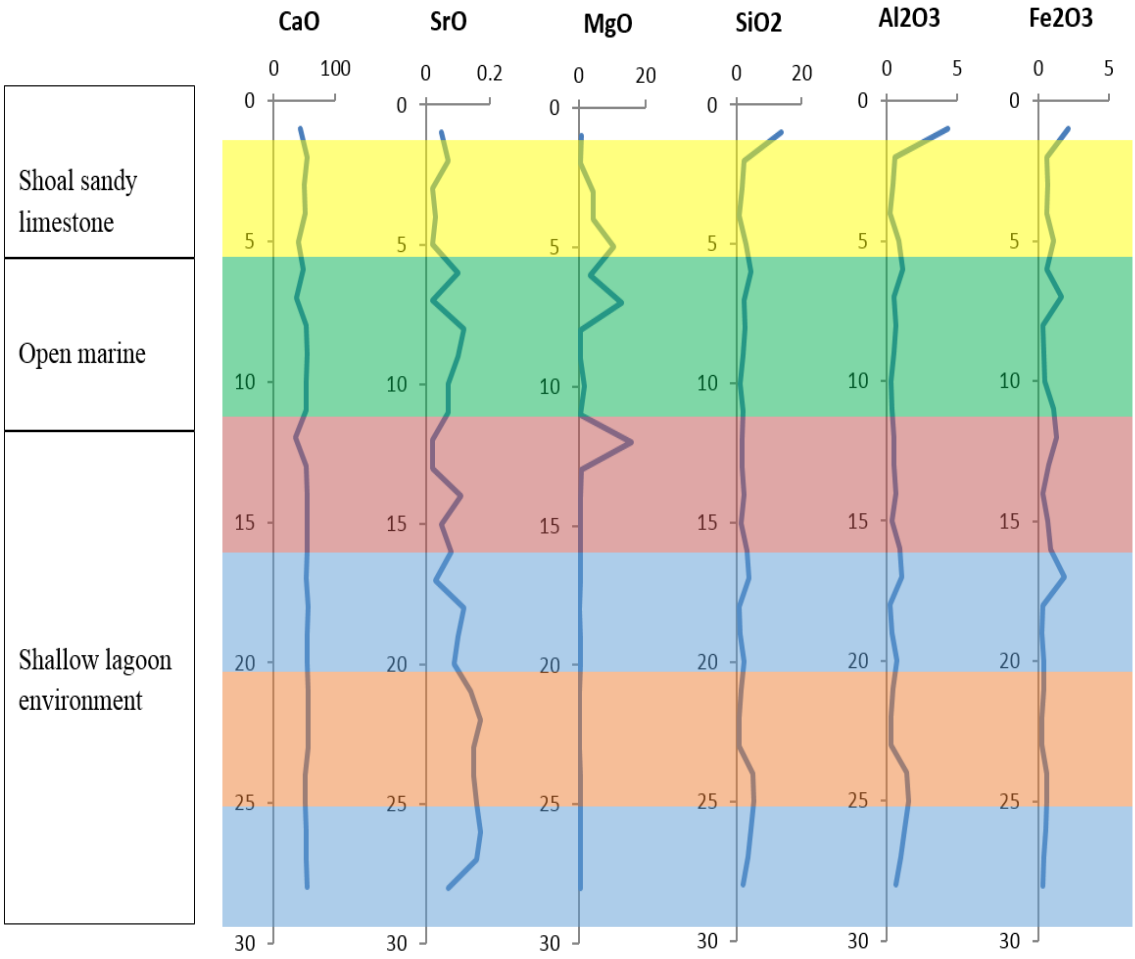

Figure 3.21 Geochemical profile signature reflect the chemical behavior trend within shollow lagoon,open marine and shoal sand deposit

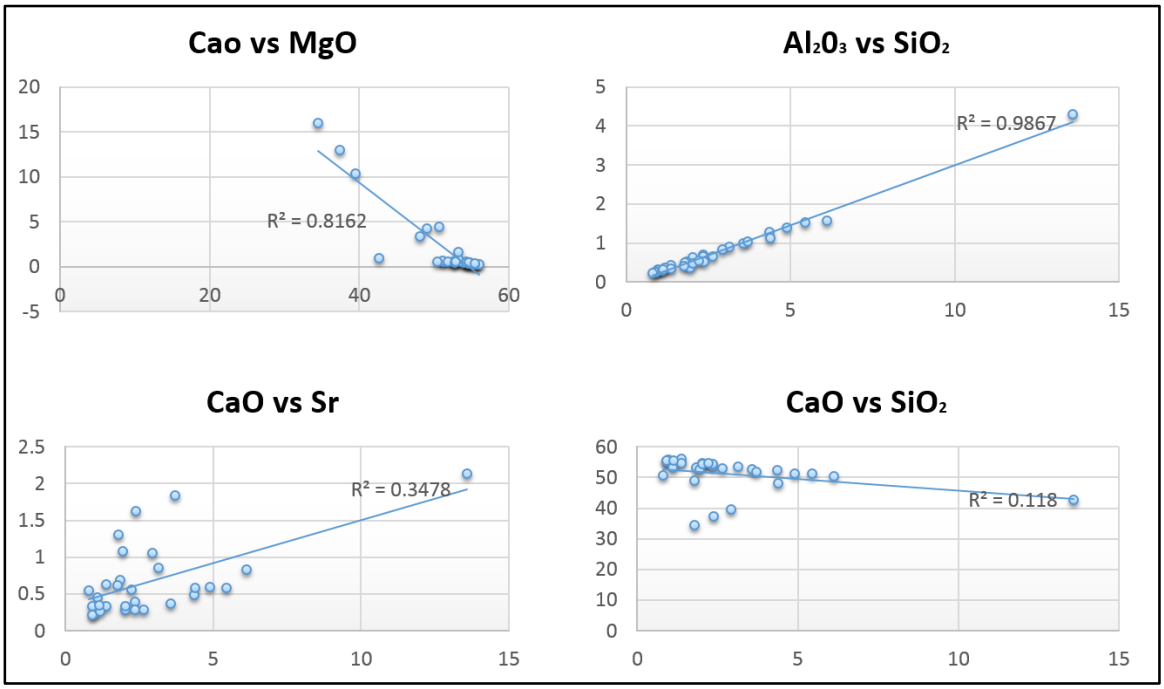

Figure 3.22 X-plot of geochemical element of Ullayah reservoir equivalent, Hanifa formation

3.5 Log Motive Gamma Ray

Spectral Gamma Ray (SGR) logging of outcrops provides an excellent technique for characterizing and modelling reservoirs. The output from SGR tools are SGR counts per second (CPS), elemental concentrations, and dose rate for potassium (K), thorium (Th), uranium (U), and their total counts (TC). SGR tools have been used effectively by many investigators (Dennison et al. 1997; Krystyniak et al. 2005; Collins et al. 2006; Evans et al. 2007; Koptíková et al. 2010; Imicek et al. 2012) to tie gamma ray log signatures to the characteristics of lithofacies at outcrops and to extract useful geological information out of these outcrops. GR detailed bulk-chemical profiling of Ulayyah reservoir equivalent shows that potassium (K) and thorium (Th) are mutually correlated and are a direct index of siliciclastic (aluminosilicate) content, whereas uranium (U) is uncorrelated with K, Th, and

all other chemical components measured. Uranium tends to be enriched in thin shale and argillaceous carbonate layers within otherwise carbonate-dominated intervals. Uranium is thus associated with aluminosilicate minerals and is not particularly concentrated in dolomite. Two types of GR peaks are observed. Potassium thorium– dominated peaks are suggested to indicate relatively major transgressions during which aluminosilicate detritus was derived from sources interior to the Arabian shield. Uranium dominated peaks correspond with relatively minor transgressions within intervals of cyclic shallow-water carbonate deposits. Uranium-enriched aluminosilicate detritus is suggested to be the product of extended subaerial exposure of the platform, during which U was concentrated by groundwater movement. These results can be useful as a basis for applying spectral GR signature asa tool for stratigraphic interpretation in uncored or incipiently understood carbonate sections

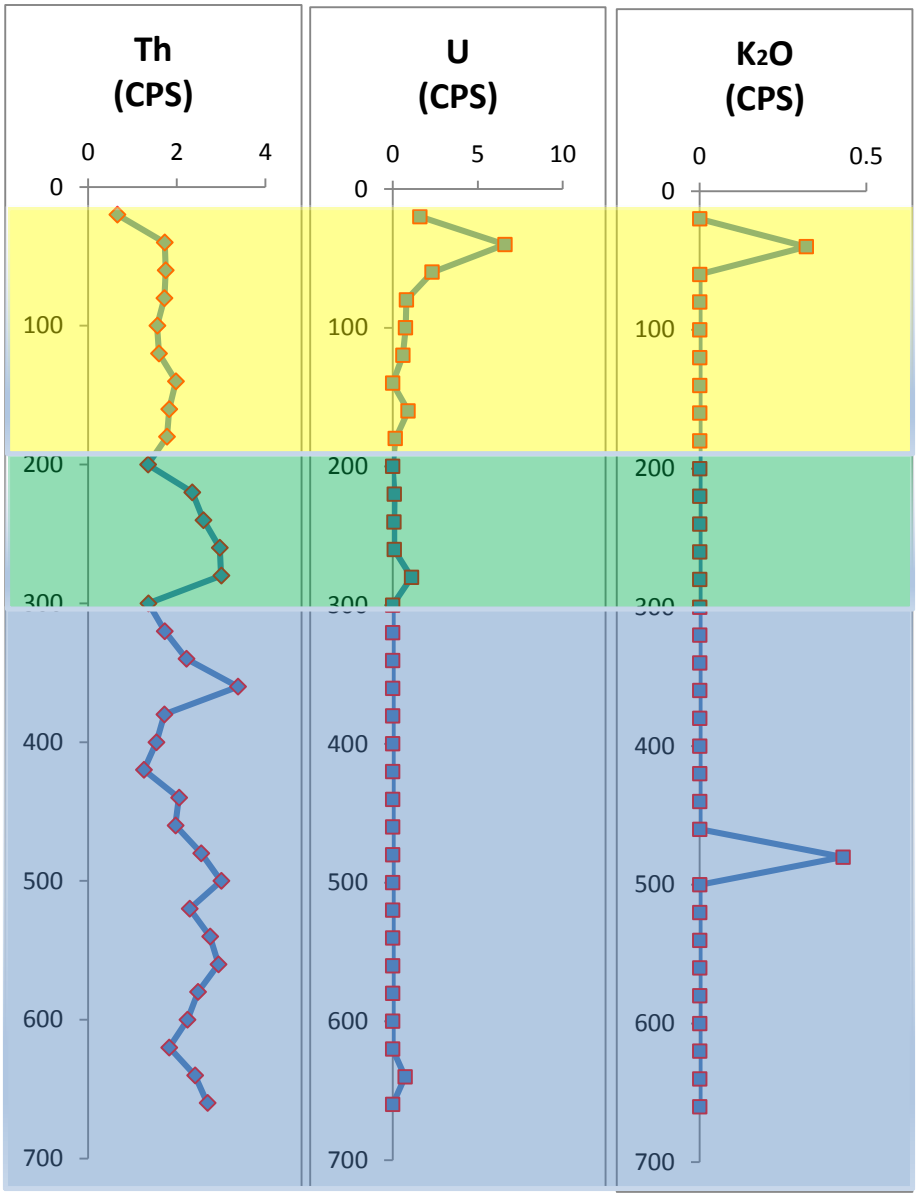

Figure 3.23 Gamma ray signature at outcrop of Ulayyah carbonate reservoir

CHAPTER 4

3D OUTCROP MODELING OF FACIES, POROSITY AND PERMEABILITY

4.1 Introduction

Sub-surface reservoirs are normally characterized by limited information from widely spaced wells (1D sections) and relative low-resolution seismic data (2D or 3D sections) making any derived geological model highly subjective. The richness of detail offered by outcrop exposures to study the sedimentary architecture (e.g. stacking patterns, lateral continuation, facies proportions and distribution) at a wide range of scales (km to mm) in continuous 3D accessible sections make them ideal analogues to help bridge the gap in resolution between seismic and well data in reservoir studies.

4.2 Significance of outcrop modeling

Geostatistics offers a way of describing the spatial variability (e.g. continuity, correlation) of geological phenomena (Isaaks and Srivastava 1989). In reservoir characterization the most commonly used geostatistical tool to investigate and model geological spatial variability is the variogram (Gringarten and Deutsch 1999). The quality of the derived spatial variability described by the variogram is crucial to develop "realistic" reservoir simulations that honor the geologic complexity. For the geostatistical modelling of heterogeneous sub-surface reservoirs it is, however, problematic to obtain accurate quantitative measures of the spatial variability lithofacies, porosity and other petrophysical

properties. For each of these properties the spatial variability is different and generally directional dependent (spatial anisotropy) (Hohn 1999; Deutsch 2002). For example, the maximum lateral continuity (major horizontal direction) of shallow marine carbonate sedimentary structures normally depends on the direction of deposition, thus the mean vector of paleoflow distribution. The structure furthermore typically displays a smaller continuity in the directions which are oblique-perpendicular to paleoflow (minor horizontal direction) and the smallest one perpendicularly to the stratigraphy (vertical direction). Thus in order to compute reliable directional variograms, a sound understanding of the geology and a substantial amount of data is needed to analyze the spatial variability of each property in their correct major and minor horizontal direction as well as vertical (Daws and Prosser 1992; Olea 1994; Jensen et al. 1996; Deutsch 2002). The inherent problem in sub-surface reservoir characterization is that measures of spatial variability rely on one-dimensional core and well log data. This makes it more or less straightforward to compute a variogram in the vertical direction, although the reliability of this vertical variogram may be debated as sub-surface well data describes less than 0.1% (North and Prosser 1993) of the reservoir volume and the well orientation might not be perpendicular to the stratigraphy. For the latter coordinate transformation can be carried out to correct the potential overestimation of the vertical continuity (Deutsch 2002). Nevertheless, a more imprtant problem is that well data does not provide any information on the lateral variations of lithofacies and petrophysical properties. Normally only a few widely scattered wells are available, so a spatial analysis cannot capture features smaller than the well spacing and therefore does not contain much detail on the lateral geological heterogeneity. Even the increased popularity of horizontal wells, formerly

believed to have potential to provide information on the lateral variability (Kupfersberger and Deutsch 1999), has not significantly helped with computing reliable horizontal variograms. Horizontal wells normally cross stratigraphic time-lines which results in a reduced correlation and underestimation of the horizontal continuity. Therefore, secondary information needs to be considered, such as seismic data (Wolf et al. 1994), conceptual models (Bashore et al. 1994) and outcrop analogues (Frykman 2006), to provide additional data on spatial variability (Deutsch 2002). Data obtained from outcrop studies allow the strongest control on the gathered information, hence suitable transects can be selected to provide representative measures of lateral and vertical variability. However, in these studies measurements taken along a two-dimensional transect in the field (Eisenberg et al. 1994; Grant et al. 1994; North and Taylor 1996) or from outcrop architectural panels (Falivene et al. 2006). Therefore, these studies commonly neglect the anisotropy of lateral spatial variability within the horizontal plane that is the differences minor and major directions of continuity, related to the deposition of sedimentary structures (Daws and Prosser 1992; Jensen et al. 1996). Another issue of outcrop studies is the spacing between samples and the distribution of transects used to represent the spatial variability, which might not correctly characterize the complexity diversity of the property. McKinley et al., 2004, for example, shows how variation can change using different sample spacing's to measure the permeability variability in a homogeneous sandstone. This, however, does not mean that sampling along transects needs to be per definition intensive and the amount of used transects very large. It is more important to understand the observed geology and collect a representative dataset to measure and subsequently correctly model the spatial variability of the lithofacies and associated petrophysical properties (Jensen et al. 1996).

4.3 Grid Construction

Four surfaces were reconstructed from the correlated stratigraphic sections (Figure 5-1), these surfaces are

Surface 1: The boundary between uppermost part of Ullayah reservoir of Hanifa formation and the Jubail Formation which is marked by

Surface 2: The top of open marine deposit which is transition between the relatively thick grainy layers of massive, skeletal oolitic foraminiferal shallow lagoon and cross-bedded laminated sandy grainstone of shoal environment.

Surface 3: The base of the uppermost part of Ullayah reservoir of Hanifa formation defined by the last appearance of deep limestone of Lower Ullayah member and

Surface 4: the bottom of exposed strata

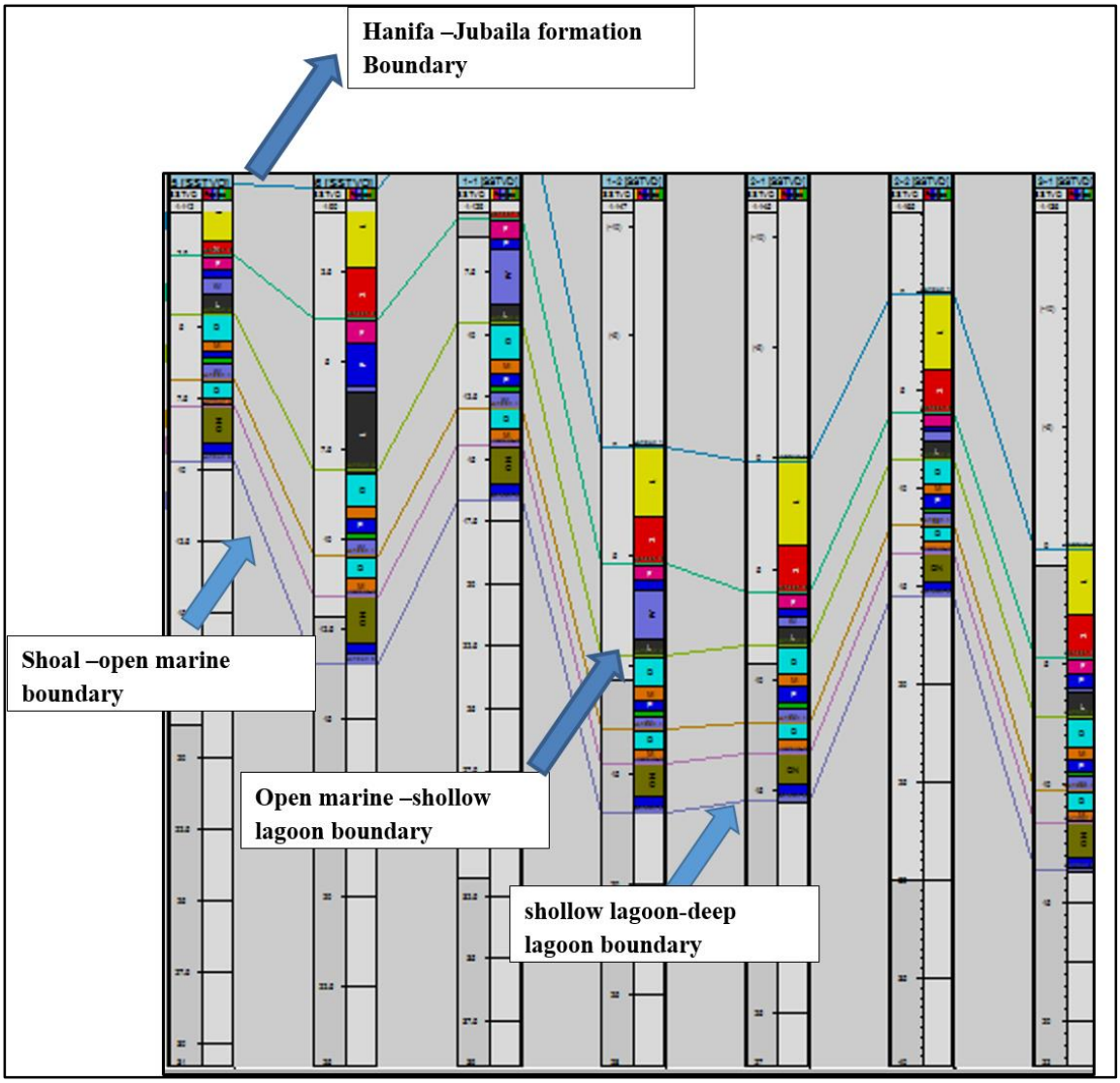

Figure 4.1 Cross section in the study area showing all stratigraphic sections and the six correlated surfaces (time lines)

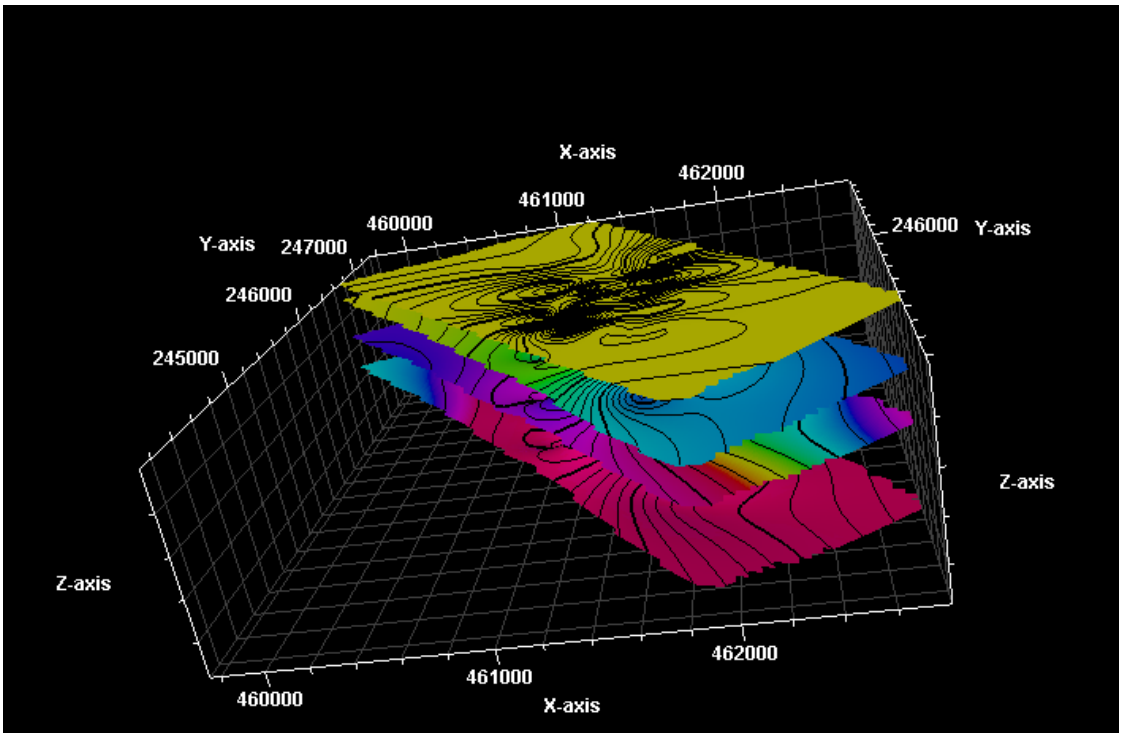

Figure 4.2 Six surfaces reflect the stratigraphy of Ulayyah reservoir for each HFS

Table 4.1 Distribution of cells in different zones in the three-dimensional grid with their corresponding stratigraphic interval in the outcrop

Gridding System	Stratigraphic Zone	Thickness of zone (m)	Number of Layers	Number of Cells	Average cell thickness
3-D grid of the outcrop	Upper Ulayyah reservoir	14	60	8000	0.45
Zone-1 grid	Deep lagoon	7	25	4000	0.6
Zone-2 grid	Shallow lagoon	3	15	1000	0.3
Zone-3 grid	Shoal lime sand	4	20	3000	0.6

4.4 Spatial Analysis (Semivariogram)

In order to analyze the spatial variability and possible correlation structures for the lithofacies of the Ulayyah reservoir. Classified point-cloud directional variograms were computed in three sample directions, a major horizontal, minor horizontal and vertical direction. The directional semivariograms were computed following the standard method described in detail by Isaaks and Srivastava (1989), Deutsch and Journel (1998) and Deutsch (2002). It involves the calculation of experimental semivariograms, for each lithofacies in the selected directions, and fitting models that honor these experimental semivariograms. The

experimental semivariogram is defined as a measure of the average squared difference between two measurements (pairs) separated by distance vector h.

$$\gamma(h) = \frac{1}{2N(h)} \sum (z_x - z_{(x+h)})^2$$

where y(h) is the measured semivariance ,N(h) the number of pairs used for computing sum ,z_x the observed value at location x and z(x+h) , the corresponding observation at location x + h. For the separation vector h (lag distance) one can specify for a direction (for example a major, minor and vertical direction) and a set of search tolerance parameters. Although the above equation formally represents the calculation of a semivariogram, the term "semivariogram" may be used for reasons of convenience and to avoid excessive jargon (Hohn 1999).

The experimental variograms were calculated using PETREL^{tm} (version 2009), in order to analyze the SIS, the dataset was up-scaled to the high-resolution modelling grid of the Ulayyah reservoir geocellular model. The quality of the resulting up-scaled data was qualitatively compared with original dataset to make sure the sedimentary architecture was correctly represented The variogram directions are defined from the spatial anisotropy present in the depositional system under investigation, therefore a sound geological understanding of the system is essential In the shallow marine carbonate platform dominated deposits of the Ulayyah reservoir outcrop area the spatial anisotropy of the lithofacies will be predominately characterized by the thickness. Although a geologically meaningful direction of major continuity is crucial for the spatial analysis, the nature of exposure of the study area also needs to be considered. The classified indicator

semivariogram dataset has to represent the spatial distribution and continuity of the analyzed property in the major and minor horizontal directions as well as vertically to be able to compute more reliable directional variograms. The calculation of reliable vertical variograms for an outcrop dataset is relatively straightforward, as it is for well data, however care has to be taken in the selection of a representative outcrop area to capture the lateral horizontal components The search parameters utilized to calculate experimental variograms commonly require some iterative refinement. As a rule, in the computation of reliable directional experimental variograms the search radius is about one half to maximum two thirds of the total study area size (maximum distance between data points) while the data spacing of the dataset is used to define the calculation steps (lag distance). Caers and Zhang (2004) argue that the search radius should not exceed one half the size of the area because otherwise not enough samples would be available to provide a reliable estimate of the variance. Furthermore, to make sure that the spatial anisotropy and resolution of variance are resolved in detail the tolerance search parameters in the calculation should be restricted as much as possible (Deutsch, 2002). The search parameters used to calculate each experimental variograms of the Ulayyah reservoir .In the final step of the spatial analysis a theoretical variogram model is fitted honoring the sample points of the experimental variogram to describe the variance for all distances. In PETREL^{tm} this is an iterative process involving adjusting the variable parameter of the theoretical model (nugget, sill, and range) until an acceptable fit of the curve to the experimental sample points and theoretical sill is achieved. Note, that the theoretical model needs to fit all the directional experimental variograms for each analyzed property to accurately interpret and model the experimental variogram a systematic is followed

(Gringarten and Deutsch 1999), where the structures are modeled from a short scale to a larger scale. Therefore a close fit at the origin (small nugget) and at small lags are more crucial than accurately honoring slight periodicities, minor zonal anisotropies, and long range trends (Journel and Huijbregts 1978; Ma and Jones 2001; Deutsch 2002). The theoretical model can be described by any positive definite function, however the most widely used functions in literature are spherical, exponential, Gaussian and hole effect variogram model (for examples see Deutsch 2002). For my study only spherical and exponential variogram models were utilized in the experimental variogram interpretations to allow direct application of the results in the facies modelling process of PETREL™ .The discussion below follows the principles for systematic variogram interpretation and modeling, where structures are modelled from small to large scale (prioritizing detail on short over large distances) (Gringarten and Deutsch 1999). However, in the variogram modelling the requirements for the subsequent facies simulation of the Ullayyah geocellular model in PETREL™ are also taken into account. Thus, the final variogram model associated with the computed experimental variogram is either a spherical or exponential function which are controlled with a nugget effect, correlation range or theoretical sill. The finest-scale variance is defined by the nugget, representing the apparent discontinuity at the origin of the variogram. This discontinuity is the sum of measurement error and geological variability at a scale below the lag distance (Ulayyah dataset: horizontal < 1 m; vertical < 0.25 m). The nugget must be equal in all directions of each lithofacies and should as a rule be determined from that directional experimental variogram which shows the lowest variance. Pure nugget effect variogram models, without any spatial correlation, are not desirable in geostatistical modelling (Isaaks and Srivastava 1989) and a geologically

realistic nugget effect should normally not exceed 30% of the total variance (Deutsch 2002). The low nugget values for the vertical variograms are most likely related to the relative smaller lag distances used to calculate them compared to horizontal directions (lag distances of 0.25 versus 1 m). Therefore the vertical spatial variability could be captured in greater detail, hence resulting in a potentially smaller measuring error and relative low nugget. McKinley et al. (2004) observed a similar effect when comparing the experimental variograms of permeability variability calculated using a small and large sampling resolution (1 cm versus 4 cm lag distance). However, in the experimental variograms of the wackstone the horizontal direction defined the nugget effect. This might be the result of the used variogram search parameters and their relation to the geocellular modelling grid versus the limited thickness of the wackstone unit (< 40 cm). The vertical experimental variograms of both lithofacies have an undulating appearance illustrating a periodic phenomenon, such as the repetitive shallowing upward carbonate Hanifa formations semivariogram for all lithofacies that has very good vertical and spatial continuity, and is interpreted to have been deposited on shallow lagoon to shoal deposit lithofacies exists only above the mudstone and wackestone in three repeated cycles in the Upper Ulayyah at the outcrop. Its presence depends on the allochthonous transportation and therefore this facies has a amalgamated skeletal packstone, massive and oolitic skeletal grainstone deposits that are characterized by nearly continuous layer but have limited vertical extension.

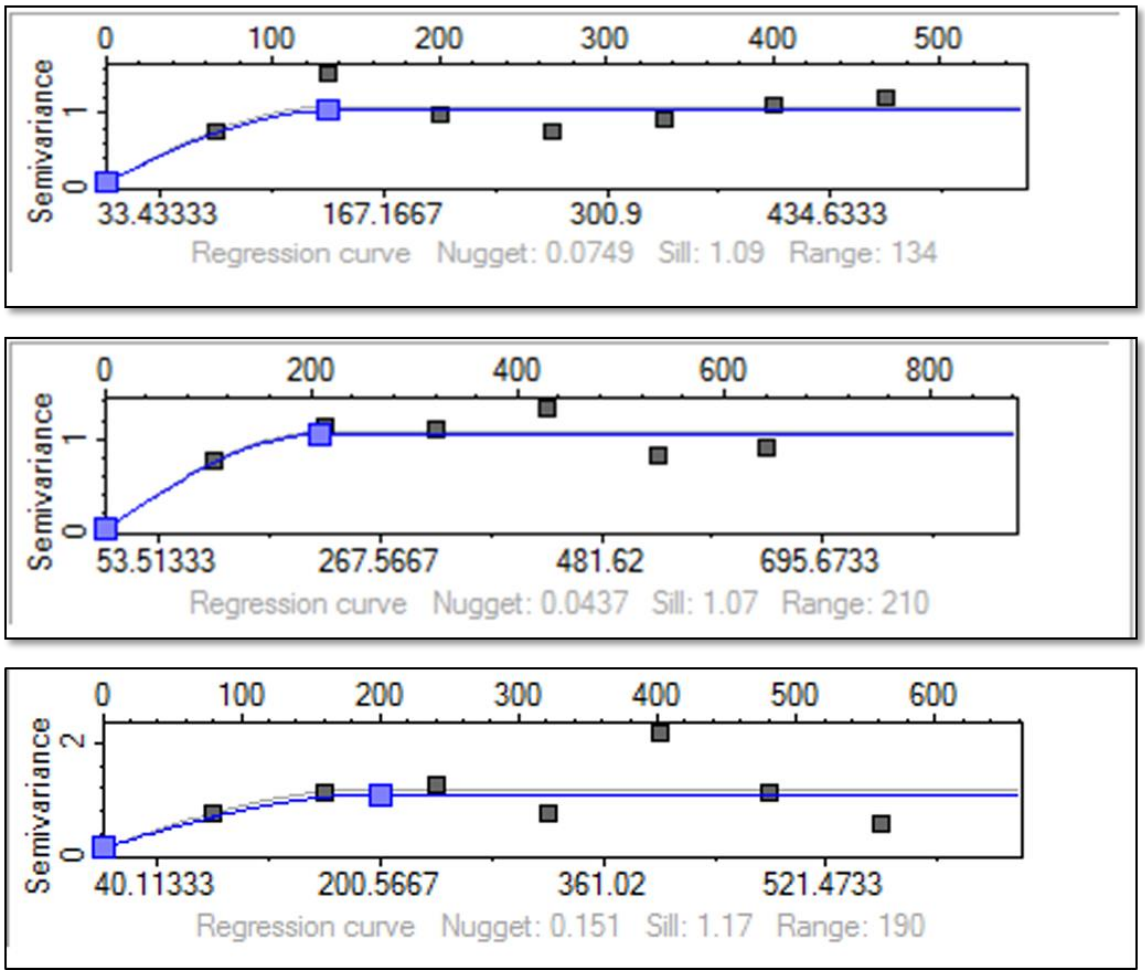

Figure 4.3 Semivariogram major (N-S), minor (S-W) and vertical direction of the lime mudstone lithofacies

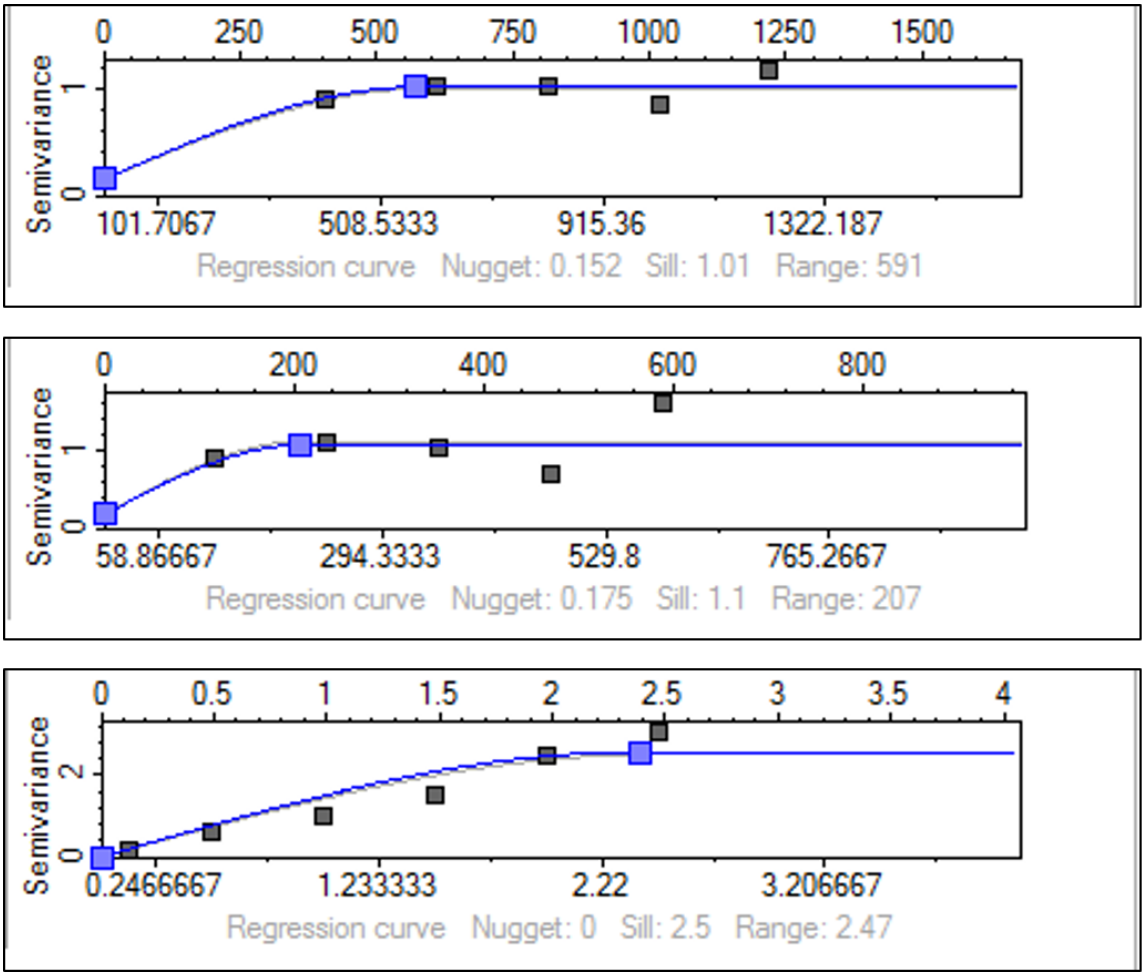

Figure 4.4 Semivariogram in major (N-S), minor (S-W) and vertical direction of the wackstone lithofacies

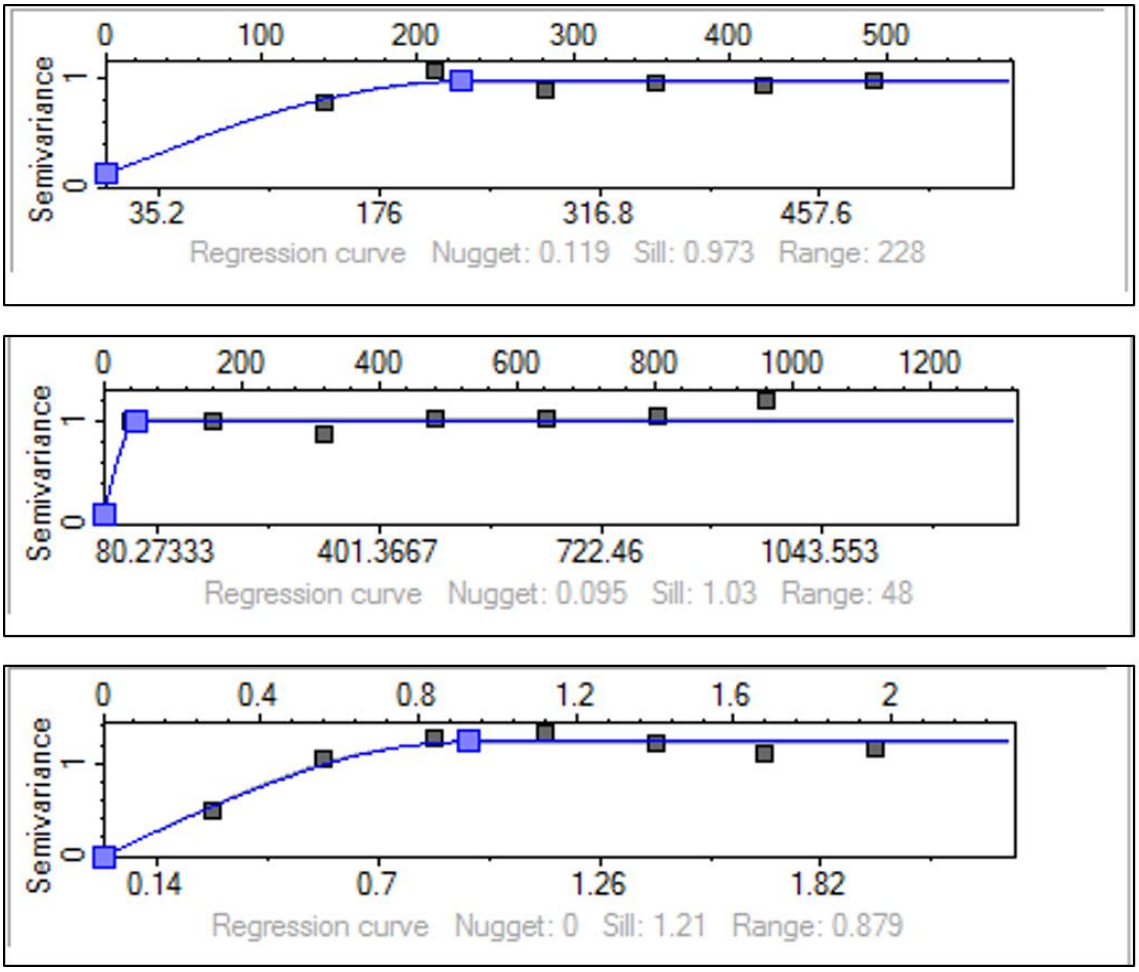

Figure 4.5 Semivariogram in major (N-S), minor (S-W) and vertical direction of the packstone lithofacies

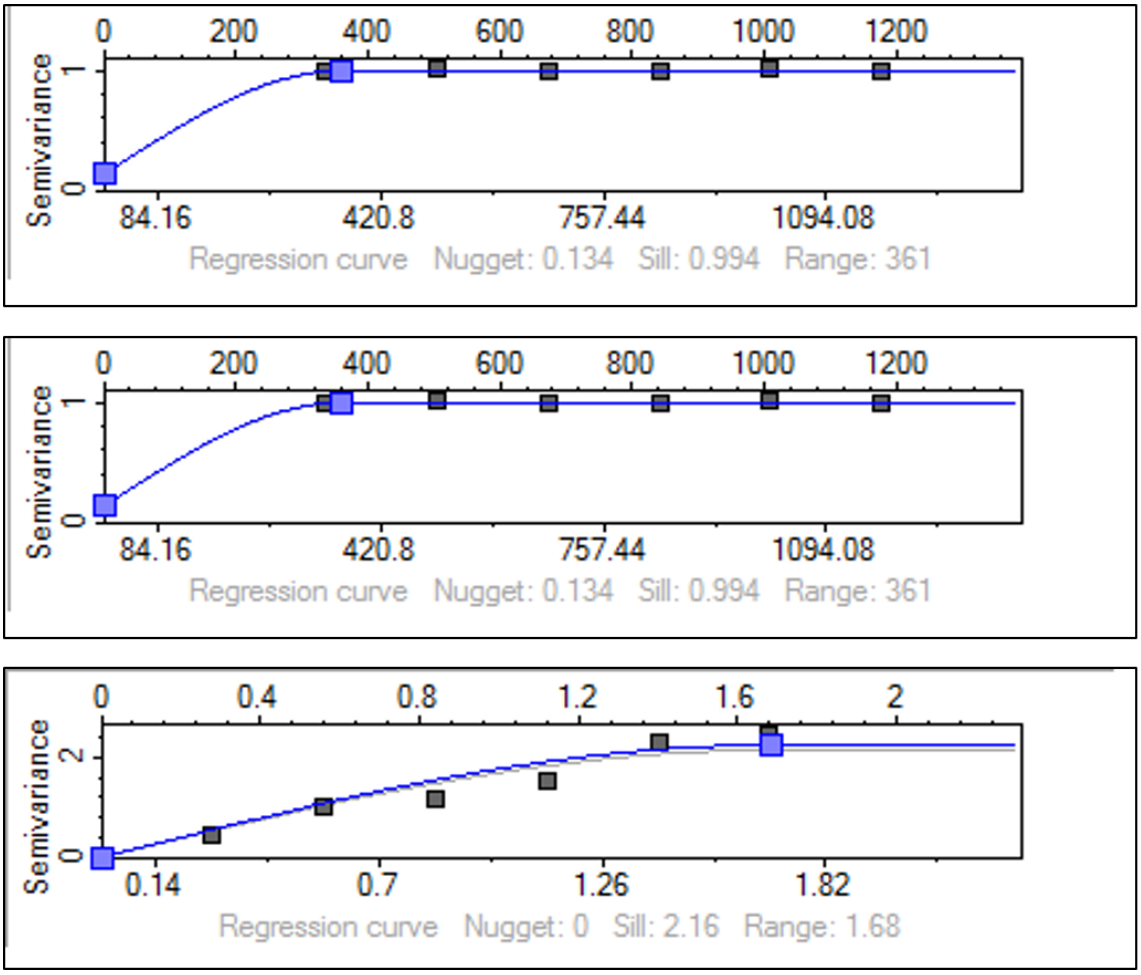

Figure 4.6 Semivariogram in major (N-S), minor (S-W) and vertical direction of the oncoidal lithofacies

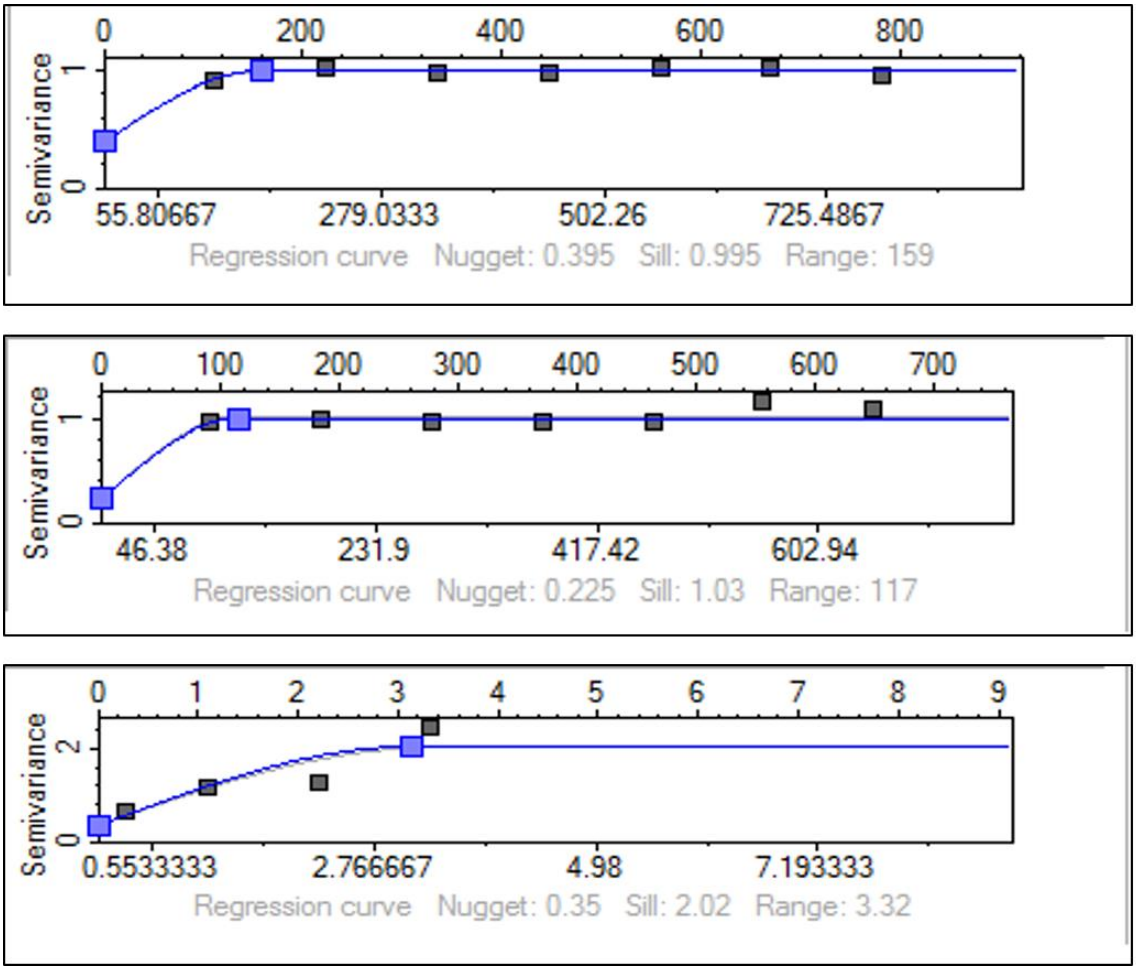

Figure 4.7 Semivariogram in major (N-S), minor (S-W) and vertical direction of the massive lithofacies

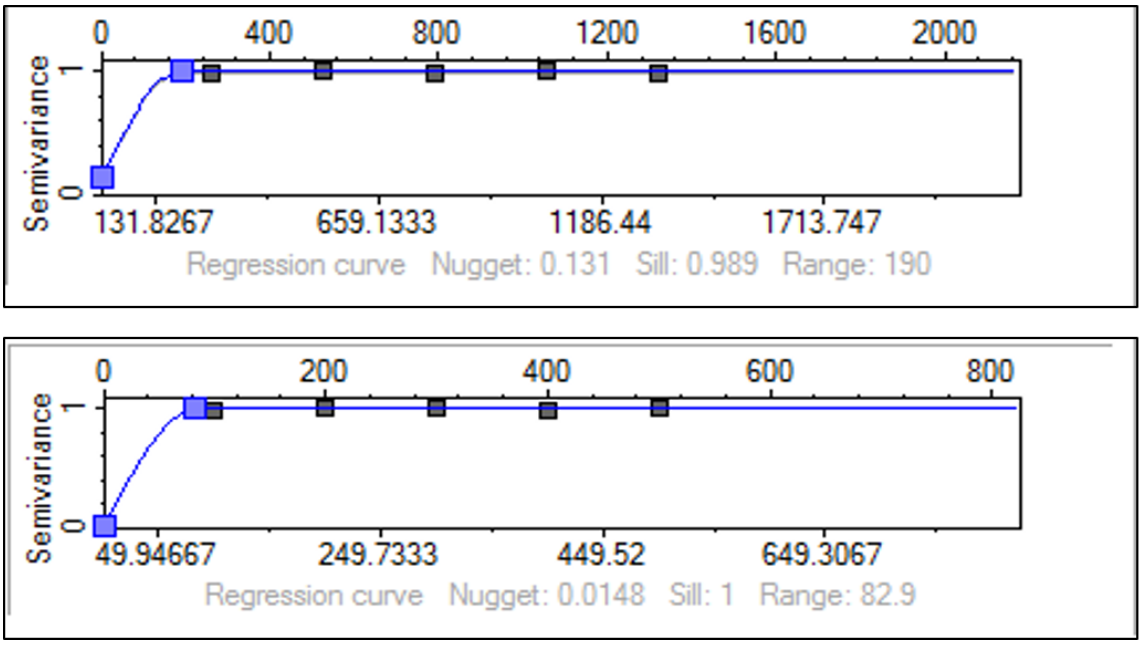

Figure 4.8 Semivariogram in major (N-S), minor (S-W) and vertical direction of the oolitic lithofacies

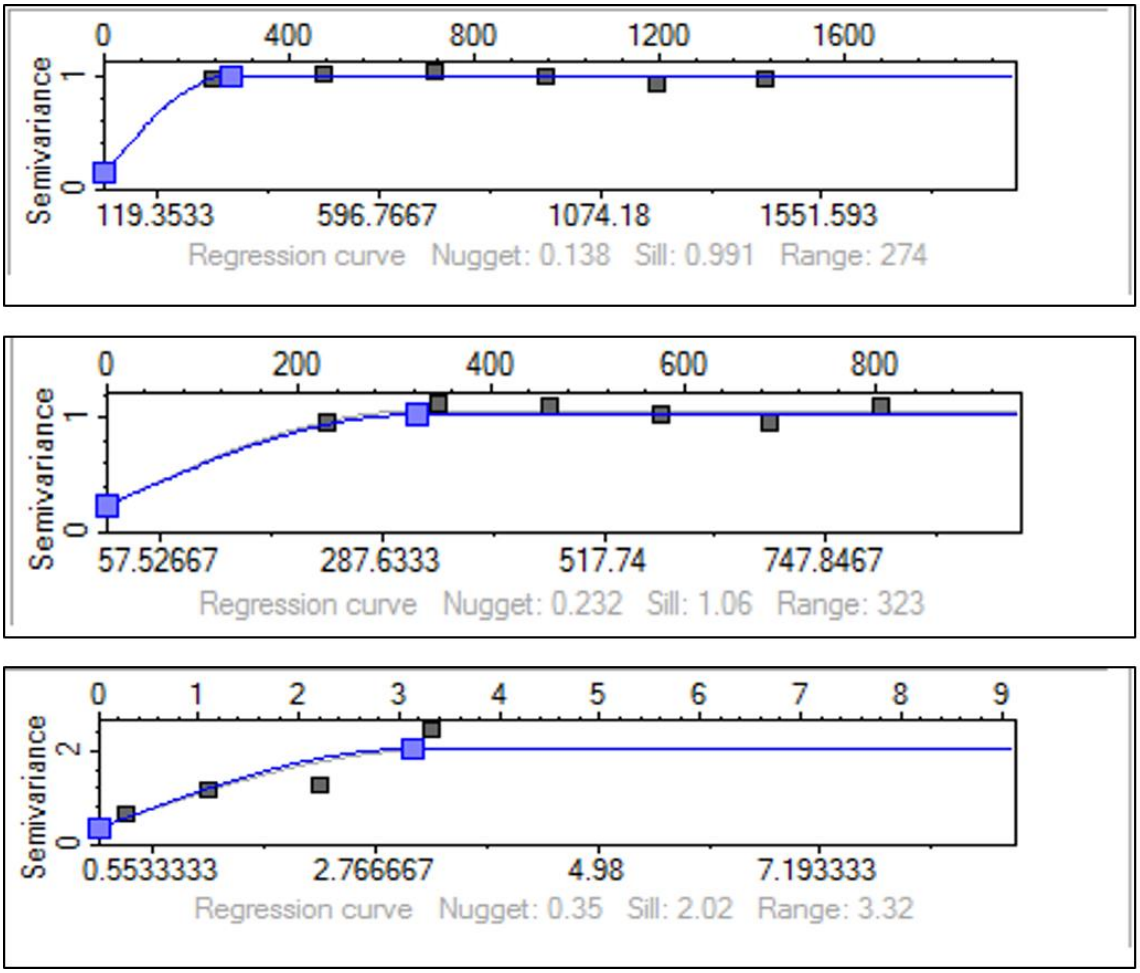

Figure 4.9 Semivariogram in major (N-S), minor (S-W) and vertical direction of the stromatoporoid lithofacies

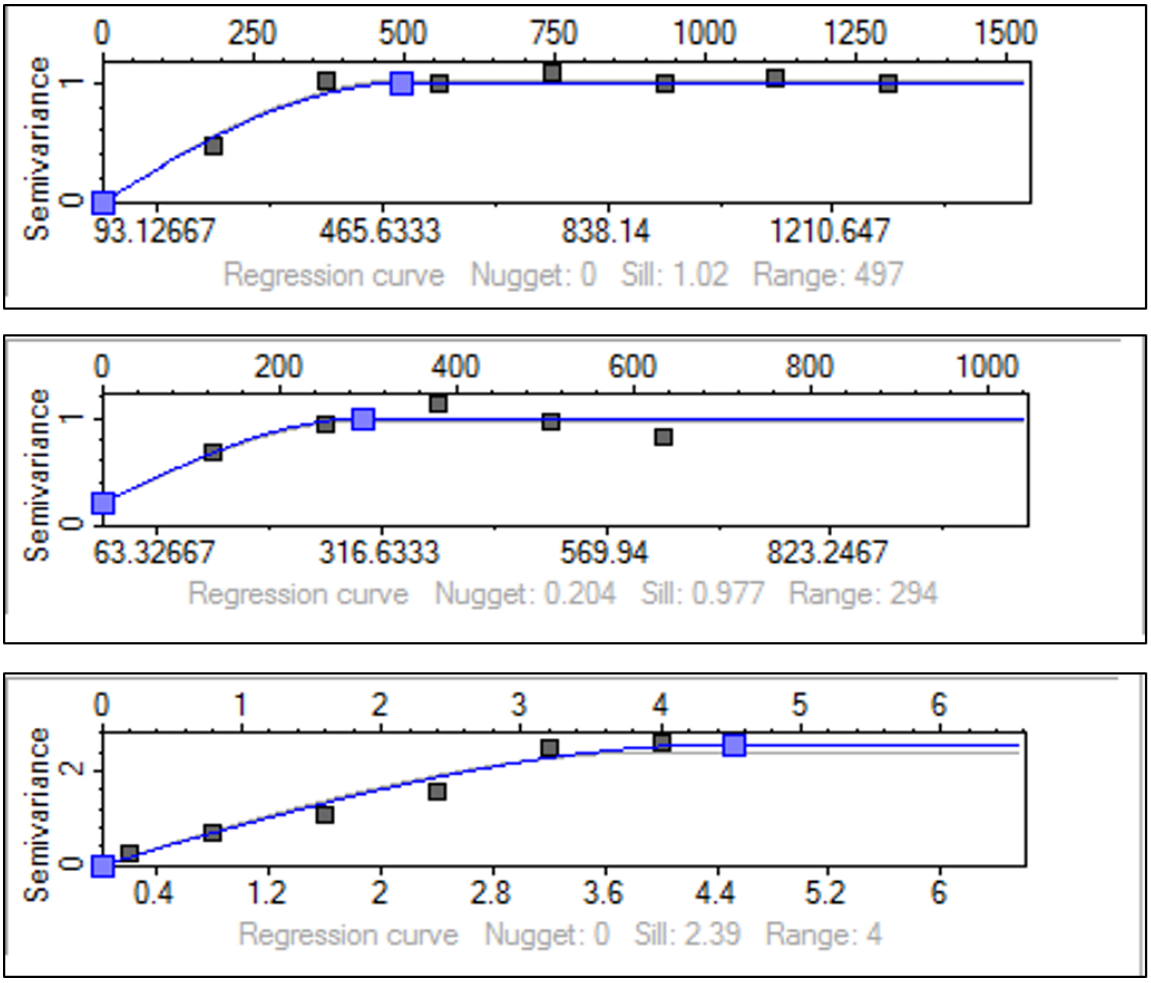

Figure 4.10 Semivariogram in major (N-S), minor (S-W) and vertical direction of the foraminiferal lithofacies

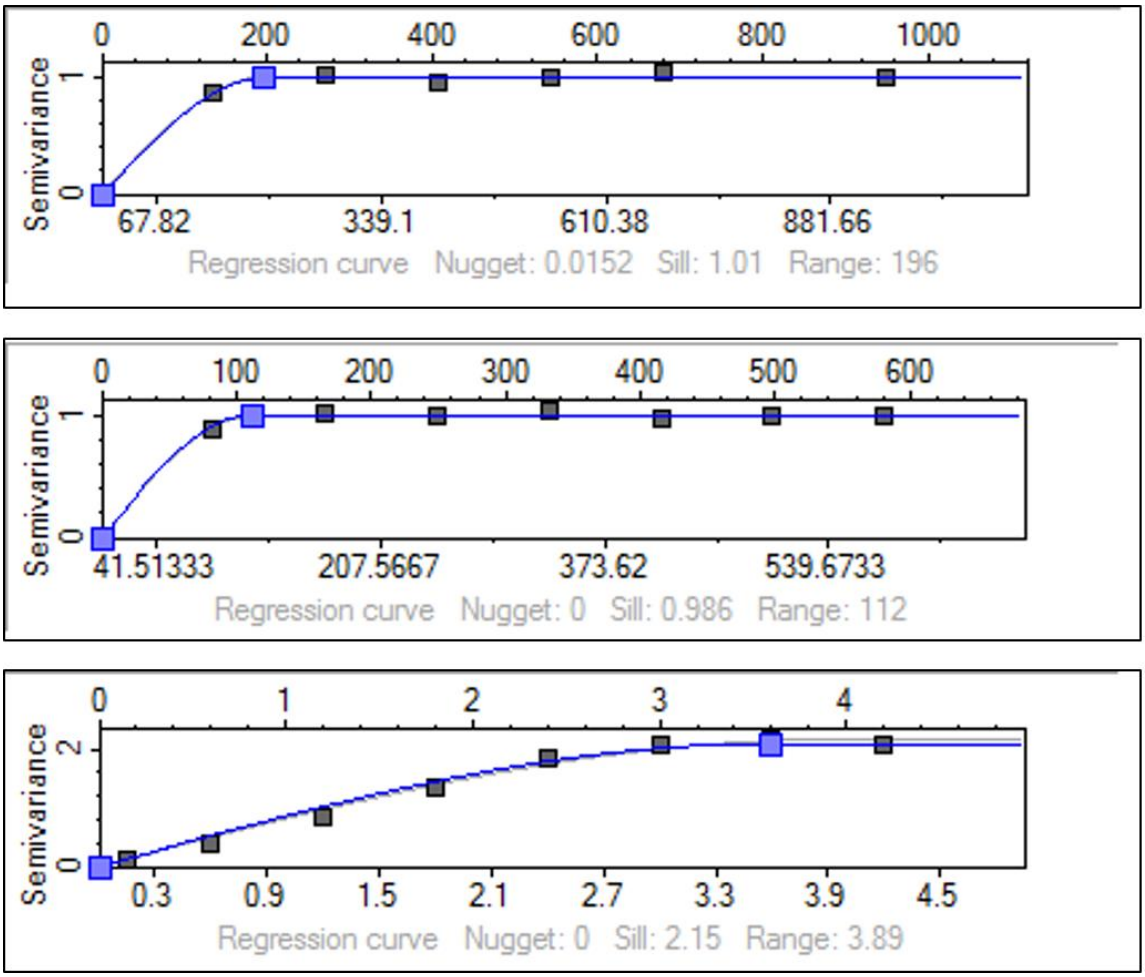

Figure 4.11 Semivariogram in major (N-S), minor (S-W) and vertical direction of the cross bed lithofacies

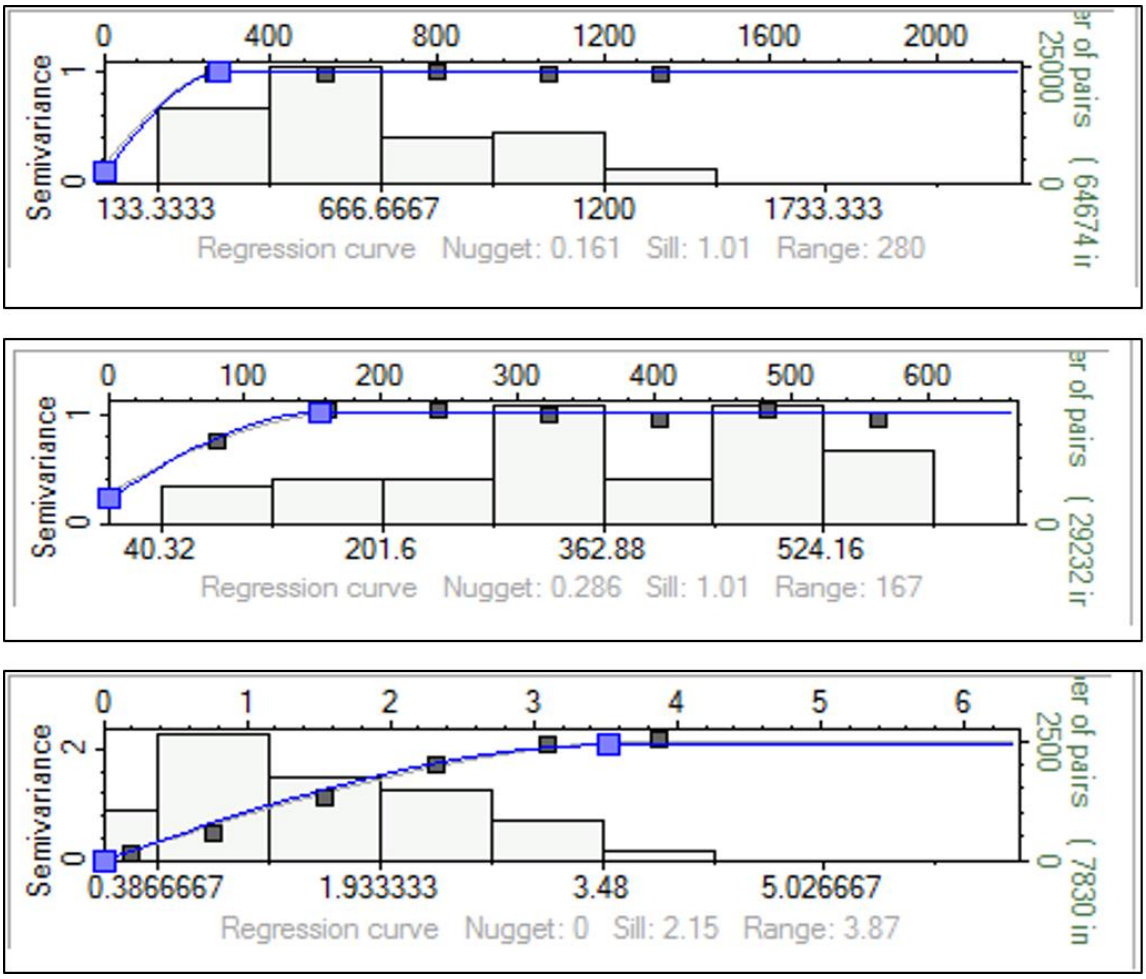

Figure 4.12 Semivariogram in major (N-S), minor (S-W) and vertical direction of the laminated sandy lithofacies

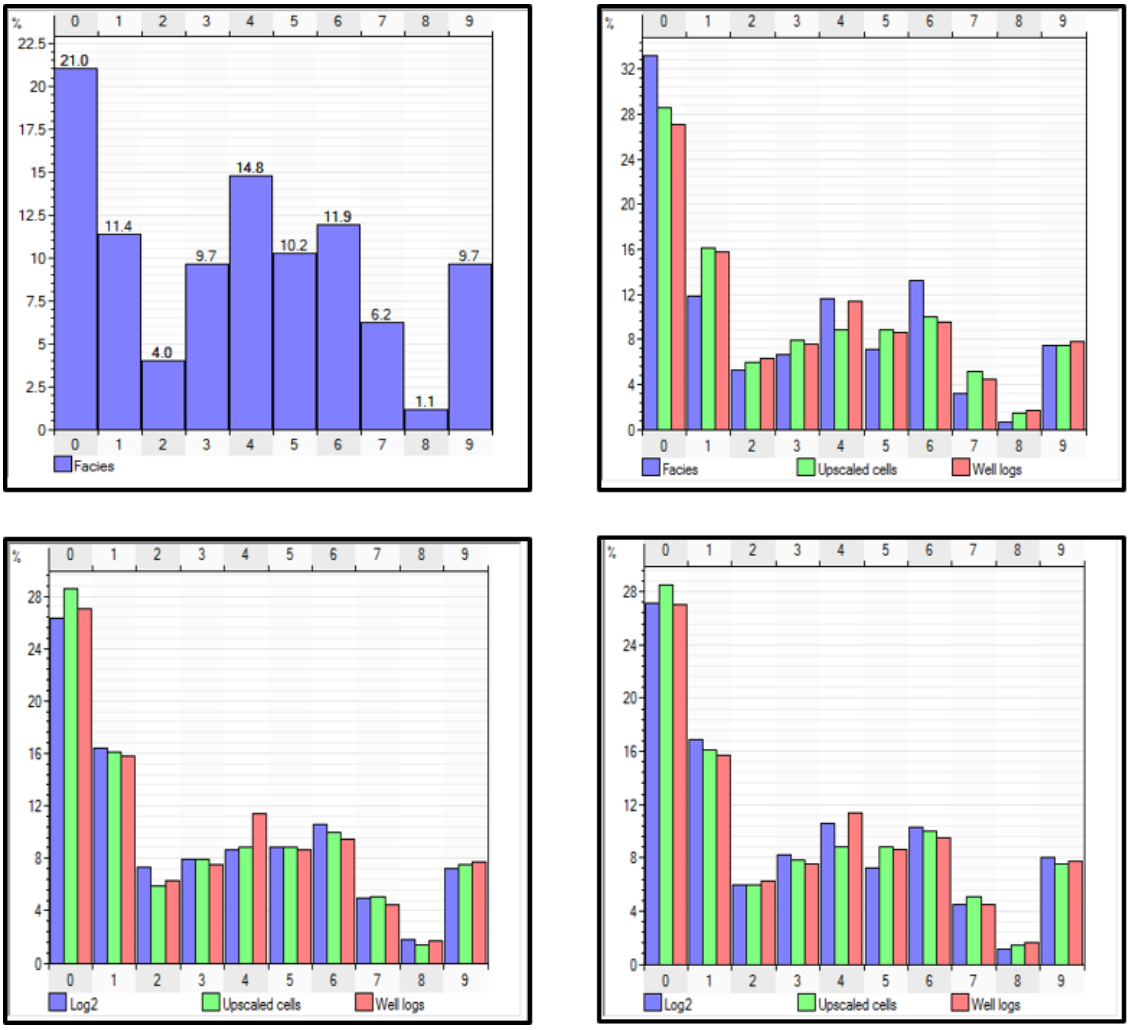

Figure 4.13 Lithofacies percentage in the 3-D model for three realizations that generated stochastically with up scaled cells for each pseudo well logs. The left diagram shows the outcrop lithofacies characterized only by 9 lithofacies

4.5 3D Outcrop Facies Model

The generated facies models show how the lithofacies are distributed in three dimensions based on the variogram models. In order to evaluate the geological integrity of these facies models, the field observations are compared with the multiple realizations of facies model by visual inspection. The facies models show an overall similar sedimentary architecture to that observed in outcrop, the large-scale features in the outcrop were visually examined to test the satisfactory match with the 3-D facies model. An ideal way to check the accuracy of the model can be directly comparing the high-resolution outcrop pictures with the model. This could be done by comparing small scale features such as the thin oncolitic layer in the lower section of Upper Ulayyah member with the model. While, the overall lithofacies proportions and distribution represent a good match to the original field data, some differences and potential modeling errors are observed. An expected difference is the absence of thin layers in the foraminiferal lithofacies a consequence of associated to the selected modeling grid resolution The model resolution is not sufficient to resolve these often thin layers (< 0.25 m), furthermore they would disappear in the upscaling process.

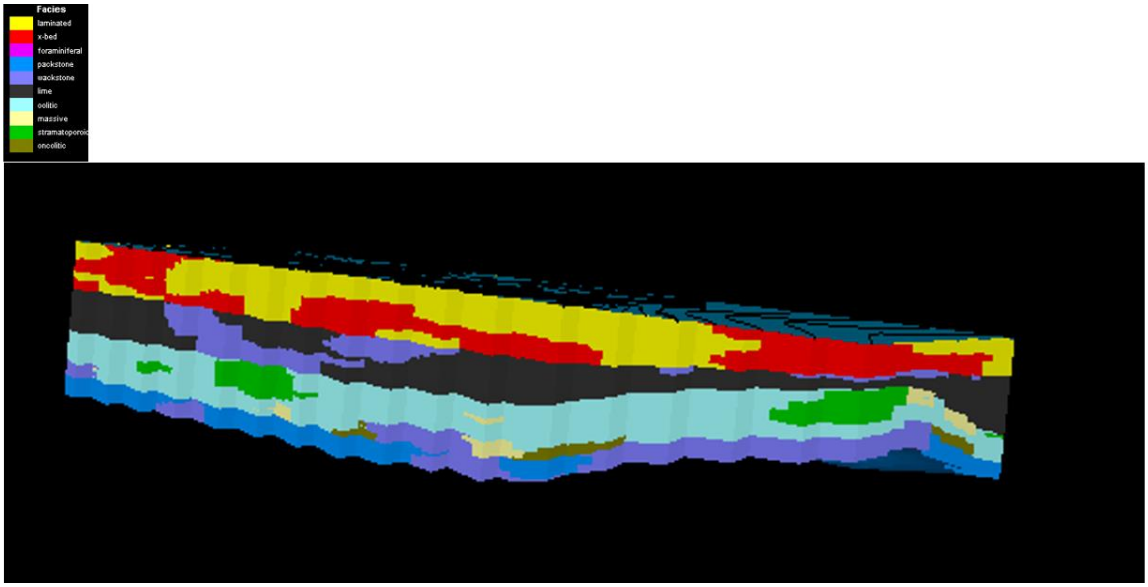

Figure 4.14 3-D facies model with outcrop stratigraphy shows three zones

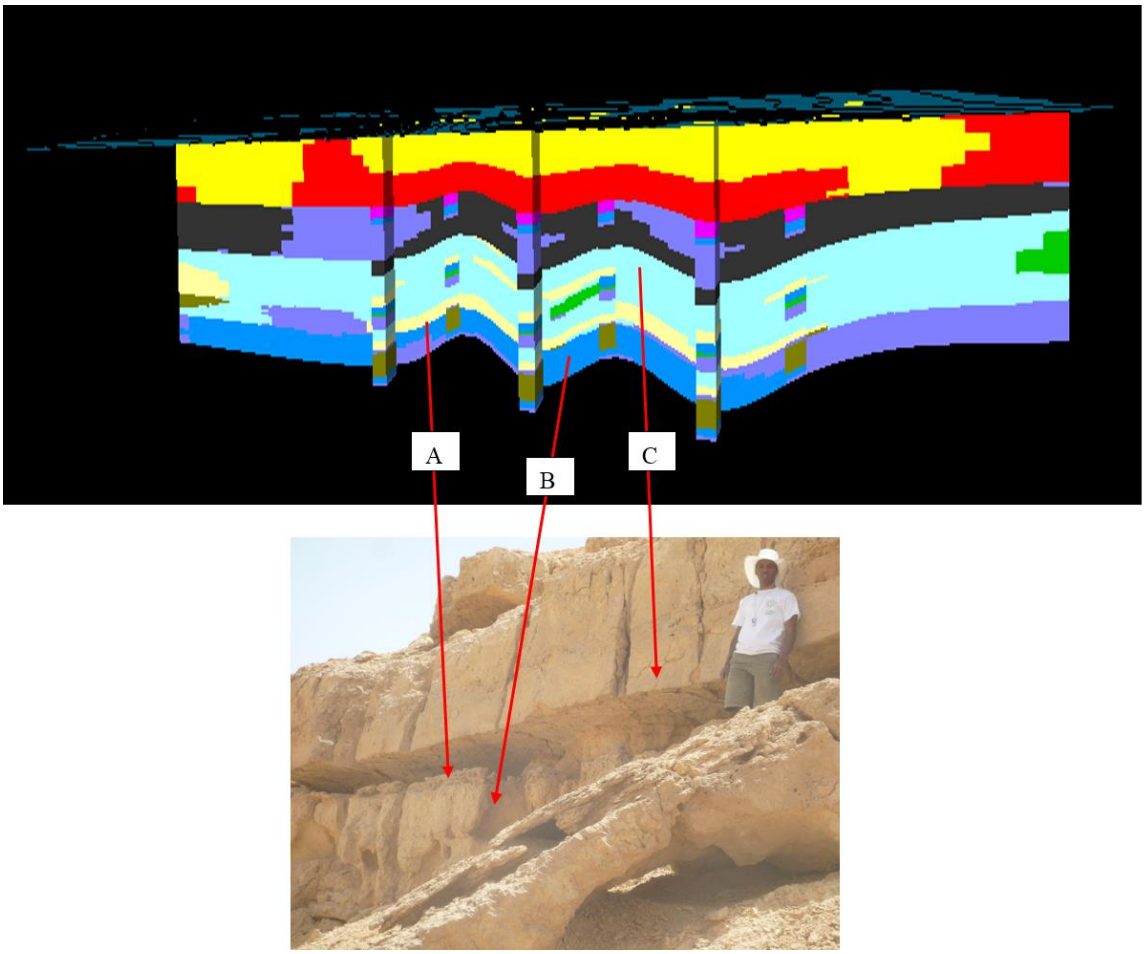

Figure 4.15 : 3-D facies cross section model with outcrop stratigraphy. Outcrop picture of Jabbal Abkyan was used to compare the small scale features of the outcrop with the 3-D facies model

4.6 Petrophysical Model

The three-dimensional geological (Petrel 2009) modeling software offers a wide range of possibilities for modeling the distribution of petrophysical properties. In contrast to the subsurface, outcrop analogue studies allow a direct determination of the spatial distributions of reservoir properties. Also outcrop data can be used to constrain the algorithms applied in the modeling process. Reservoir properties within a facies body, in the same stratigraphic position, remains in the same order of magnitude for hundreds of metres laterally. On a kilometre scale, facies bodies, reservoir properties and diagenetic

trends show gradual lateral changes, whereas the mostly stratigraphic cycle-controlled vertical differences vary commonly on a decimeter scale.

These observations within this particular setting were considered for the construction of the geological model. The detailed, deterministic geo-model was used as a main input for geostatistical data analysis and modeling the distribution of reservoir properties.

The model covers area on the scale of outcrop and provides both (a) high resolution sequence stratigraphic reservoir layering and (b) a detailed facies distribution. The high vertical resolution provides the possibility to model detailed variations of reservoir properties within individual reservoir bodies. Furthermore, the data distribution suggest a deterministic approach for modelling reservoir properties.

The investigation of thin sections showed that preservation and creation of pore space are restricted to high-energy shoal and grainstone shallow lagoon facies types and are modified by diagenetic history. Therefore, the primary facies types can be clearly subdivided into reservoir and non-reservoir facies.

These observations and the fact that the software requires a constant sampling rate led to the following steps in preparing the dataset for 3D modelling after the insertion of the plug measurements as point values .Subsequently, the porosity and permeability values of all non-reservoir facies types were set to zero. The step of data preparation was furthermore used for a quality control of the dataset. The upscaling process transfers porosity and permeability plug measurements to the neighboring grid cells.

In contrast to porosity, permeability tends to change exponentially and therefore requires a different averaging method for the upscaling process:

(1) Porosity: arithmetic average of point data upscaled on neighbor cells.

(2) Permeability: geometric average of point data upscaled on neighbour cells.

However, owing to the extraordinary high vertical resolution (average 1 m) of the 3D grid, which corresponds to the sampling rate of the plug measurements, the upscaling had no considerable impact on the quality of the model.

In order to establish the necessary input parameter I carried out geostatistical variogram analysis (Gringarten & Deutsch 2001) on the complete dataset with the original log data spaced between cm and a hundred meter. Based on the observations described above, the reservoir properties were analyzed for each facies type and each association with various lags, ranges, and so on. A reasonable variogram model could only be found for the facies associations, by using relatively large bin sizes and large ranges that are in the order of the observed facies changes

The small-scale heterogeneity of the lithofacies created in the lithofacies model was represented by small-scale porosity and permeability variability, which could represent high porosity zones or permeability barriers. The reservoir lithofacies (cross bedded skeletal grainstone and laminated sandy grainstone) have higher porosity and permeability values than the surrounding rocks.

The porosity model was compared to the facies model. The facies model shows a high degree of continuity, but low porosity patches were also captured in the model, and may represent a potential permeability barriers

In this regard, the constructed lithofacies model of the study area was intended to be equivalent to one cell of the subsurface reservoir models, assuming that one cell of the reservoir model covers an area nearly the same as one cell of subsurface models (Douglas, 1996; Al-Khalifah and Makkawi, 2002).

Studying outcrops equivalent to the Upper Ulayyah reservoir of Hanifa Formation at this higher resolution helps to better understand reservoir heterogeneity reservoir stacking patterns, sequence hierarchy, and their lateral correlations. Although the 3-D facies model has a layer cake pattern at low resolution, it exhibits a higher degree of heterogeneity when examined at higher resolutions.

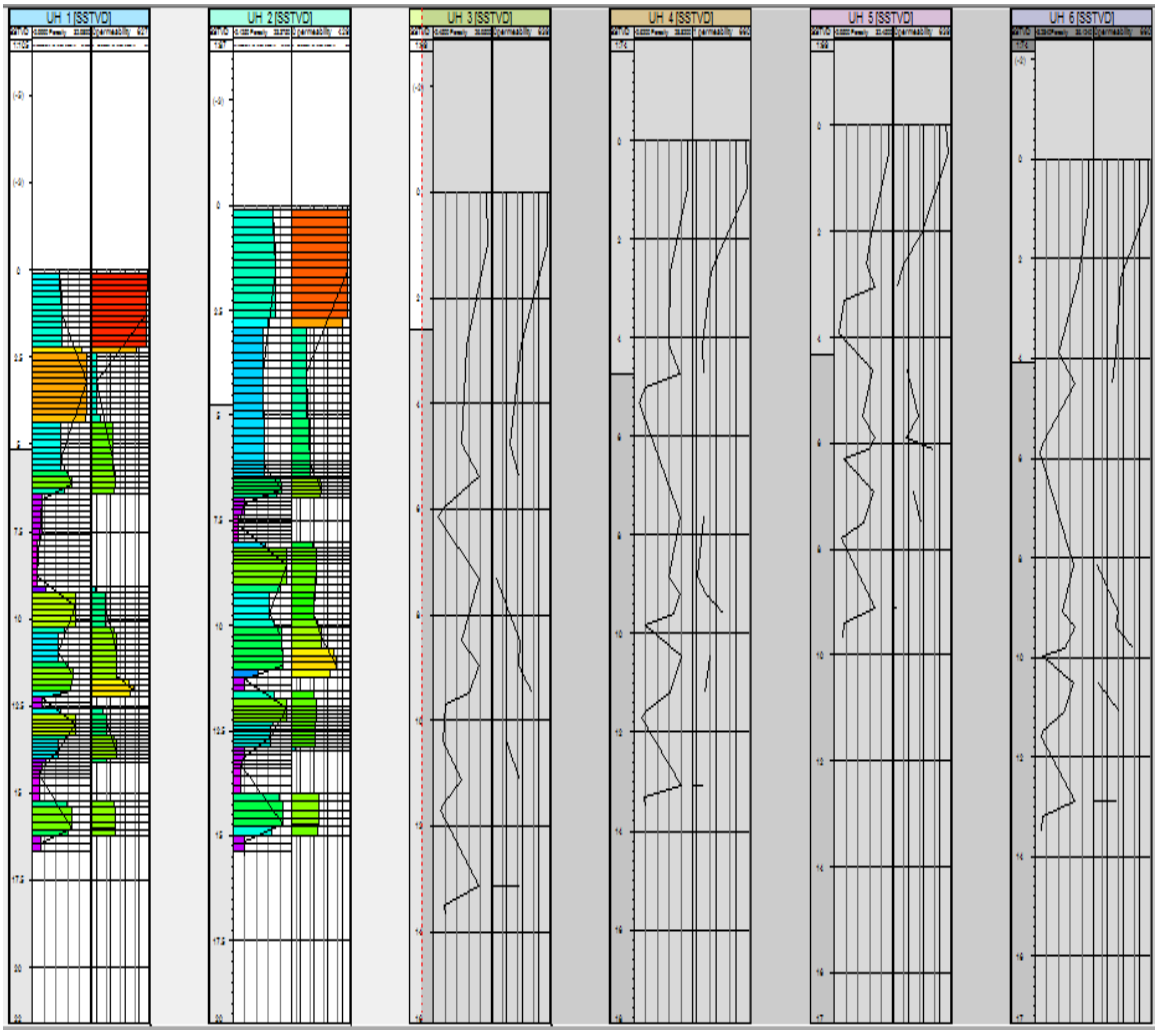

Figure 4.16 Upscaling of petrophysical properties distribution in the outcrop sections

Major direction

Minor direction

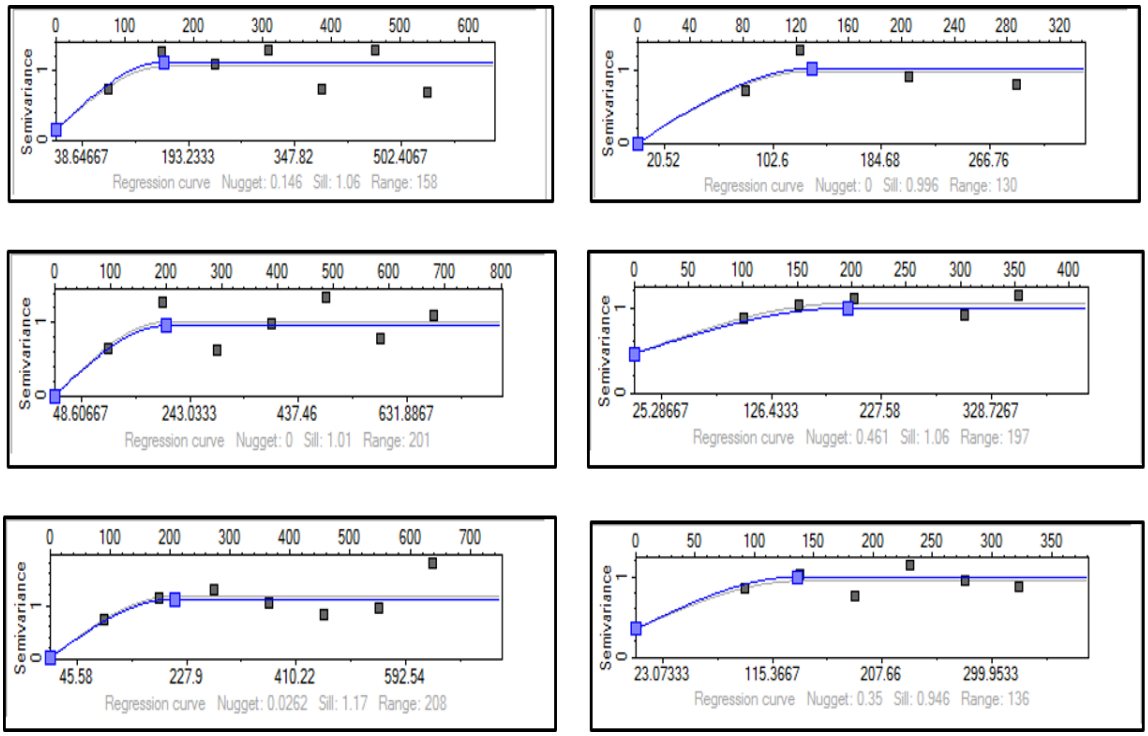

Figure 4.17 Semivarigram model of porosity of three facies association zones

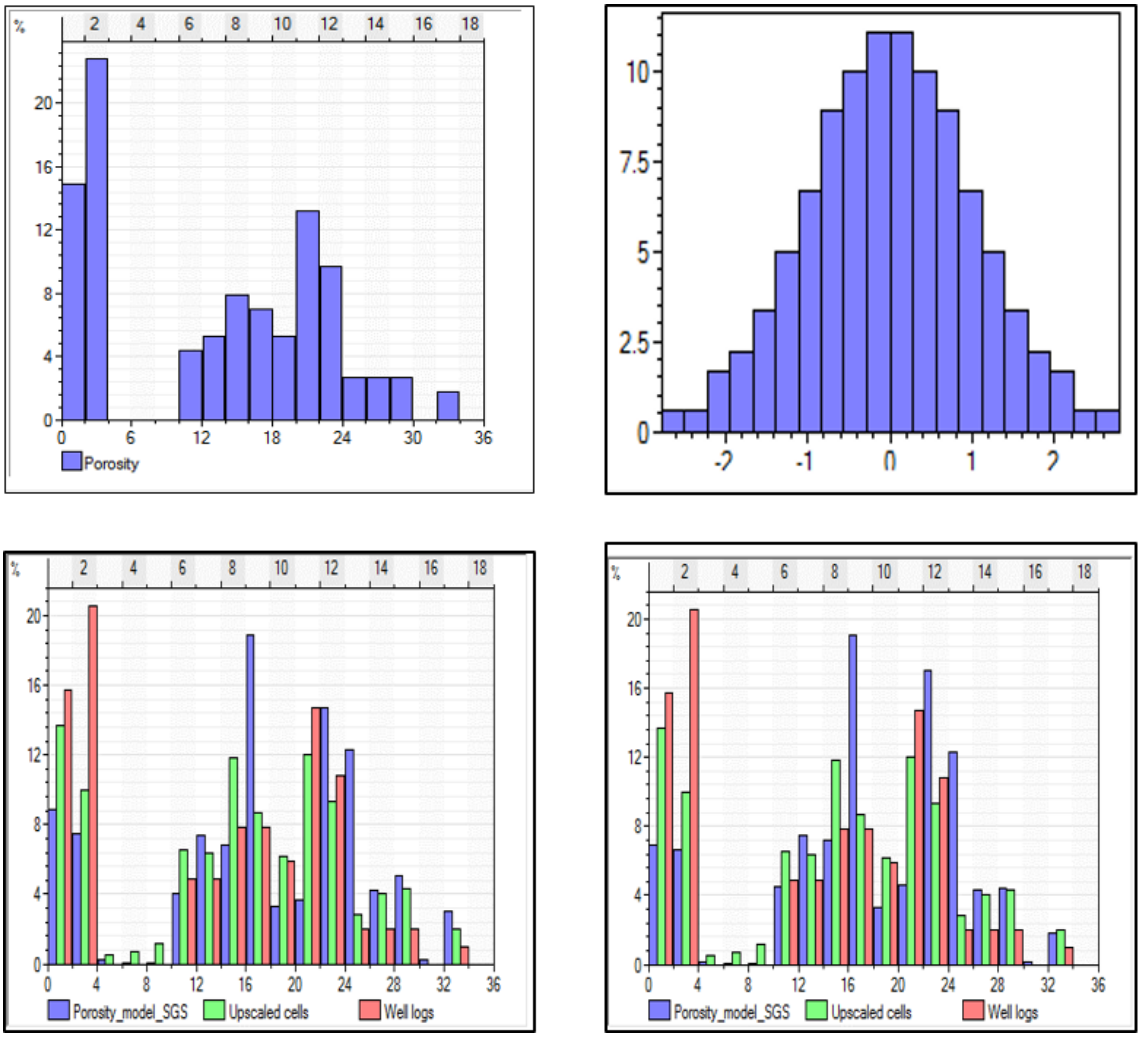

Figure 4.18 Realizations of Porosity model of upper Ulayyah reservoir equivalent

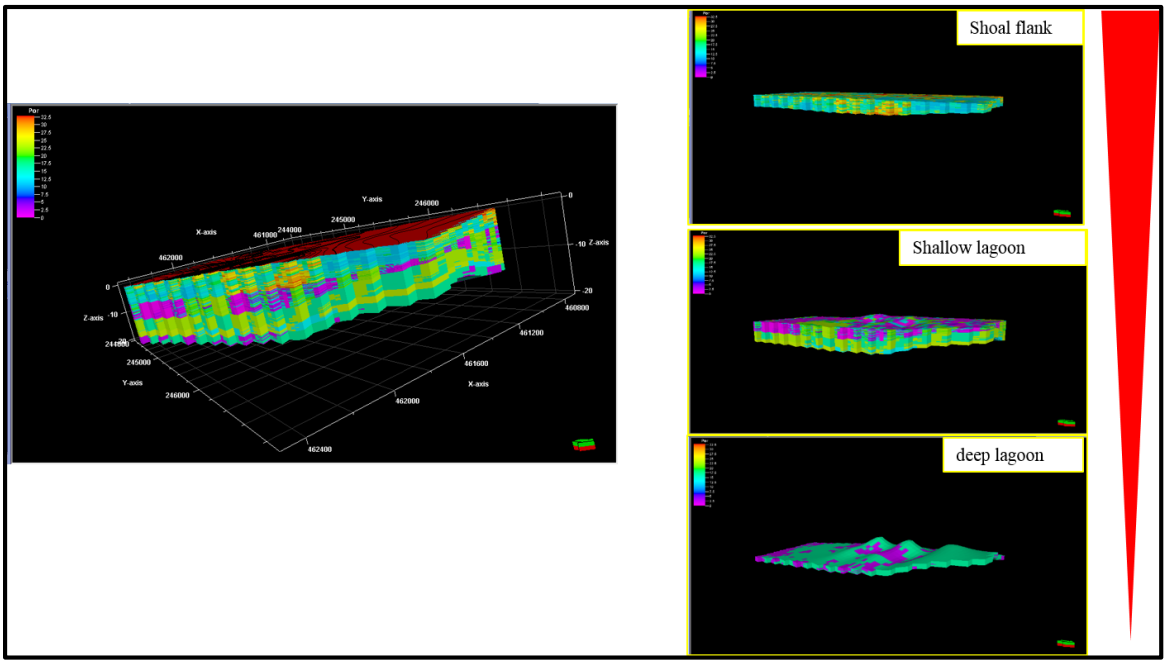

Figure 4.19 3-D porosity model of Upper Ulayyah reservoir generated by SGS. The small-scale heterogeneity created in the lithofacies model was represented by small-scale porosity variability

Major direction

Minor direction

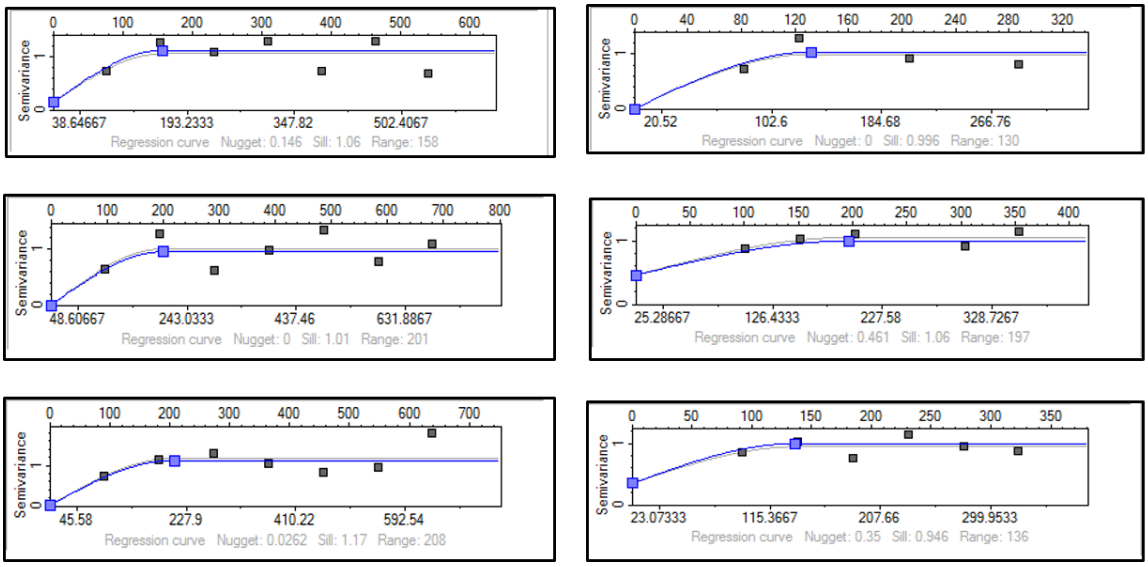

Figure 4.20 Semivarigram model of permeability of three facies association zones

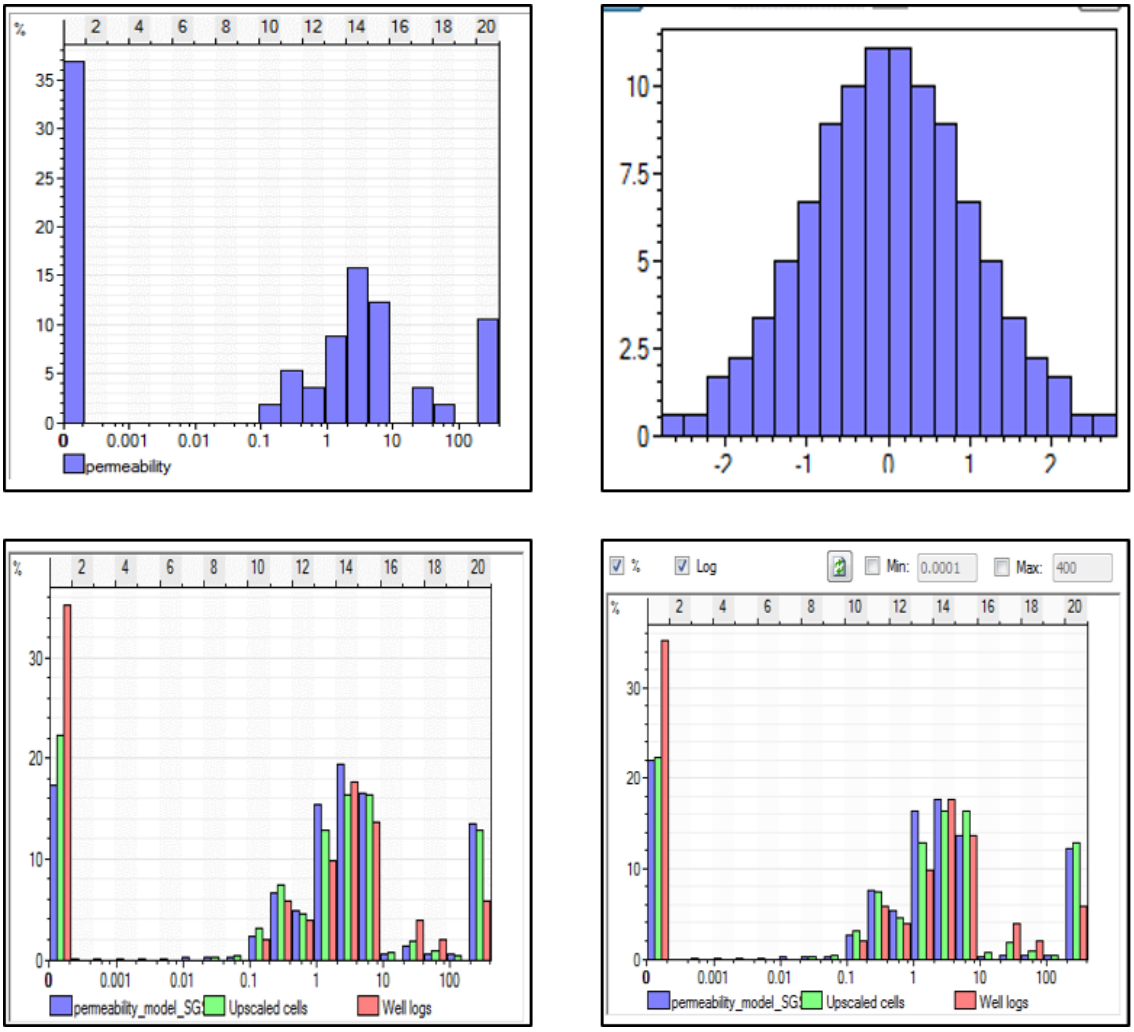

Figure 4.21 Realizations of permeability model of upper Ulayyah reservoir equivalent

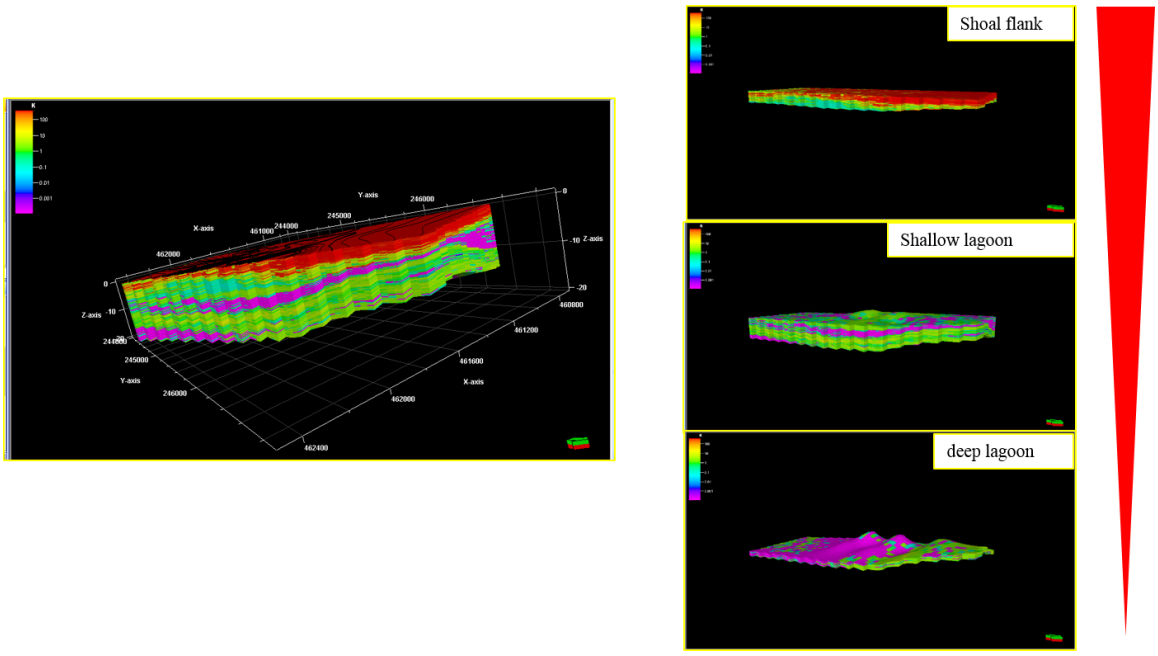

Figure 4.22 3-D permeability model of Upper Ulayyah reservoir generated by SGS. The small-scale lithofacies heterogeneity created in the lithofacies model was represented by small-scale permeability variability

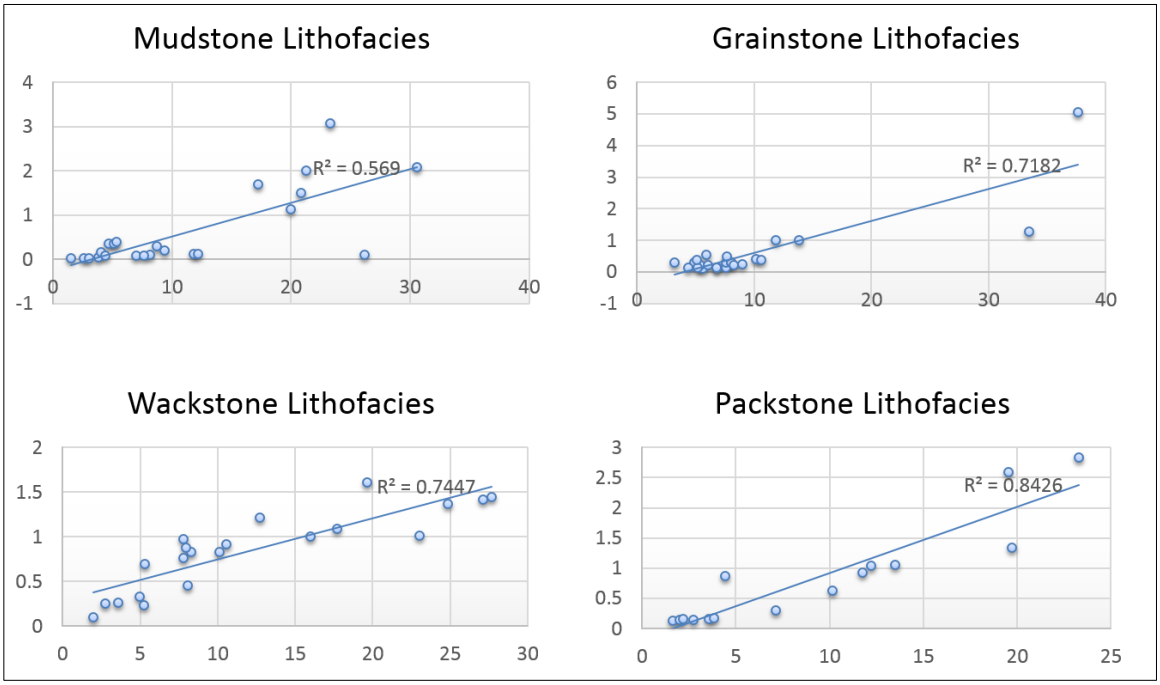

Figure 4.23 X-plot shows porosity vs permeability of lithofacies associations at outcrop sections.

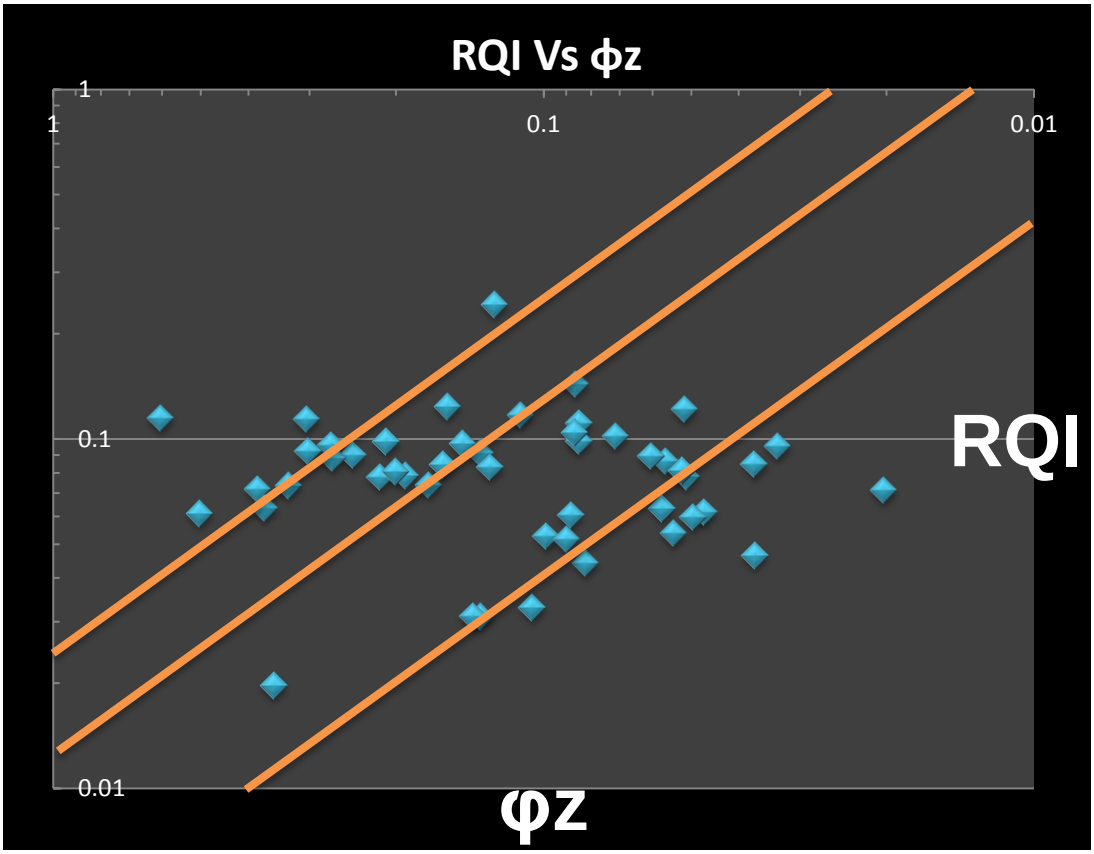

Figure 4.24 Reservoir quality index of three lithofacies associations in upper Ulayyah reservoir equivalent

CHAPTER 5

CONCLUSIONS AND RECOMMENDATIONS

5.1 Conclusions

The reservoir properties show a close relationship to the lithofacies and the associated matrix mud content. Porous facies types are restricted to the high-energy shoal facies, whereas both open marine muddy and shallow lagoon are commonly tight since the muddy matrix protects the sediment from diagenetic fluids and associated moldic porosity creation. Reservoir heterogeneities within the shoal bodies are mainly related to the mud content and early diagenesis.

All three hierarchies of stratigraphic cycles have an impact on quality and presence of the flow units: (a) large-scale cycle – controls the lateral extent, as well as retro- and pro-gradation of the reservoir bodies; (b) medium-scale cycles – control the stratigraphic presence of the reservoir facies associations; and (c) small-scale cycles – control the mud content and early moldic porosity creation in facies types with primary porosity, which are considered as key drivers for systematic vertical and horizontal changes in porosity and permeability within the reservoir bodies.

The primary aim of reservoir models is to estimate and maximize the amount of recoverable hydrocarbons or potable water. In traditional sedimentological research the emphasis lays on producing geological models relevant to hydrocarbon exploration, however the increasing demand for potable water around the world might steer research to also consider these reservoir types more frequently. The importance of the internal

reservoir architecture was greatly under estimated in previous study, even though approximately 60% of moveable oil in carbonate reservoirs are trapped within such heterogeneities (Tyler and Finley 1991). This directly affects the recovery efficiency, which is in general low (less than 25%) even with the sophisticated recovery technologies (Tyler and Finley 1991). The reservoir architecture describes the internal heterogeneities and is a product of depositional and diagenetic processes, and ultimately controls the fluid flow path that is large-scale permeability (North and Prosser 1993). It is therefore of utmost importance to locate and describe reservoir heterogeneities. The accessibility of outcrops versus sub-surface reservoir data makes it easier to study the variability and distribution of geological properties in such an outcrop analogue, especially in three-dimensions and to resolve sub-seismic features. These studies allow better reservoir characterization by reducing uncertainties and analyzing geological variability (e.g. Cuevas Gozalo and Martinius 1993; Beaty 1997; Knox 1997; Hornung and Aigner 2002a, 2002b; Sullivan et al. 2004; Brandse£ter et al. 2005). A suitable analogue should have an excellent three-dimensional exposure over an area large enough to capture the required heterogeneities and discontinuities (preferably at a scale comparable scale with the reservoir). Outcrop studies have provided fundamental information and improved our understanding of the sedimentary architecture of depositional systems. It however remains difficult to extract quantitative data on the size, shape and the vertical and lateral stacking of sedimentary bodies (Bryant and Flint 1993; Adams et al. 2005). For example, in the last two decades geologists have made detailed geological descriptions, interpretations and conceptual models (e.g. numerous papers in Miall and Tyler 1991), however how this largely qualitative information can be utilized in reservoir models as an aid to geostatistical

modelling remains problematic (Bryant and Flint 1993; North and Prosser 1993; McCaffrey et al. 2005).

The analysis of the variograms has a large interpretative component, structures such as nugget effect and periodicity can be ascribed to several causes, including sampling variability, measurement errors and geological features. However, sometimes in these interpretations little regard is paid to the possible geological causes of the structures in considerations of statistical factors. This practice decrease the utility of variograms as a diagnostic tool.

The resultant variogram models should therefore better describe the spatial variance of the lithofacies and subsequently should provide more accurate facies distribution models by directly linking the observed geology to the reservoir model. In addition, the classified point-cloud dataset provides continuous conditioning and accurate lithofacies probability curves along the studied section. These parameters are considered critical to accurately model the facies distribution (Falivene et al. 2006). In a comparison study of continuous (vertical transects) versus normally widely spread (sedimentary sections) conditioning data the continuous conditioning data illustrated that it helps to reduce uncertainty related to lateral facies distribution by assisting the facies modelling process to better populate the entire modelling grid. Furthermore the observed variation of the stochastic realizations was reduced, which implies an increase in model precision (Journel and Deutsch 1993).The variograms computed using the classified point-cloud dataset could also offer a better understanding of the relationship between geological features and how these feature are displayed in the structures of the experimental variograms and which short to long range structures are most important for the subsequent facies modelling. This enhanced insight

may in addition help to better model experimental variograms in scenarios when results are more erratic, for example variograms calculated from well data, and analyze how outcrop results should be modified for sub- surface reservoir conditions. Another major issue is related to the study area selection, where the exposure needs to be accurately analyzed spatially additionally to make accurate field-based interpretations and minimize errors. In order to compute reliable directional variograms a substantial amount of data is required (Olea 1994) alongside a sound understanding of the geology. The numerous uncertainties and limitations that need to be considered for outcrop modeling in general (Enge et al. 2007; Verwer et al. 2007; Van Lanen et al. 2009; Fabuel-Perez, 2010). In my study the individual data points of the experimental variogram were not available for further analysis as the variogram calculation module in PETREL^{TM} does not provide them. This has limited the variogram analysis (e.g. modeling variograms using various nested functions) and therefore future more refined variogram calculations are recommended using some other software, for example, the Geostatistical Library (GSLIB) (Deutsch and Journal 1998) or Stanford Geostatistical Modelling Software (SGeMS) (Remy et al. 2009).

5.2 Recommendations

Though the need for quantitative analysis in outcrop studies, and a better integration of the results in the geostatistical modelling process, have been realized (e.g. Kerans et al., 1995), for long no real progress has been made. The primary reason has been the difficulty of capturing the two- and three dimensional geometry of stratal horizons or boundaries between lithofacies and genetic units in a reliable and accurate manner. The awareness

that more accurate quantitative information on the sedimentary architecture might be beneficial has led to several advances in digital data collection techniques over the last decade. Stafleu et al.,1996; Bracco-Gartner and Schlager, 1997 revolutionized traditional outcrop studies using respectively photogrammetric methods and total-station laser ranging equipment to capture and quantify morphologic data from outcrop cliff faces. However, these technologies were expensive and no software packages were available to properly process and analyze the data. Recent advances in digital mapping tools as well as computer hardware and software development made the integration with traditional geologic outcrop studies more straightforward. The digital tools such as differential GPS (Global Positioning System) and (terrestrial and airborne) LiDAR (Light Detection and Ranging) equipment allow rapid acquisition of high resolution three-dimensional digital outcrop datasets in their correct geospatial position. Bellian et al. (2005) and Slob and Hack (2004) provided the first comprehensive reviews of incorporating this technique in outcrop studies. The acquired three-dimensional point cloud is geo-referenced by the integral DGPS measurement taken of the scan station position. Digital photogrammetry techniques allow draping of ortho-rectified images of both aerial and ground-based derived photographs over the acquired datasets or color-coding the point clouds. These datasets can be viewed interactively in modeling software packages from any desired orientation to gain more insight in three-dimensional geometries and the distribution of geological properties (Jones et al. 2004; Pringle et al. 2004, 2006; Verwer et al. 2007. The integration of traditional and spatial outcrop data forms a digital outcrop model (DOM). The DOM functions as a digital database holding all possible collected outcrop data in their correct geographical spatial position. I strongly recommend to use LIDAR teqnique

for the Ulayyah reservoir equivalent of the Hanifa formation. I recommend to do comprehensive analysis in term of diagenesis and to identify the numerous reservoir units within the Ulayyah reservoir member.

References

Abu Ali, M., Grover, G., Hwang, R., and Baskin, D., 1995. Geochemical analysis of reservoir continuity and connectivity, Arab-D and Hanifa reservoirs, Abqaiq Field, Saudi Arabia. AAPG Bulletin, 79, 1191.

Adams, E.W., Grotzinger, J.P., Watters, W.A., Schro¨der, S., McCornick, D.S. and Al-Siyabi, H.A., 2005 Digital characterization of thrombolite-stromatolite reef distribution in a carbonate ramp system (terminal Proterozoic, Nama Group, Namibia). AAPG Bull., 89, 1293–1318.

Al-Husseini, M.I., 1997. Jurassic sequence stratigraphy of the western and southern Arabian Gulf. GeoArabia (Manama), 2, 361-382.

Al-Husseini, M.I., 2000. Origin of the Arabian Plate structures; Amar collision and Najd Rift. GeoArabia (Manama), 5, 527-542.

Alsharhan, A. S. and Kendall, C. 1986. Precambrian to Jurassic Rocks of Arabian Gulf and Adjacent Areas: Their Facies, Depositional Setting, and Hydrocarbon Habitat, *American Association Petroleum Geologists Bulletin* 70 (8): 977–1002

Alsharhan, A. S. and A. E. M. Nairn, 1997. Sedimentary basins and petroleum geology of the Middle East.

Aigner T, 1985 Storm depositional systems. Dynamic stratigraphy in modern and ancient shallow-marine sequences. Lect Notes Earth Sci 3:1–174.

Aigner, T., Braun, S., Palermo, D. and Blendinger, W., 2007 3-D geological modelling of a carbonate shoal complex: reservoir analog study using outcrop analogs. First Break, 25, 65–72.

Alesi EJ, 1984 Der Trigonodus-Dolomit im Oberen Muschelkalk von SW-Deutschland. Arb Geol Pala¨ont Inst Univ Stuttgart N F 79:1–53

Ayres, M. G., M. Bilal, R. W. Jones, L. W. Slentz, M. Tartir and A. O. Wilson., 1982. Hydrocarbon Habitat in Main Producing Areas, Saudi Arabia. *American Association of Petroleum Geologists* 66 (January): 9.

Bashore, W.M., Araktingi, U.G., Levy, M. and Schweller, W.J., 1994. Importance of a geological framework and seismic data integration for reservoir modeling and subsequent fluid- flow predictions. In: Stochastic modeling and geostatistics: principles, methods, and case studies (Volume I) (Eds J.M. Yarus and R.L. Chambers), 177 - 199. AAPG Computer Applications in Geology 3, Tulsa.

Bellian, J.A., Beck, R. and Kerans, C., 2007. Analysis of hyperspectral and lidar data: remote optical mineralogy and fracture identification. Geosphere, 3: 491 - 500.

Bellian, J.A., Kerans, C. and Jennette, D.C., 2005. Digital outcrop models: Applications of terrestrial scanning LiDAR technology in stratigraphic modeling. Journal of Sedimentary Research, 75: 166 - 176.

Bond, C.E., Shipton, Z.K., Jones, R.R., Butler, R.W.H. and Gibbs, A.D., 2007. Knowledge transfer in a digital world: field data acquisition, uncertainty, visualization, and data management. Geosphere, 3: 568 - 576.Brigaud BFG, Vincent DC, Deconinck GF, Blanc P, Trouiller A., 2010. Acoustic properties of ancient shallow marine carbonates: effect of depositional environments and diagenetic processes (Middle Jurassic, Paris

Basin, France). J Sediment Res 80:791–807

Brandseter, I., McIlroy, D., Lia, O., Ringrose, P. and Nes, A., 2005. Reservoir modelling and simulation of Lajas Formation outcrops (Argentina) to constrain tidal reservoirs of the Halten Terrace (Norway). Petroleum Geoscience, 11: 37 - 46.

Buonocunto FP, D'Argenio B, Ferreri V, Raspini A., 1994. Microstratigraphy of highly organized carbonate platform deposits of Cretaceous age. The case of Serra Sbregavitelli, Matese (Central Apennines). Giorn Geol 56:179–192

Bryant, I.D. and Flint, S.S. 1993. Quantitative clastic reservoir geological modelling: problems and perspectives. In: The geological modelling of hydrocarbon reservoirs and outcrop analogues (Eds I.D. Bryant and S.S. Flint), 15, 3 - 20. International Association of Sedimentologists Special Publication.

Cabello, P., Falivene, O., Lopez-Blanco, M., Howell, J.A., Arbues, P. and Ramos, E., 2010. Modelling facies belt distribution in fan deltas couling sequence stratigraphy and geostatistics: The Eocene San Llorenc del Munt example (Ebro foreland basin, NE Spain). Marine and Petroleum Geology, 27: 254 – 272.

Caers, J.F. and Zhang, T. 2004. Multiple-point geostatistics: A quantitative vehicle for integrating geologic analogs into multiple reservoir models. In: Integration of outcrop and modern analogs in reservoir modeling (Eds G.M. Grammer, P.M. Harris and G.P. Eberli), 1 - 22. AAPG Memoir 80.

Carle, S.F. and Fogg, G.E. 1997. Modeling spatial variability with one and multidimensional continuous-lag Markov chains. Mathematical Geology, 29: 891 - 918.

Clarkson, E. N. K. 1998. Invertebrate paleontology and evolution. 4th Edition. Blackwell Science, Oxford.

Collins, L.B., Read, J.F., Hogarth, J.W., and Coffey, B.P., 2006. Facies, outcrop gamma ray and C-O isotopic signature of exposed Miocene subtropical continental shelf carbonates, North West Cape, Western Australia. Sedimentary Geology, 185, 1-19.

Cuevas-Gozalo, M.C. and Martinius, A.W. 1993. Outcrop data-base for the geological characterization of fluvial reservoirs: an example from distal fluvial fan deposits in the Loranca Basin, Spain. In: characterization of Fluvial and Aeolian Reservoirs (Eds C.P. North and D.J. Prosser), 73, 79 - 94. Geological Society of London, Special Publication, London.

Daws, J.A. and Prosser, D.J. 1992. Scales of permeability heterogeneity within the Brent Group. Journal of Petroleum Geology, 15: 397 - 418.

Deutsch, C.V. 2002. Geostatistical Reservoir Modeling. Oxford University Press, New York, 376 p.

Deutsch, C.V. and Journel, A.G. 1998. GSLIB: Geostatistical software library and user's guide. Oxford University Press, Oxford, 350 p.

Douglas, J.L., 1996. Geostatistical model for the Arab-D Reservoir, North 'Ain Dar Pilot, Ghawar Field, Saudi Arabia; an improved reservoir simulation model. GeoArabia (Manama), 1, 267-284.

Dennison, J.M., Filer, J.K., Cavallo, L.J., Drake, R.A., and Middleton, J.D., 1997. Subsurface to surface; use of outcrop gamma-ray logs to interpret structurally complex exposures of Appalachian Devonian strata. AAPG Bulletin, 81, 1549.

Doveton, J.H, 1994. Theory and applications of vertical variability measures from Markov Chain analysis. In: Stochastic modeling and geostatistics: principles, methods, and case studies (Volume (Eds J.M. Yarus and R.L. Chambers), 177 - 199. AAPG Computer Applications in Geology 3, Tulsa.

Edgell, H.S., 1987. Stratigraphic Control of Oil and Gas Accumulation in Saudi Arabia.In, Short Course on Hydrocarbon Exploration, 23.

Eisenberg, R.A., Harris, P.M., Grant, C.W., Goggin, D.J. and Conner, F.J., 1994. Modeling reservoir heterogeneity within outer ramp carbonate facies using an outcrop analog, San Andres Formation of the Permian Basin. AAPG Bulletin, 78: 1337 - 1359.

Enge, H.D., Buckley, S.J., Rotevatn, A. and Howell, J.A., 2007. From outcrop to reservoir simulation model: workflow and procedures. Geosphere, 3: 469 - 490.

Enge, H.D. and Howell, J.A. 2010. Impact of deltaic clinothems on reservoir performance: Dynamic studies of reservoir analogs from the Ferron Sandstone Member and Panther Tongue, Utah. AAPG Bulletin, 94: 139 -161.

Evans, R., Mory, A.J., and Tait, A.M., 2007. An outcrop gamma ray study of the Tumblagooda Sandstone, Western Australia. Journal of Petroleum Science and Engineering, 57, 37-59.

Enay, R., Le Nindre, Y.M., Mangold, C., Manivit, J., and Vaslet, D., 1987. The Jurassic of central Saudi Arabia; new data on lithostratigraphy, paleoenvironments, ammonite fauna, ages and correlations Le Jurassique d'Arabie Saoudite centrale; nouvelles donnees sur la lithostratigraphie, les paleoenvironnements, les faunes d'ammonites, les ages et les correlations. Geobios, Memoire Special, 9, 13-65.

Fabuel- Perez, I., Hodgetts, D. and Redfern, J., 2009. A new approach for outcrop characterization and geostatistical analysis of a low-sinuosity fluvial-dominated succession using digital outcrop models: Upper Triassic Oukaimeden Sandstone Formation, central High Atlas, Morocco. AAPG Bulletin, 93: 795 - 827.

Fabuel- Perez, I., Hodgetts, D. and Redfern. J. 2010. Integration of digital outcrop models

(DOMs) and high resolution sedimentology - workflow and implications for geological modelling: Oukaimeden Sandstone Formation, High Atlas (Morocco). Petroleum Geoscience, 16: 133 - 154.

Falivene, O., Arbues, P., Gardiner, A., Pickup, G.E., Munoz, J.A. and Cabrera, L., 2006. Best practice stochastic facies modeling from a channel-fill turbidite sandstone analog (the Quarry outcrop, Eocene Ainsa basin, northeast Spain). AAPG Bulletin, 90: 1003 - 1029.

Frykman, P. 2006. Spatial variability of porosity in chalk: comparison of an outcrop and a North Sea reservori. In: Stochastic modeling and geostatistics: principles, methods, and case studies Eds T.C. Coburn, J.M. Yarus and R.L. Chambers), 279 -288. AAPG Computer Applications in Geology 5, Tulsa.

Flugel, 2010. Microfacies of carbonate rocks analysis, interpretation and application. Springer, Berlin Heidelberg New York

Flugel, Erik, 2004. Microfacies of carbonate rocks; analysis, interpretation and application. Springer.

Galloway, W.E., 1989. Genetic stratigraphic sequences; flooding-surface-bounded depositional units in terrigenous shelves and seaways. International Geological Congress, Abstracts Congres Geologique International, Resumes, 28, Vol. 1, 1-525.

Galloway, W.E., 1989, Genetic stratigraphic sequences in basin analysis. I. Architecture and genesis of flooding-surface bounded depositional units. American Association of Petroleum Geologists Bulletin **73**: 125–142.

Geel T, 2000. Recognition of stratigraphic sequences in carbonate platform and slope deposits: empirical models based on microfacies analysis of Paleogene deposits in southeastern Spain Paleogeogr Paleoclimatol Paleoecol 155:211–238.

Grant, C.W., Goggin, D.J. and Harris, P.M., 1994. Outcrop analog for cyclic-shelf reservoirs, San Andres Formation of Permian Basin: Stratigraphic framework, permeability distribution, geostatistics, and fluid-flow modeling. AAPG Bulletin, 78: 23 – 54.

Gringarten, E. and Deutsch, C.V. 1999. Methodology for variogram interpretation and modeling for improved reservoir characterisation. In: Proceedings: 1999 SPE Annual Technical Conference and Exhibition, SPE 56654, 1 - 13. Society of Petroleum Engineers, Houston, Texas

Gringarten, E. and Deutsch, C.V. (2001) Teacher's Aide Variogram Interpretation and Modeling. Math. Geol., 33, 507–534.

Grammer, G.M., Harris, P.M. and Eberli, G.P., 2004. Integration of outcrop and modern analogs in reservoir modeling: Overview with examples from the bahamas. In: Integration of outcrop and modern analogs in reservoir modeling (Eds G.M. Grammer, P.M. Harris and G.P. Eberli), 1 - 22. AAPG Memoir 80.

Haq, B. U., Hardenbol, J., and Vail, P. R., 1986, Chronology of fluctuating sea levels since the Triassic: *Science*, 235.

Hallock, Pamela and Schlager,. 1986. Nutrient excess and the demise of coral reefs and carbonate platforms. *Society of Economic Paleontologists and Mineralogists* **1**(4): 389-398.

Hughes, G.W., 1996. Environmentally-induced biofacies events in the Arab-D reservoir of Saudi Arabia. GeoArabia (Manama), 1, 150.

Hughes, G.W., 2004a. Middle to Late Jurassic biofacies of Saudi Arabia. Rivista Italiana di Paleontologia e Stratigrafia, 110, 173-179.

Hughes, G.W., 2004b. Palaeoenvironmental and sequence stratigraphic implications of Pseudocyclammina lituus events in the Upper Jurassic (Oxfordian), Hanifa Formation of Saudi Arabia. Grzybowski Foundation Special Publication, 8, 209-216.

Hughes, G.W., Varol, O., Hooker, N.P., and Enay, R., 2008. New aspects of Saudi Arabian Jurassic biostratigraphy. GeoArabia (Manama), 13, 174.

Hughes, G.W., 2009. Using Jurassic micropaleontology to determine Saudi Arabian carbonate paleoenvironments. Special Publication - Society for Sedimentary Geology, 93, 127-152.

Kendall, C.G.G.S.C., Alsharhan, A., and WHITTLE, G., 1994, Field Guidebook to Examine the Holocene Carbonates/Evaporites of Abu Dhabi, United Arab Emirates: for the International Geological Correlation Program (IGPCP-349): Abu Dhabi, U.A.E. University Publication Department, 46 p

Hips K, Haas J ., 2009 Facies and diagenetic evaluation of the Permian–Triassic boundary interval and basal Triassic carbonates: shallow and deep ramp sections, Hungary. Facies 55: 421–442

Hohn, M.E 1999. Geostatistics and Petroleum Geology. Kluwer Academic Publishers, Dordrecht, the Netherlands, 235 p

Isaaks, E.H. and Srivastava, R.M. 1989. An introduction to applied geostatistics. Oxford University Press, New York, 561

Journel, A.G. and Deutsch, C.V. 1993. Entropy and spatial disorder. Mathematical Geology, 25: 329 – 355

Journel, A.G. and Huijbregts, C.J. 1978. Mining geostatistics. Academic Press, New York, 600 p

Jensen, J.L., Corbett, P.W.M., Pickup, G.E. and Ringrose, P.S., 1996. Permeability semivariograms, geological structure, and flow performance. Mathematical Geology, 28: 419 - 435.

Kavoosi MA, Lasemi Y, Sherkati S, Moussavi-Harami R (2009) Facies analysis and depositional sequences of the Upper Jurassic Mozduran Formation, a carbonate reservoir in the Kopet Dagh Basin, NE Iran. J Petrol Geol 32:235–260

Krystyniak, A.M., Paxton, S.T., and Coffey, W.S., 2005. Detailed outcrop gamma-ray characterization of the Woodford Shale, south-central Oklahoma. Abstracts: Annual Meeting - American Association of Petroleum Geologists, 14, A76.

Koptikova, L., Babek, O., Hladil, J., Kalvoda, J., and Slavik, L., 2010. Stratigraphic significance and resolution of spectral reflectance logs in Lower Devonian carbonates of the Barrandian area, Czech Republic; a correlation with magnetic susceptibility and gamma-ray logs. Sedimentary Geology, 225, 83-98

Koehrer, B., Zeller, M., Aigner, T., Poeppelreiter, M., Milroy, P., Forke, H., and Al-Kindi, S., 2010a, Facies and stratigraphic framework of a Khuff outcrop equivalent; Saiq and Mahil formations, Al Jabal al-Akhdar, Sultanate of Oman: GeoArabia (Manama), v. 15, no. 2, p. 91-156.

Koehrer, B.S., Heymann, C., Prousa, F. and Aigner, T., 2010. Multi-scale facies and reservoir quality variations within a dolomite body – outcrop analog study from the Middle Triassic, SW German Basin. Mar. Petrol. Geol., 27, 386–411.

Kerans, Charles and Tinker, Scott W. 1997. Sequence stratigraphy and characterization of carbonate reservoirs. *Society of Sedimentary Geology: SEPM Short Course Notes*, 40

Kerans, Charles; Fitchen, W. M., 1995. Sequence hierarchy and facies architecture of a carbonate-ramp system; San Andres Formation of Algerita Escarpment and western Guadalupe Mountains, West Texas and New Mexico. Report of Investigations-Texas, University, Bureau of Economic Geology

Kerans, C., Lucia, F.J., Senger, R.K., 1994 Integrated characterization of carbonate ramp reservoir using Permian San Andres Formation outcrop analogs. AAPG Bull., 78, 181–216.

Konert, G., Afifi, A.M., Al-Hajri, S.A., de Groot, K., Al Naim, A.A., and Droste, H.J., 2001. Paleozoic stratigraphy and hydrocarbon habitat of the Arabian Plate. AAPG Memoir, 74, 483-515

Kupfersberger, H. and Deutsch, C.V. 1999. Methodology for integrating analog geologic data in 3-D variogram modeling. AAPG Bulletin, 83: 1262 - 1278.

Le Nindre, Y.M., Farjanel, G., Giot, D., and Remond, G., 1987. Application of crystalline luminescence properties to the petrography of sedimentary rocks Application des proprietes de luminescence cristalline a la petrographie des roches sedimentaires. Principaux Resultats Scientifiques - Bureau de Recherches Geologiques et Minieres, 1987, 85-86.

Le Nindre, Y.M., Vaslet, D., and Manivit, J., 1996. Quantitative subsidence analysis of the Arabian Shelf during the Jurassic. Conference and Technical Exhibition - European Association of Geoscientists and Engineers, 58.

Lindsay, R.F., Cantrell, D.L., Hughes, G.W., Keith, T.H., Mueller, H.W., and Russell, S.D., 2006. Ghawar Arab-D; widespread porosity in shoaling-upward carbonate cycles, Saudi Arabia. Abstracts: Annual Meeting - American Association of Petroleum Geologists, 15, 64.

Ma, Y.Z. and Jones, T.A, 2001. Modeling holl-effect variograms of lithology-indicator variables. Mathematical Geology, 33: 631 - 648.

Martini R, Cirilli S, Saure C, Abate B, Ferruzza G, Cicero GL., 2007. Depositional environment and biofacies characterisation of the Triassic (Carnian to Rhaetian) carbonate succession of Punta Bassano (Marettimo Island, Sicily). Facies 53:389–400

Mattner J. and Al-Husseini M. I, 2002. Essay: applied cyclo-stratigraphy for the Middle East E&P industry. *GeoArabia*, **7**:734-744

Murris, R. J., 1980. Middle East: Stratigraphic Evolution and Oil Habitat. *American Association of Petroleum Geologists* 64(5): 597-618.

McKinley, J.M., Lloyd, C.D. and Ruffell, A.H., 2004. Use of variography in permeability characterization of visually homogeneous sandstone reservoirs with examples from outcrop studies. Mathematical Geology, 36: 761 - 779. Journal of Petroleum Geology, 15: 397 - 418.

McGuire, M. D., R. B. Koepnick, J. R. Markello, M. L. Stockton, L. E. Waite, G. S. Kompanik, M. J. Al-Shammery and M. O. Al-Amoudi., 1993. Importance of Sequence

Stratigraphic Concepts in Development of Reservoir Architecture in Upper Jurassic Grainstones, Hadriya and Hanifa Reservoirs, Saudi Arabia. *Society of Petroleum Engineers*, 489-499.

Miall, A.D. and Tyler, N. (Eds), 1991. The three-dimensional facies architecture of terrigenous clastic sediments and its implications for hydrocarbon discovery and recovery, Concepts in sedimentology and paleontology, 3. SEPM, Tulsa, 309 p.

North, C.P. and Prosser, D.J, 1993. Characterization of fluvial and aeolian reservoirs: problems and approaches. In: Characterization of fluvial of aeolian reservoirs (Eds C.P. North and D.J. Prosser), 73, 1 - 6. Geological Society Special Publication.

Olea, R.A., 1994. Fundamentals of semivariogram estimation, modeling, and usage. In: Stochastic modeling and geostatistics: principles, methods, and case studies (Volume I) (Eds J.M. Yarus and R.L. Chambers), 177 - 199. AAPG Computer Applications in Geology 3, Tulsa.

Palma RM, Lopez-Gomez J, Piethe RD., 2007. Oxfordian ramp system (La Manga Formation) in the Bardas Blancas area (Mendoza Province) Neuquen Basin, Argentina: facies and depositional sequences. Sediment Geol 195:113–134

Papaioannou FP, Kostopoulou V (2008) Microfacies and cycle stacking pattern in Liassic peritidal carbonate platform strata, Gavrovo-Tripolitza platform, Peloponnesus, Greece. Facies 54:417–443

Pérez-López, A., 2001, Significance of pot and gutter casts in a Middle Triassic carbonate platform, Betic Cordillera, southern Spain: Sedimentology, v. 48, no. 6, p. 1371-1388.

Pemberton, S. G. 1992. Applications of Ichnology to Petroleum Exploration. *SEPM Core Workshop*, 17

Pringle, J.K., Howell, J.A., Hodgetts, D., Westerman, A.R., and Hodgson, D.M., 2006. Virtual outcrop models of petroleum reservoir analogues: A review of the current stateof-the-art. First Break, 24, 33-42

Pomar, L. and Hallock, P. 2008. Carbonate factories; a conundrum in sedimentary geology. *Earth-Science Reviews* 87(3-4): 134-169.

Palermo, D., Aigner, T., Nardon, N. and Blendinger, W., 2010. Three-dimensional facies modeling of carbonate sand bodies: outcrop analog study in an epicontinental basin (Triassic, Southwest Germany). AAPG Bull., 94, 475–512.

Phelps, R.M., Kerans, C., Scott, S.Z., Janson, X. and Bellian, J.A., 2008. Three-dimensional modelling and sequence stratigraphy of a carbonate ramp-to-shelf transition, Permian Upper San Andres Formation. Sedimentology, 55, 1777–1813.

Powers, R. W. 1962. Arabian Upper Jurassic Carbonate Reservoir Rocks. *American Association of Petroleum Geologists,* 1: 122-192.

Powers, R. W., L. R. Ramirez, C. D. Redmond, and E. L. Elberg., 1966. Sedimentary geology of Saudi Arabia: Geology of the Arabian Peninsula: U.S. Geological Survey Professional Paper 560-D, 150 p

Qi, L., Carr, T.R. and Goldstein, R.H., 2007. Geostatistical three-dimensional modeling of oolite shoals, St. Louis Limestone, southwest Kansas. AAPG Bull., 91, 69–96.

Romero J, Caus E, Rossel J., 2002. A model for the palaeoenvironmental distribution of larger foraminifera based on Late Middle Eocene deposits on the margin of the south Pyrenean Basin (SE Spain). Paleogeogr Paleoclimatol Paleoecol 179:43–56

Raspini, 2001. Stacking pattern of cyclic carbonate platform strata; Lower Cretaceous of Southern Apennines, Italy. *Journal of the Geological Society of London*, 158(2): 353-366

Schauer M, Tebingen TA (1997) Cycle stacking pattern, diagenesis and reservoir geology of peritidal dolostones, Trigonodus- Dolomit, Upper Muschelkalk (Middle Triassic, SW Germany). Facies 37:99–114

Schlager, Wolfgang 2000. Sedimentation rates and growth potential of tropical, cool-water and mud-mound carbonate systems. Geological Society Special Publications, 178: 217-227

Schlager, Wolfgang. 2003. Benthic carbonate factories of the Phanerozoic. *International Journal of Earth Sciences*. 92(4): 445-464

Sech, R.P., Jackson, M.D. and Hampson, G.J., 2009. Three dimensional modeling of a shoreface-shelf parasequence reservoir analog: Part 1. Surface-based modeling to capture high-resolution facies architecture. AAPG Bull., 93, 1155– 1181.

Sharland, P.R., Boote, D., Casey, D.M., Davies, R.B. and Simmons, M.D., 2001. North Africa and Arabian Plate first and second order sequence stratigraphy. Annual Meeting Expanded Abstracts - American Association of Petroleum Geologists, 12, 156.

Senalp, M. and Al-Duaiji, A.A., 2001. Qasim Formation; Ordovician storm- and tidedominated shallow-marine siliciclastic sequences, central Saudi Arabia. GeoArabia (Manama), 6, 233-268.

Toland, C., 1994, Late Mesozoic stromatoporoids: Their use as stratigraphic tools and paleoenvironmental indicators Micropaleontology and hydrocarbon exploration in the Middle East: London, Chapman and Hall, p. 113–125

Taylor, A. M.and Gawthorpe, R. L, 1993. Application of sequence stratigraphy and trace fossils analysis to reservoir description; examples from the Jurassic of the North Sea. Geological Society of London, 4: 317-335

Toma´ s, S., Zitzmann, M., Homann, M., Rumpf, M., Amour, F., Benisek, M., Marcano, G., Mutti, M. and Betzler, C. (2010) from ramp to platform: building a 3D model of depositional geometries and facies architectures in transitional carbonates in the Miocene, northern Sardinia. Facies, 56, 195–210

Tolosana-delgado, R., Pawlowsky-Glahn, V. and Egozcue, J.-J., 2008. Indicator kriging without order relation violations. Math. Geosci., 40, 327–347.

Verwer, K., Adams, E.W. and Kenter, J.A.M., 2007. Digital outcrop models: technology and applications. First Break, 79, 57–63.

Verwer, K., Merino-tome O., Kenter, J.A.M. and Della Porta, G., 2009. Evolution of a high-relief carbonate platform slope using 3D digital outcrop models: Lower Jurassic Djebel Bou Dahar, High Atlas, Morocco. J. Sed. Res., 79, 416–439

Vaslet, D., Manivit, J. and Le Nindre, Y.-M., 1989. Proposal for new reference sections of the Early Triassic Sudair Shale, Kingdom of Saudi Arabia. Professional Papers - Kingdom of Saudi Arabia, Ministry of Petroleum and Mineral Resources, PP3, 45-59

Van Lanen, X.M.T., Hodgetts, D., Redfern, J. and Fabuel-Perez, I., 2009. Applications of digital outcrop models: two fluvial case studies from the Triassic Wolfville Fm., Canada and Oukaimeden Sandstone Fm., Morocco. Geological Journal, 44: 742 - 760.

Wilson JL, 1975. Carbonate facies in geologic history. Springer, Berlin Heidelberg New York.

Wilson, A.O., 1981. Jurassic Arab-C and -D Carbonate Petroleum Reservoirs, Qatif Field, Saudi Arabia. Society of Petroleum Engineers of AIME, (Paper) SPE, 171-177.

Wilmsen M, Fu¨rsich FT, Seyed-Emami K, Majidifard MR, Zamani PM (2010) Facies analysis of a large-scale Jurassic shelf-lagoon: the Kamar-e-Mehdi Formation of east-central Iran. Facies 56:59–87

White, C.D., Novakovic, D., Dutton, S.P. and Willis, B.J., 2003. A geostatistical model for calcite concretions in sandstone. Math. Geol., 35, 549–575

Wolf, D.J., Withers, K.D. and Burnaman, M.D., 1994. Integration of well and seismic data using geostatistics. In: Stochastic modeling and geostatistics: principles, methods, and case studies (Volume I) (Eds J.M. Yarus and R.L. Chambers), 177 - 199. AAPG Computer Applications in Geology 3, Tulsa.

Zappa, G., Bersezio, R., Felletti, F. and Giudici, M., 2006. Modeling heterogeneity of gravel-sand, braided stream, alluvial aquifers at the facies scale. J. Hydrol., 325, 134–153.

Ziegler, M.A., 2001. Late Permian to Holocene paleofacies evolution of the Arabian Plate and its hydrocarbon occurrences. GeoArabia (Manama), 6, 445-504.

Ziegler, M.A., 2001. Late Permian to Holocene paleofacies evolution of the Arabian Plate and its hydrocarbon occurrences. GeoArabia (Manama), 6, 445-504.

Vitae

Name	Hussam Eldin Elzain Osman Elzain
Nationality	Sudanese
Date of Birth	8/1/1989
Email	hejo777@hotmail.com
Address	Khartoum-Sudan
Academic Background	MSc Geology
Research of Interest	Carbonate Sedimentology and Reservoir modeling
Publication	Conference paper in International Association of Sedimentologist (IAS)